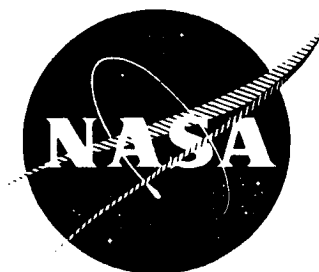N65-36781

NASA CR-54731

FINAL REPORT

DEVELOPMENT OF A
HIGH TEMPERATURE BATTERY

by

W. J. Subcasky, T. M. Place, D. N. Stamires, W. G. Anderson, H. A. Parker Jones, G. Segovia, and R. G. Salisbury

prepared for

NATIONAL AERONAUTICS AND SPACE ADMINISTRATION

CONTRACT NAS3-6002

OCTOBER 15,1965

Request for copies of this report should be referred to:

    National Aeronautics and Space Administration
    Office of Scientific and Technical Information
    Washington, D. C. 20025
    Attention: AFSS-A

NASA CR 54731
Aeronutronic Publication No. U-3313
W.O. 2261

FINAL TECHNICAL REPORT

DEVELOPMENT OF A HIGH
TEMPERATURE BATTERY

by

W. J. Subcasky, T. M. Place, D. N. Stamires, W. G. Anderson,
H. A. Parker-Jones, G. Segovia and R. G. Salisbury

prepared for

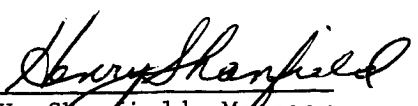NATIONAL AERONAUTICS AND SPACE ADMINISTRATION

October 15, 1965

Technical Management
NASA Lewis Research Center
Cleveland, Ohio
Space Power Systems Division
Meyer R. Unger

Approved by _[signature]_
H. Shanfield, Manager
Chemistry Laboratory

APPLIED RESEARCH LABORATORIES
Aeronutronic Division
Philco Corporation
Newport Beach, California

Request for copies of this report should be referred to:

ABSTRACT

This report covers the results of a program to develop a battery capable of
operation for 72 hours at an ambient temperature of 800°F$(425^\circ$C). Two types
of cells were constructed and discharged for this time period. In one cell
type a zeolite separator was used with a lithium-magnesium alloy anode and
a molten cuprous chloride cathode. The initial open circuit voltage of
this cell was 3.29 volts. This high voltage was due to the lithium content
of the anode and to cupric ion impurities in the cathode. After removal of
these cupric ions the IR free cell voltage was 2.50 volts at a current
density of 6.7 mamps/cm^2 of zeolite separator area. At these current
densities only resistance polarization was found, i.e. the IR free and open
circuit voltages of the cell were identical. At the end of the test the IR
free cell voltage had dropped to 1.93 volts probably because of depletion
of lithium from the alloy anode. The resistivity of the zeolite separator,
initially 5030 ohm-cm, rose to a maximum of 12,700 ohm-cm in five hours
before decreasing to 314 ohm-cm at the end of the 72 hour test. Evidence
is cited in the report that this high resistivity was caused by contaminants
from the flexible sealants used in the assembly of the cell. At the end of
the test a crack containing metallic copper was visually observed within the
membrane. The relatively high cell resistance and cell voltage at the end
of the test would indicate that this copper did not lead to any significant
shorting of the cell compartments.

In the final cell tested on this program, a specially designed flexible
seal of AgCl was used in a cell with a magnesium anode separated from the

cuprous chloride cathode by a zeolite membrane. When this cell test was discontinued at 51 hours, the cell voltage under a load of 6.7 mamps/cm^2 of zeolite separator area was 1.60 volts. Total cell resistance was only 10 ohms. The zeolite separator was found intact and no copper was found in the anode compartment.

In the second type of cell a porous glass separator was used between the lithium-magnesium alloy anode and a solid cupric oxide cathode. This cell showed terminal voltages (no correction for IR drop) of the order of 2.1 volts under a drain of 6.7 mamps/cm^2 of separator area with new anodes. After depletion of the surface lithium content of the anode, the terminal cell voltage stabilized at 1.5 volts. The maximum cell resistance was 15 ohms but during most of the discharge period the cell resistance was less than five ohms. Thus for this current density the IR drop would be of the order of 0.025 volts. This cell was discharged a total of 159 hours. Failure at this time was attributed to cracking of the glass cell compartments. This type of failure did not permit an analysis of the cell after test. However, a previous analysis after 48 hours of operation showed a total of 46.2 x 10^{-6} moles of Cu present in the anode compartment. A second cell of this same type had an IR free cell voltage of 1.36 volts after 72 hours of discharge and 1.28 volts after 96 hours.

Additional cells were constructed and tested utilizing a zeolite separator with a molten sodium anode and a molten cuprous chloride cathode. Initial open circuit voltages were 3.3 to 3.5 volts for these cells. After removal of cupric ions present as an impurity in the cathode, the cell voltage was about 2.6 volts. At a current density of 6.7 mamps/cm^2 of zeolite area, only resistivity polarization was found. Membrane resistivities were greater than 1000 ohm-cm. Again the high resistivity was attributed to contamination by material derived from the flexible sealants. Maximum cell life was 22 hours. Failures in these cells were usually due to cracking and attack of the zeolite membranes by molten sodium thereby permitting direct chemical reaction between the cell components.

Cells utilizing molten sodium anodes and zeolite separators did not have life time capabilities for satisfying the 72 hour requirement. Attack of the zeolite by the molten sodium limited the life of these cells. Magnesium-cuprous chloride cells appeared to be capable of achieving the required 72 hours of operation if suitable sealants which would accommodate dimensional changes in the zeolite with temperature and ion exchange were used. These sealants must be flexible and stable at the operating temperature. With such sealants the zeolites were effective as low resistance separators in magnesium-cuprous chloride cells.

Various methods were developed for fabricating zeolite membranes. These methods were vacuum, hot pressing; sintering with binder or aids such as sodium silicate or phosphoric acid; self sintering; and hot pressing. These techniques were investigated for Type A zeolite in the sodium ion form and for Type X zeolite in both the sodium and the lithium ion form. All techniques with the exception of vacuum hot pressing, were found to cause some loss of zeolite structure when the forming conditions were such as to yield membranes with suitable strength. In general, increases in temperature or times used in the fabrication technique caused an increase in the strength, density, and resistivity and a decrease in porosity, thermal expansion, and crystallinity of the zeolites.

In general the Type X zeolite had lower a.c. resistivities than the Type A; and zeolites in the sodium ion form had lower resistivities than those in the lithium ion form. At 425°C. the following a.c. resistivities were found for the zeolite membranes in the absence of fused salts: NaA, 6500 ohm-cm; NaX, 440 ohm-cm; and LiX-PJ, 10,000 ohm-cm. Type A in the sodium ion form (NaA) had the highest temperature stability. Although a transformation with loss of the zeolite crystal structure was noted at 770°, a complete fusion could not be obtained even at temperatures above 1000°C. The NaX zeolite sintered and fused at temperatures below 1000°C. However, loss of the zeolite structure occurred before sintering. The LiX zeolite

had a very sharp melting and transformation point at approximately 700°C. This transformation was accompanied by a loss of zeolite structure.

Electrochemical performance, as cathodic half cells, was determined for the chlorides of silver(I), copper(I), copper(II), iron(III), bismuth (III), and compounds of chromium(VI) and vanadium(V). These metals were tested as pure molten salts or as solutions in other salts. Chromium(VI) compounds either reacted with chloride electrolytes or formed insoluble films with high resistances upon reduction. V_2O_5 reacted with molten chlorides and in addition appeared to have a very high equivalent weight. All of the molten chlorides, with the exception of ferric chloride, showed very little polarization under current drain. Ferric chloride was subject to concentration polarization at high current drains. Silver chloride showed good electrochemical performance but had a high equivalent weight. Cupric chloride was the strongest oxidizing agent studied as a possible cathode material. Its extreme reactivity with practical electrode materials and proposed cell cases made it unsuitable for use in the present application. Although bismuth trichloride shows excellent electrochemical properties, its volatility and the formation of soluble or liquid reduction products would make its containment and utilization very difficult. Cuprous chloride was found to be the most suitable cathode based upon its electrochemical properties and compatibilities with other cell components.

Compatibility test showed that the molten alkali metals destroyed the zeolite or porcelain separators. Suitable compatibilities were found for other materials to be used in the proposed cell design.

CONTENTS

APPENDICES

ILLUSTRATIONS

TABLES

SECTION 1

INTRODUCTION

1.1 OBJECTIVE

The objective of this program is the development of a high energy density battery capable of operation for 72 hours under ambient conditions as are believed to exist on the planet Venus. For purposes of the program, such conditions were specified to include a temperature of $800^{\circ}F$, an atmospheric pressure of 10 bars, and a composition of 90% nitrogen and 10% carbon dioxide.

1.2 PROGRAM REVIEW

A battery system utilizing a salt electrolyte fusible below $800^{\circ}F$ (i.e., a "thermal battery") was chosen as most suitable to the Venus environment. The specified duration of 72 hours imposed much more stringent limitations on the self-discharge rate than is the case with conventional thermal batteries. It was anticipated that the self-discharge process most likely to limit battery life would be that resulting from the diffusion of electrode materials through the separator. Two methods of controlling this process exist: (1) use of insoluble or only slightly soluble electrodes, or (2) development of a separator having selective permeability to ions and dissolved species. In the latter case the separator would be required to have a high permeability to ions of the electrolyte, but very low permeability

to the dissolved electrode materials. An additional factor of importance in this connection was that insoluble electrodes generally produce lower potentials and greater polarization problems than do soluble electrodes. This consideration and the importance of high energy density for the intended mission decreed that a battery system involving soluble electrodes and the second of the above two methods for controlling self discharge be adopted.

Two types of materials exist potentially capable of meeting the separator requirements. These are the synthetic zeolites and certain porcelains or glasses. The latter had been subjected to considerable investigation and were known to have good ion selectivity but resistivities greater than 500 ohm-cm at $800^{o}F$. The zeolites had been extensively studied in aqueous electrolytes at temperatures up to $200^{o}C$. In such electrolytes they have good conductivity and appreciable if not well documented ion selectivity. No information was available on their conductivity in fused salts. However, some data existed on their intrinsic ion conductivity at $800^{o}F$ and above, and this together with the results of theoretical reasoning indicated that a zeolite could be found having the right combination of ion conductivity and specific ion permeability required for the purposes of this program. There appeared to be good reasons for believing that the synthetic zeolites were most promising.

In accordance with the foregoing, the program was initiated with the working hypothesis that a suitable semipermeable separator would be obtainable, and initial work on cathode materials stressed soluble electrodes. For reasons as discussed in this report, CuCl and $BiCl_3$ were selected as the most promising, and ultimately, attention was centered on CuCl. A not unimportant reason for its selection was that it could be conceived as intermediate to the development of $CuCl_2$ as a depolarizer. This latter material develops about the highest cathode potential possible in fused chloride melts.

Anodes of interest were exclusively those of the alkali metal or alkaline earth groups, all of which exhibit satisfactory polarization behavior and which develop a potential of about -2.6 to -2.8 volts with respect to AgCl,

-2-

with the exception of Mg and Be with potentials of about -1.82 and -1.25 volts, respectively. The only point to be decided was whether a solid or a liquid anode would be most suitable. This decision was dependent upon details of final cell design. Selection of a liquid anode was tentatively made based upon ease of maintaining contact with the current collector and also with the separator without the need for a reservoir of electrolyte in the anode compartment.

Research and development work on the separator problem occupied, by far, a major part of the program. It was directed primarily to the various zeolite materials, with a small amount of work on the porcelains and on porous materials such as alumina and glass. In some cases porcelains formed from zeolites were fabricated by fusing to destroy the zeolite structure. In general it was found that the Type X zeolite had lower resistance than Types A or Y, and further that resistance was lowest for the sodium zeolite form. Aside from the general problem of devising a membrane material having all of the desired properties, the difficulties which were encountered may be summarized as falling into three different categories: (1) attack on the zeolite by the anode material, (2) sealing problems, and (3) disruption of the membrane structure by exchange with foreign ions from the electrode materials or the electrolyte. Because of these difficulties, it was not possible to demonstrate unequivocally that the materials studied had the desired selective permeability or electrical conductivity. However, the experimental efforts indicated that by the use of a less active anode and with suitable sealing techniques, zeolite membranes would be suitable for operation at $800^{\circ}F$ for 72 hours.

Data on the attack of separator and cell materials by molten alkali metals is presented in this report. As a result of this work, it was concluded that the problem could not be solved within the scope of the present program. Consequently the concept of a liquid anode was abandoned and replaced by the alternative of a solid anode, i.e., Mg or Li-Mg alloy. In this case physical contact between the anode and the separator would be avoided, electrical contact being maintained by means of a film of electrolyte.

The sealing problem provided a major impediment to the program, and was particularly annoying because it was one which manifested itself much more importantly in the membrane development than it is expected to do in the actual construction of a practical cell. The screening of separator compositions required that each membrane specimen be sealed to the appropriate part of the test cell structure. If a rigid seal be used, the wide thermal range to which the cell was exposed required a close match (probably within 1%) in coefficient of expansion between the membrane, support, and sealant, if cracking of the membrane was not to occur. Since different membrane materials had different coefficients of expansion, meeting this requirement for each material was very laborious. Use of a flexible sealing material would materially alleviate the problem. Extensive use had been made of the only flexible sealant available, namely an RTV silicone rubber, which appeared to withstand the cell operating temperature. However, the evidence obtained in the program strongly indicated that due to the ubiquitous antiwetting character of silicones, conductivities obtained from measurements on membranes sealed in place with such material were subject to serious question. Additionally it was found that at the cell operating temperature the silicone rubber slowly decomposed with the evolution of gas.

Finally, in those cases where satisfactory seals had been obtained, there was strong evidence that cracking of the membrane occurred due to changes in material volume consequent upon the exchange of ions with the surroundings. Earlier work in the program had been with sodium zeolites and ceramics in the sodium ion form. In the cell, the membrane was in contact with the KCl-LiCl eutectic and with CuCl. Exchange of the Na with either K, Li or Cu, or any combination thereof could occur. Such exchange would lead to the observed effect. Therefore in the later portion of the program the membrane materials were subjected to various exchanging reactions prior to incorporation in the cells.

Towards the end of the program conferences with NASA program monitors led to the decision to concentrate on zeolite materials, and this decision was implemented. Most recent work was concerned with the synthesis of lithium

zeolites and their fabrication into membranes, and the effect of various fabrication techniques upon the properties of the zeolites.

Also presented in this report are data on two cell tests carried out using insoluble electrodes and fritted glass porous separators. The electrodes were Li-Mg alloy and CuO. Durations of over 72 hours were obtained with little difficulty. No measurement was made of electrode utilization, but qualitative observations indicated a very low rate of self discharge. These results suggest that the quickest path to a 72 hour thermal cell would be through use of insoluble electrodes and porous separators. An approach utilizing soluble or molten cathodes and a zeolite separator would be of longer range but if successful should provide for the maximum attainable energy density.

SECTION 2

LITERATURE SURVEY

During the initial portion of this program, a literature survey was directed towards the areas of immediate importance, namely anodes, cathode, and solid electrolyte with particular emphasis upon the synthetic crystalline zeolites. The purpose of this survey was to define areas of most promise for further study.

2.1 ANODES

The alkali and alkaline earth metals are generally used as anodes in thermal cells. The equivalent weight of the most important anode materials, their approximate potentials as measured versus a Pt/Pt(II) reference in actual thermal cells,[1] and their melting points are shown in Table I.

The potential given for calcium is undoubtedly that of the calcium-lithium alloy which invariably forms when metallic calcium is brought in contact with molten electrolytes containing lithium ions. The alloy which is formed by the reduction of lithium ions by metallic calcium is a liquid at the operating temperature of the battery. The potential of sodium is estimated from the calculated reversible decomposition voltage of NaCl at 450°C.[2] Sodium is expected to have an activity only slightly lower than calcium and hence a Li-Na alloy would probably form in the presence of Li^+.

Although beryllium looks attractive on the basis of its very low equivalent weight, its potential (as estimated from the decomposition voltage of $BeCl_2$) indicates it is not as desirable as magnesium.

A commercially available Li-Mg alloy called LA141 has been used as an anode in thermal cells.[3] This alloy contains 13-15 percent lithium and 1.0 to 1.5 percent aluminum. It reportedly gives cell voltages both on open circuit and under drain about 0.5 to 0.6 volts higher than pure magnesium. The particular advantage of this alloy is high electrochemical activity without the formation of a liquid anode.

TABLE I

CHARACTERISTICS OF ANODE MATERIALS

Material		Potential Versus Pt-Pt(II)	Equivalent Weight	M.P. (^{o}C)
Aluminum		-1.71	8.99	659.7
Lithium		-3.34	6.94	186
Magnesium		-2.55	12.16	651
Calcium		-3.23	20.04	842
Sodium	Approx.	-3.23(a)	23.0	97.5
Beryllium	Approx.	-2.00(a)	9.01	1278
Li-Mg Alloy	Approx.	-3.10(b)	--	600

(a) Potential calculated from Reference 2. See text.
(b) From Reference 3. See text.

2.2 CATHODES

Practical cathode systems for high temperature applications are almost exclusively those involving compounds between oxygen and the transition and nonmetallic elements. The cathode depolarizers are generally in the form of oxides. Examples of various oxides which have been used as cathodes in thermal batteries are CuO,[4] Sb_2O_3,[4] and FeO_x.[5] The oxides are used because they are only slightly soluble in the molten LiCl-KCl electrolyte generally used in thermal batteries. The oxides have the required thermal stability and many appear to be reversible.[6] The slight solubility of some of the oxides would be expected to decrease the active life of a

thermal battery especially in batteries designed for extended periods of operation.

It is anticipated that using an insoluble cathode depolarizer will decrease, to some extent, the energy and power densities of a thermal cell. As would be predicted by the Nernst equation, the potential of a metal-metal oxide electrode is more negative (IUPAC, Stockholm Convention) than that of the corresponding metal-metal ion electrode. Table II shows this shift for a few systems in molten LiCl-KCl eutectic. A more negative cathode would give a lower cell voltage when coupled with an anode.

It is highly possible that in a cell using a solid electrolyte as a separator, a pure molten cathode depolarizer could be used. In other words, little or no additional molten electrolyte is needed in the cathode compartment. The omission of the inert electrolyte would obviously increase the energy density of the cell.

Standard potentials for possible cathode depolarizers both as pure molten halides and in a LiCl-KCl eutectic at 450°C. are given in Table II. Potentials of Li, Ca, and Mg are given for comparison. The reference electrode for both systems is Ag(I)-Ag and the concentration units are expressed in mole fraction of cation. The voltages for the pure salts[2] were calculated from thermodynamic data while those for the LiCl-KCl solution were experimentally determined. Many of these potentials have been confirmed in thermal cells using a LiCl-KCl electrolyte.[1]

The standard potentials listed in Table II can be used to estimate the voltage of complete cells by the relation:

$$E_{cell} = E_{cathode} - E_{anode} \qquad (1)$$

The unpublished work of H. A. Laitinen and his students[10] contains much information concerning the electrochemical properties of possible cathode

TABLE II

ELECTRODE POTENTIALS AT 450°C.

Couple	Pure Salt		LiCl-KCl Eutectic
Li(I)-Li	-2.773		-2.773
Ca(II)-Ca	-2.659		-2.66
Mg(II)-Mg	-1.809		-1.943
NiO-Ni	- -		-0.771[6]
Cr(III)-Cr	-0.763		- -
Cr(II)-Cr	-0.657		-0.758
Cu_2O-Cu	- -		-0.750[6]
V(III)-V	-0.665	(227 D)	- -
Fe(II)-Fe	-0.686		-0.535[7]
Fe(III)-Fe	-0.405	(319 V)	- -
V(III)-V(II)	- -		-0.217[7]
Cu(I)-Cu	-0.424		-0.214
Ni(II)-Ni	-0.493		-0.158
Sb(III)-Sb	-0.408	(221 V)	-0.033
Cr(III)-Cr(II)	- -		-0.006
Ag(I)-Ag	0.000		0.000
Bi(III)-Bi	-0.233	(441 V)	+0.049
Cu(II)-Cu	+0.053		- -
PtO-Pt	- -		+0.118[6]
Pd(II)-Pd	+0.124		+0.421
Cr(VI)-Cr(III)	- -		+0.545[8]
Cu(II)-Cu(I)	- -		+0.592
Fe(III)-Fe(II)	- -		+0.617[7]
Pt(II)-Pt	+0.312		+0.637
Au(I)-Au	+0.574		+0.948
Cl_2-Cl	+0.611		+0.953[7]

References: Pure Salt[2]; LiCl-KCl eutectic[9] except where noted otherwise.

Concentrations expressed as mole fraction of cations. Value in brackets indicate temperatures in °C. at which vaporization (V) or decomposition (D) occurs. Potentials in these cases are at temperatures slightly lower than those at which the transition occurs.

depolarizers dissolved in LiCl-KCl eutectic. These results are summarized according to the various elements.

2.2.1 CHROMIUM

The reduction of Cr(VI), added as K_2CrO_4, is irreversible and occurs in the region of -0.2 to -0.9 volts versus $\underline{1m}$ Ag(I). The reduction product is insoluble and contains Li, Cr(VI), Cr(III), and $O^=$. The reduction of Cr(III), added as $CrCl_3$, is irreversible and occurs in the range of +0.5 to +0.1 volts. The reduction of Cr(II) occurs at -1.0 volts and is reversible.

2.2.2 COPPER

The Cu(II)-Cu(I) couple appears to be slow. Potentiometrically, it does not follow the Nernst equation and voltammetrically, a mixture of Cu(II) and Cu(I) shows a discontinuity in the slope of the current-voltage curve as it crosses the zero current axis. Cu(II) is a stronger oxidizing agent than Pt(II).

2.2.3 BISMUTH

A single, reversible, three-electron reduction wave at +0.12 volts versus $\underline{1m}$ Ag(I) was observed with Bi(III).

2.2.4 IRON

Fe(III) undergoes a reversible, one-electron reduction to Fe(II) at +0.8 volts. The Fe(II) itself is reversibly reduced to Fe at -0.60 volts.

2.2.5 GOLD

Potentiometric measurements indicate that the Au(I)-Au couple is reversible with a standard potential of +0.948 volts versus $\underline{1m}$ Ag(I).

2.3 SOLID ELECTROLYTES

There are three general types of solid electrolytes which might be considered

for use in a high temperature battery. These are:

        (1) Oxide deficient structures.

        (2) Porcelains and ceramics.

        (3) Synthetic, crystalline zeolites.

Each of these will be considered separately. However, since the proposed system used a zeolite solid electrolyte, the major portion of the survey was directed toward this subject.

2.3.1 OXIDE DEFICIENT STRUCTURES

Oxide deficient materials of the form $(ZrO_2)_{0.85}$ $(Y_2O_3)_{0.15}$ or $(ZrO_2)_{0.85}$ $(CaO)_{0.15}$ have been used as solid electrolytes in high temperature fuel cells. The CaO system seems to form cubic crystals of the fluorite type, with all cation lattice sites occupied, but with one anion site vacant for each CaO molecule included. Transfer of oxide ions from one vacant anion site to another accounts for the conductivity of these materials. However, the temperature must be rather high (about 1000°C.) before the resistivity drops below about 400 ohm-cm.[11]

2.3.2 PORCELAINS AND CERAMICS

The electrolytic conductivity of glass at elevated temperatures has been known for some time. This conductivity has been used in the preparation of sodium coulometers and reference electrodes. When used as a diaphragm between two fused salts, glass has a resistance of 2000 to 5000 ohms in the temperature range of 350 to 550°C.[12]

More recently, porcelain-type materials (sodium aluminum silicates) have been used for reference electrodes.[13] The porcelain used in these electrodes is prepared by fusion of various glass and clay compositions and can be used at higher temperatures than corresponding electrodes using glass. In addition, the resistivity of the porcelain is lower than that of the glass. Resistivities of some porcelain materials as a function of composition and temperature are shown in Table III. Conductivity of these

porcelain materials has been shown to be solely by sodium ions and not by transfer of electrons or oxide ions. These porcelains may then be considered to be solid electrolytes where the transference number of sodium ions is unity.

TABLE III

RESISTIVITY IN OHM-CM OF PORCELAINS[13]

Temperature °C	2.5% Na_2O, 73.1% SiO_2 24.4% Al_2O_3	10% Na_2O, 54% SiO_2 36% Al_2O_3
400		730
450		420
550		140
650		64
700		42
860		25
900	430	20
940	380	
1000	300	

Ion exchange studies[14] with porcelains containing the higher Na_2O concentration in certain molten salts showed that with potassium, rubidium, or silver melts, exchange was complete and reversible; in lithium, cuprous, or cesium melts partial exchange occurred. No exchange was noted with melts containing NH_4^+, Mg^{++}, Ba^{++}, Zn^{++}, Pb^{++}, or Cd^{++}. The extremely small probability of two cation sites which are simultaneously vacant and sufficiently close together to accept a divalent cation was given as the reason for lack of exchange of divalent cations. A similar reason was given for the lack of electromigration of divalent cations in glass.

Porcelain membranes have been used as a barrier to prevent mixing of the liquid anolyte and catholyte of secondary molten salt cells while still maintaining electrolytic conductivity.[15] Cells of the type M/MCl, NaCl/P/ NaCl, AgCl/Ag where M was the anode material, MCl was its oxidized product in a chloride melt, and P was a porcelain membrane, were operated for periods as long as five or six days.

Recently a study of cells using tin alloys of sodium and lithium as anodes and various porcelains and glasses as separators has been reported.[16] All of these separators had resistivities greater than 10^2 ohm-cm at a temperature of about $550^\circ C$.

High temperature cells using a porcelain electrolyte to separate two dissimilar metals have been prepared. The cells, called Austin Cells, generate electrical energy by the oxidation of one metal electrode while the other metal, usually silver, serves as an inert electrode for the reduction of oxygen. The glass or porcelain enamel separating the two metals served as the electrolyte or ionic conductor.[17]

2.3.3 ZEOLITES

The natural and synthetic zeolites are aluminosilicates of the alkali or alkaline earth metals. The synthetic zeolites are usually prepared by crystallization from aluminosilicate gels. The zeolites prepared in this manner have the general composition

$$Na_x \left[(AlO_2)_x (SiO_2)_y \right] \qquad (2)$$

and consist of alumina and silica tetrahedra arranged in an orderly fashion so as to form basic cubo-octahedra units, which in turn are linked together in various types of arrangements to form the unit cell. It is these arrangements which give rise to the different types of zeolites. Thus the structure of so-called "Type A" zeolite has been found[18] to consist of 12 alternating AlO_4 and SiO_4 tetrahedra per unit cell. Each unit cell also contains 12 sodium ions in the interstices. The arrangement of the tetrahedra in the unit cell produces a large central cage, 11.4 $\overset{\circ}{A}$ in diameter, connected to six similar cages by 8-membered oxygen rings having an opening of 4.2 $\overset{\circ}{A}$. In addition, the large cage is linked to eight smaller cavities 6.6 $\overset{\circ}{A}$ in diameter by opening 2.0 $\overset{\circ}{A}$ in diameter. It is these well-defined passages in the zeolite lattices which gives these materials their molecular sieve properties. In the Type X and Y zeolites, the large cavities are connected by channels of approximately 12 $\overset{\circ}{A}$ diamter.[19]

The four-fold coordination of Al atoms with oxygen in the zeolite lattice creates a uninegative charge on each of the (AlO_4) units. This requires the occlusion of one monovalent or a half of a divalent cation in the lattice for electrical neutrality. A small fragment of the lattice can be represented as follows:
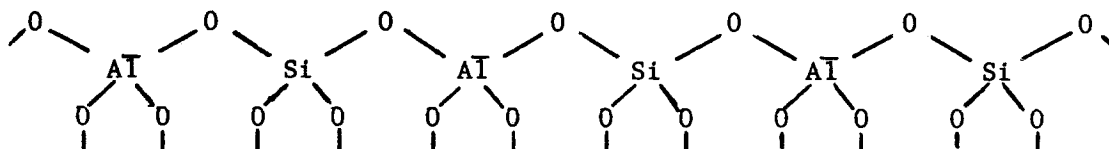
The negative lattice sites are fixed in the framework and interact with the cations, primarily through coulombic forces. This type of bonding and the open crystal framework permits easy exchange and diffusion of the cations in the lattice.[20]

a.   Preparation and Characterization

Synthetic zeolites are usually prepared by crystallization from alumino-silicate gels in the presence of excess alkali. The hydrous gels are prepared with various amounts of sodium silicate, sodium aluminate, and sodium hydroxide. In some cases, all or a portion of the sodium salts are replaced by the corresponding potassium salts. By varying the amounts of materials used to form the gels and by varying the temperature of crystall-ization, various synthetic zeolites have been prepared. A list of some crystalline zeolites that have been prepared is given in Table IV. The type designation is that assigned by Union Carbide Corporation to its various types of molecular sieves. The compositions as given are those which are usually obtained. Slight variation in composition are possible without modifying the zeolite type. In fact, the zeolite type is deter-mined not by its composition but by its x-ray diffraction pattern.

The gel composition and crystallization temperature are quite critical in determining the type of zeolite which is produced. As a specific example, Type F and Type J zeolites have practically the same composition with the

TABLE IV

SYNTHETIC ZEOLITE CHARACTERISTICS

Type	Composition (1) a Na_2O	b K_2O	c Al_2O_3	d SiO_2	"d" Spacings in Order of Line Intensity (2)	Reference
A	1	0	1	2		21
B	1	0	1	3-5		22
D	0 to 1	1-a (3)	1	4.7	2.94, 6.89, 9.42	23
E	0 to 1	1-a (3)	1	2	9.53, 2.86, 3.00	24
F	0	1	1	2	6.95, 2.96, 3.09	25
G	0	1	1	3.6		22
H	0	1	1	2		22
J	0	1	1	1.9-2.3	2.89, 3.13, 6.86	26
L	0	1	1	5.9-6.9	15.8, 4.57, 3.91	27
M	0	1	1	2.0-2.2	3.10, 2.60, 4.25	28
Q	0	1	1	2.2	11.8, 3.01, 2.67	29
R	1	0	1	3.45-3.65	2.95, 9.51, 4.37	30
S	1	0	1	4.6-5.9	7.16, 2.97, 4.12	31
T	0.1 to 0.8	1-a (3)	1	6.4-7.4	11.3, 3.72, 2.85	32
W	0	1	1	3.3-4.9	3.25, 3.17, 2.96	33
X	1	0	1	2.0-3.0	14.47, 3.81, 2.88	34
Y	1	0	1	3-5	14.4, 5.69, 3.78	35

(1) Composition of material as usually prepared based on the empirical formula $aNa_2O \cdot bK_2O \cdot cAl_2O_3 \cdot dSiO_2$

(2) Generally the fully hydrated form as usually prepared.

(3) Amounts of Na_2O and K_2O can be varied within the limits shown with the condition that the total Na_2O and K_2O equal unity.

exception of the noncritical water content. The oxide ratio of the materials used to prepare the gel are different (Table V) and both zeolites are crystallized at 100°C. The x-ray diffraction patterns are completely different as shown in Table VI.

TABLE V

OXIDE RATIO OF GELS

	Type F	Type J
K_2O/SiO_2	1.4 - 4.0	4
SiO_2/Al_2O_3	1.0 - 3.0	4
H_2O/K_2O	10 - 20	10

TABLE VI

X-RAY POWDER DIFFRACTION DATA FOR POTASSIUM ZEOLITES

Type F[25]		Type J[26]	
"d" Spacing Å	Relative Intensity	"d" Spacing Å	Relative Intensity
6.95	100	6.86	54
6.51	11	4.77	32
3.48	21	4.72	16
3.09	56	4.27	15
2.96	72	4.00	51
2.81	39	3.23	46
2.25	8	3.13	93
1.74	6	3.04	40
1.69	6	3.00	41
1.64	5	2.97	36
		2.89	100
		2.87	61
		2.66	20
		2.64	25
		2.58	23

The "d" spacings for the three most intense lines of the other types of zeolites are also shown in Table IV. The "d" spacings are for the zeolites as prepared. Slight changes in relative intensities and positions of the diffraction lines are noted when the cation of the zeolite is changed. This shift is shown in Table VII for the 111 plane in Type X zeolite. Small

changes in line positions are also noted with changes in the water content of the zeolite.

TABLE VII

SHIFT OF d_{111} FOR TYPE X ZEOLITE AS A FUNCTION OF EXCHANGED CATION[34]

Cation	Percent Exchanged	d_{111} Å
Na^+	100	14.47
Ca^{++}	89	14.37
Ag^+	85	14.37
Ce^{+3}	77	14.42
Li^+	59	14.37
NH_4^+	81	14.41
Ba^{++}	93	14.43

Crystallographic examination of various types of synthetic zeolites yield the following unit cell compositions.[20]

$$\text{Type A} \quad Na_{12}\left[(AlO_2)_{12} \quad (SiO_2)_{12}\right] \qquad (4)$$

$$\text{Type Y} \quad Na_{53}\left[(AlO_2)_{53} \quad (SiO_2)_{139}\right] \qquad (5)$$

$$\text{Type X} \quad Na_{88}\left[(AlO_2)_{88} \quad (SiO_2)_{104}\right] \qquad (6)$$
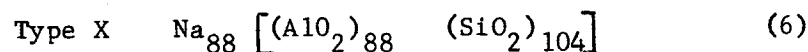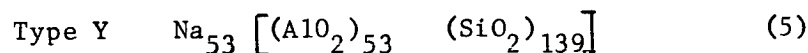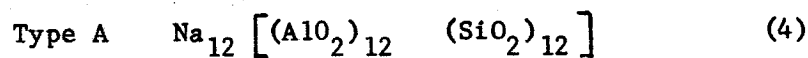
An extensive study of the hydrated forms of the Type 4A, 5A, and 13X has also been reported.[19] This study includes x-ray diffraction and electron density observations and the application of the three-dimensional Fourier method to the refinement of atomic positions and the location of cations.

Zeolites can be obtained containing various cations. In most cases, the synthetic zeolites are first prepared in the Na^+ or K^+ form, and then the desired cation form obtained by ion exchange as described in Paragraph 2.3.3b. However, it is sometimes possible to synthesize the zeolite in the desired cation form. Zeolites containing Ba^{++},[36] Rb^+ and Cs^+,[37] and Li^+[38] have been prepared. A summary of these preparations have been published.[39]

b. <u>Ion Exchange Properties</u>

As described before, the interaction between the negative lattice sites
fixed in the zeolite framework and the cations is principally through
coulombic forces. Because of this type of bonding between the cations and
the cation sites and also because of the open crystal framework, these
cations are very easily exchanged for other cations of different size and
charge without much distortion of the crystal lattice.

A summary of the studies of the ion exchange properties of some of the
various types of synthetic zeolites produced by Union Carbide Corporation
is given in Table VIII. The numerals in Table VIII indicate the percent of
the exchange which was achieved. No attempt was made to obtain complete
exchange except for the studies on the Type Y zeolite. The exchange studies
were performed by equilibrating a portion of the zeolite with an aqueous
solution of the exchanging ion. The (+) sign indicates exchange did occur
but no quantitative information on the extent of exchange was given. X-ray
diffraction patterns are given for the various exchanged forms of Types A,
D, L, Q, and X. In addition, exchange studies on Type X zeolite with K^+,
Li^+, Ca^{++}, and Ag^+ from alcoholic solutions have been made.[40] By the use
of percolating techniques,[20] almost complete exchange has been achieved in
some cases. Thus, with Type A zeolite, the exchange with Li^+ was 98.6
percent; with K^+, 99.8 percent, and with Ag^+, 99.7 percent.

c. Conductivity

The highly mobile cations in the zeolite lattice result in an unusually high
electrical conductivity for ionic crystals. It has been long recognized
that this conduction mechanism is ionic in nature[41] and is due to the self-
diffusion of cations in the crystal lattice.[20,42] That this proceeds with
a relatively low activation energy has been attributed to the high density
of the cations ($\sim 10^{22}$ monovalent cations/gram of crystal) and to weak
electrostatic interaction of the cation with the cation site (~ 10 kilocal/mole).
This low activation energy for cation diffusion is also the result of the

TABLE VIII

ION EXCHANGE PROPERTIES OF SYNTHETIC ZEOLITES

Cation	\underline{A}	\underline{D}	\underline{E}	\underline{F}	\underline{L}	\underline{M}	\underline{Q}	\underline{R}	\underline{W}	\underline{X}	\underline{Y}
Li^+	33	66	47.2	+	47.6		58	+	22.6	59	
Na^+	100	95	+	+	41.4	+	65	100	69	100	100
K^+	46	+	+	100	100	100	100	+	100		97.6
Rb^+	36										61.4
Cs^+	31										77.1
NH_4^+	39			+		+				81	
Ag^+	88					+				85	
Tl^+	~70	72		+	39.1						78
Mg^{++}	43		51.8				45	+	52.9		71.0
Ca^{++}	72	92	89.4		+	+	81	+	52	89	95.7
Sr^{++}	+	96			48.3		64	+	62.7		74.2
Ba^{++}	+				73.2		66	+		93	95.6
Zn^{++}	+	71	82.3		22.8		64	+	89		
Cd^{++}	+										
Hg^{++}	+										
Mn^{++}	+										
Co^{++}	+										
Ni^{++}	+										
Ce^{+++}										77	
Reference	18 43	23	24	25	27	28	29	30	33	34	20

open space available in the diffusion path.

The ionic conductivity[20] increases with increasing temperature and is given
by:

$$\sigma = \frac{N \lambda^2 q^2}{h} \exp\left(-\frac{\Delta G}{RT}\right) \qquad (7)$$

where

σ = conductivity

N = number of charge carriers

q = carrier charge

λ = distance between cation sites

ΔG = free energy for conduction

The effects of cation density and temperature on the conductivity are shown
in Figure 1 for a series of zeolites in the Na^+ form. The SiO_2/Al_2O_3 ratio
was varied in such a manner as to go from the Type X zeolite (2.40) to the
Type Y (5.20). The ratio is also an indication of the cation density since
electrical neutrality requires that every aluminum atom in the crystal be
balanced with a positive charge.

Figure 2 shows the effect of the radius and the charge of the cationic
carriers upon the free energy for conduction. According to Equation 7, an
increase in ΔG causes a decrease in the conductivity. For monovalent cations
the coulombic attraction between the cation and the cation site decreases as
the size of the cation increases. For larger cations, the number capable
of migration decreases because of steric hindrance. For divalent cations
the conductivity decreases with increasing size because of the greater bond-
ing to two separated negative charges with the larger, more easily polarized
cations.

The effect of various adsorbed phases upon the conductivity of various
synthetic zeolites have also been studied.[42] It was found that the potential
energy barrier for the conduction process is decreased and hence the con-
ductivity increased by adsorbed molecules. Polar molecules (e.g., H_2O and NH_3)

-20-

10^{-3}

10^{-4}

10^{-5}

10^{-6}

10^{-7}

10^{-8}

$(OHM^{-1} CM^{-1})$

ARRHENIUS PLOT	$\dfrac{SiO_2}{Al_2O_3}$
◯	5.20
✕	4.50
▢	3.80
△	3.05
◇	2.40

1.4   1.6   1.8   2.0   2.2   2.4   2.6

$10^3/T^oK$

RO5237
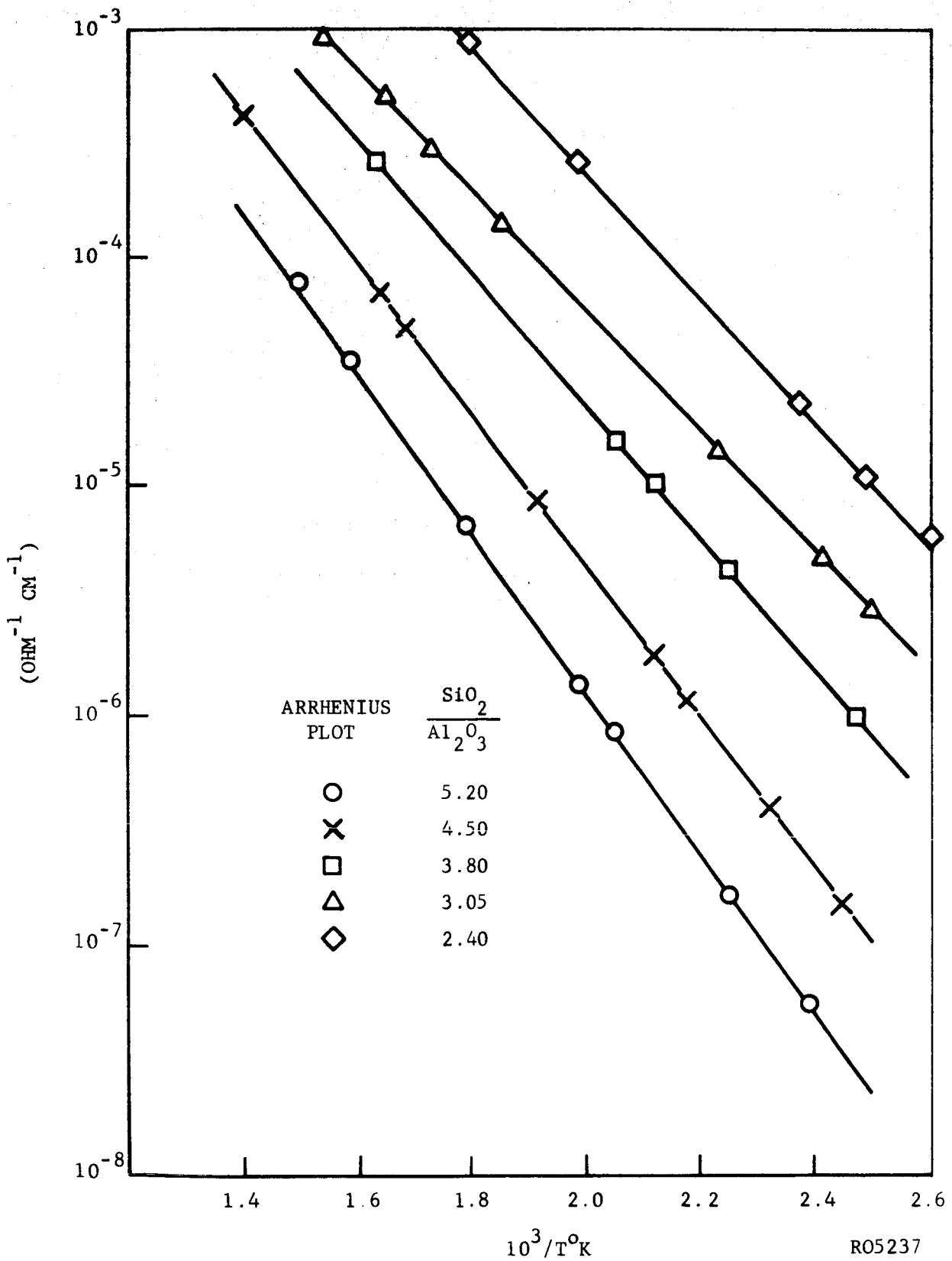
FIGURE 1. CONDUCTIVITY OF THE X-Y ZEOLITE SERIES[42]
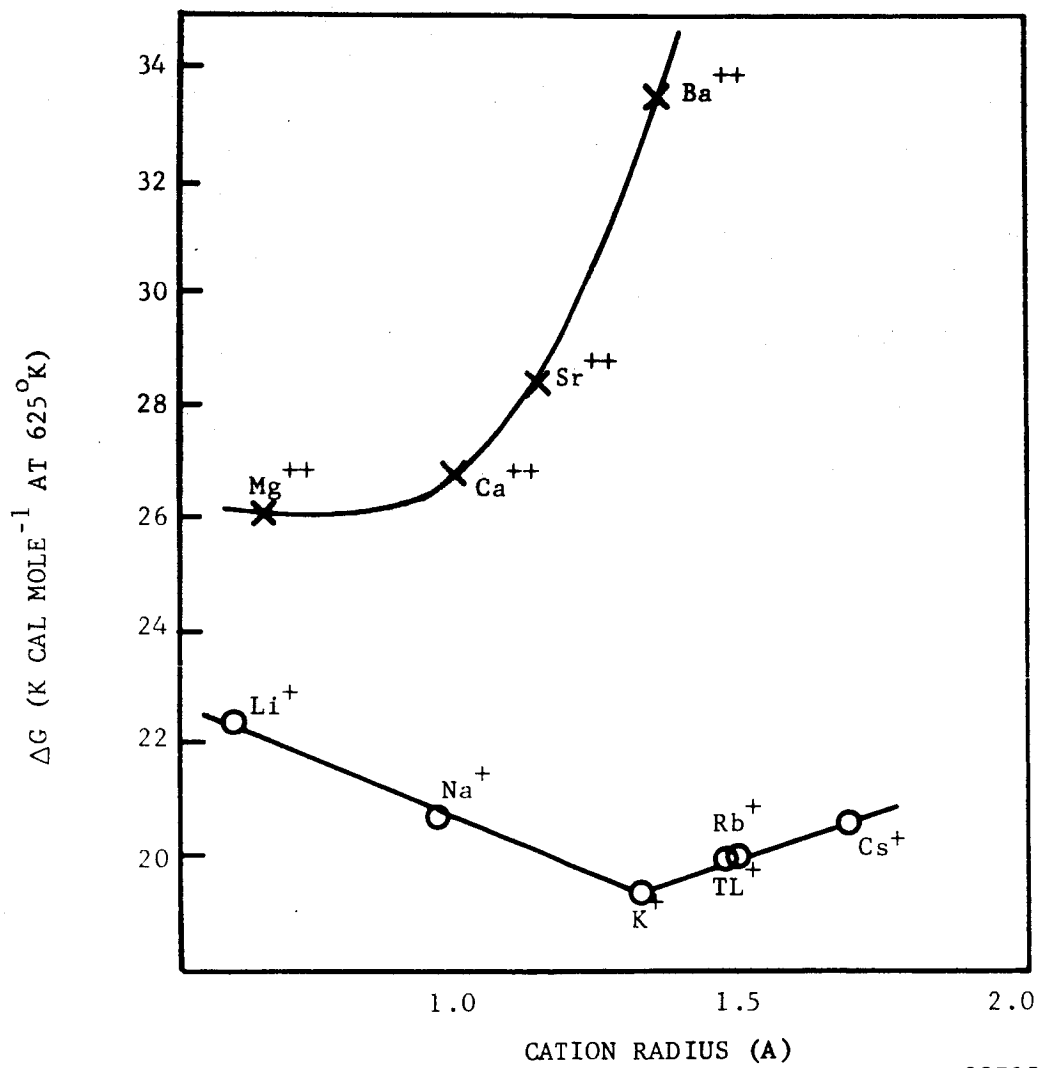
FIGURE 2. FREE ENERGY VALUES FOR MONOVALENT AND DIVALENT-CATION
EXCHANGE Y ZEOLITES

R08715

-22-

exhibit a strong association through ion-dipole interactions with the mobile cations. Completely hydrated zeolites at room temperatures have conductivities approaching that of aqueous solutions. These observations have been confirmed for zeolites containing phosphoric acid.[44]

The effect of various factors upon the conductivity of crystalline zeolites can be summarized. The conductivity increases with:

      (1) increasing temperature

      (2) increasing cation density

      (3) increasing cation charge

      (4) increasing cation radius except for very large cations where steric hindrance reduces the charge carriers available for conduction

      (5) decreasing cation radius for divalent ions

      (6) adsorption of polar molecules

d. Applications

The principal application of the synthetic zeolites is as molecular sieves to selectively adsorbed and separate various molecules. However, for this program, the application of the ionic conductivity of the zeolite as a solid electrolyte in a high temperature battery is the prime requisite. The Astropower Laboratory of Douglas Aircraft[44] have used synthetic zeolites as solid electrolytes in ambient temperature fuel cells. In this study, the zeolites were bonded into thin wafers using $ZrO_2-H_3PO_4$ cements. The large amount of phosphoric acid contained in these wafers yield specific conductivities of the order of 10^{-2} to 10^{-1} ohm^{-1} cm^{-1} for high relative humidities at temperatures below $100^{\circ}C$.

The use of another type of inorganic ion exchange material for use as a solid electrolyte in a fuel cell should be mentioned.[45] These materials were prepared from the phosphates of heavy metals such as tin, titanium, niobium, and germanium. Exchange capacities of 6 to 8 milliequivalents per gram and resistance values of the order of 1 to 10 ohm- cm^2 were obtained

for water saturated membranes. These materials might be useful as solid electrolytes at higher temperatures. Zirconium phosphate[46] was found to be a solid electrolyte with a resistivity of the order of 10^5 ohm-cm. at low temperature.

2.4 SUMMARY AND CONCLUSIONS

As a result of the literature survey, it appeared that the best solid anode was calcium and the best liquid anodes were sodium or lithium. Pure molten salts of materials which are strong oxidizing agents showed the most promise as cathodes. The synthetic zeolites appeared to be the most suitable solid electrolytes on the basis of their conductivity and exchangeability with a wide variety of cations.

SECTION 3

ANODE STUDIES

Calcium metal was first proposed as the anode for this cell. This selection
was predicated by the low equivalent weight and highly reducing nature of
calcium. However, further consideration of this anode material leads to the
conclusion that problems associated with maintaining electrical contact
between the solid zeolite electrolyte and solid calcium would be difficult
to overcome. These problems would be intensified in this application where
a considerable amount of the anode material would be consumed during cell
discharge. Consequently solid calcium anodes were dropped from consideration,
and attention focused upon anode materials which would be liquid at the cell
operating temperature.

Lithium, by reason if its low equivalent weight, was the first liquid anode
to be considered. However, the corrosive nature of molten lithium as shown
in compatibility tests (Section 3.2) eliminated the use of lithium in the
present application.

Sodium was next considered as the anode material. One of the determining
factors in this selection is the wealth of information on the technology and
properties of liquid sodium.[47] All results for sodium anodes were obtained
with complete cells -- no anode half cells were run. However, in many cases
anode potentials were measured and are reported in Section 3.1.

Because of the corrosive nature of molten sodium, efforts were shifted to a solid anode of either magnesium or a lithium-magnesium alloy operating in a LiCl-KCl anolyte.

3.1 ELECTROCHEMICAL PERFORMANCE

Cells with sodium anodes and cuprous chloride cathodes with several types of separators or solid electrolytes were constructed and tested. One of these cells used a porcelain membrane[13] to separate the anode and cathode compartments. The complete cell and its performance are described in Section 6.1. The potential of the anode was found to be -2.53 volts vs. Ag-1$\underline{m}$ AgCl at 450°C. The portion of the ceramic tube in contact with molten sodium was found to be blackened after the three hour test. Slightly less negative potentials (-2.33 to -2.44) volts were observed in cell using zeolite separators. This difference in potential could have been the result of a greater reaction rate between the liquid sodium and the zeolite.

Sodium had to be rejected as a suitable anode material for this program because of the corrosive reaction between the molten metal and the zeolite separators. To obtain as negative an anode potential as possible a lithium-magnesium alloy was considered. The use of such alloys as anodes for short duration thermal cells has been reported.[3] A lithium-magnesium alloyed designated LA141 is commercially available.[48] The chemical composition of this alloy is given as:

Li	13.00-15.00	Ni	0.005 max.
Al	1.00- 1.50	Fe	0.005 max.
Mn	0.15 max.	Na	0.005 max.
Si	0.10 max.	Other	impurities total 0.30 max.
Cu	0.04 max.	Mg	Remainder

This alloy melts at 580°C and has a density of 1.35 gm/cm^3. Since this alloy is a solid at the required operating temperature of the cell, a liquid anolyte was required to maintain adequate ionic contact between the anode and the zeolite separator. A molten LiCl-KCl eutectic was chosen for this purpose.

The alloy for the anode was used in the form of strips or pellets fabricated with chips milled from sheet stock. The milling was performed under kerosene and the chips were washed and dried with methyl ethyl ketone. Pellets 1.27 cm long were pressed in a 1.27 cm diameter die utilizing an upper punch with a 0.51 mm hole through the center of its longitudinal axis. This hole permitted integral pressing of a 0.25 mm iron wire lead spot-welded to a 180 mesh stainless steel collector screen. The collector screen and wire lead assembly were inserted into the die cavity during filling. Minimum pellet density (74% of bulk density) with sufficient strength was obtained at pressing pressures of 560 kgm/cm^2.

As with sodium, information concerning the lithium-magnesium alloy anode was obtained from complete cell tests. These cells are further described in Section 6.3. Initially the potential of the alloy anode was in the range of -2.56 to -2.60 volts vs. a Ag-1m AgCl reference electrode. However, after operating under current drain a potential shift to the region of -1.90 to -2.0 volts was observed.

The relatively high initial anodic potential observed in most tests using the lithium-magnesium alloy appeared to be that of the lithium component in the alloy. The depletion of lithium was indicated by a shift of the potential to that of the remaining magnesium. The time required for this shift to occur was a function of the size, the shape, and the porosity of the anode, other factors, such as temperature and current density, being kept constant. However, it was not considered profitable in this program to define the relations between these variables. The use of the alloy anode gives an added voltage of about 0.6 volts as compared to a magnesium anode. This added cell voltage is far outweighed by the increase in the anode weight. Since the more negative potential was due only to lithium oxidation, the anode must contain sufficient lithium to meet the ampere-hour capacity specifications. With the low lithium content of the alloy, an amount of alloy equal to six to seven times the required weight of lithium would be needed.

3.2   COMPATIBILITY TESTS

Early in the program it appeared that, in cell test, the proposed alkali
metal anodes were reacting with the zeolites being used as separators. To
further study this problem compatibility tests were run between the alkali
metals and proposed separator materials. The procedure used in these tests
was to vacuum seal the alkali metal and the separator in Pyrex ampoules.
The cleaning of the alkali metals and the loading of the ampoules was car-
ried out in a dry box containing a dry argon atmosphere. The argon was
recirculated through tubes containing magnesium perchlorate and heated
copper wool to remove moisture and oxygen, respectively. In some cases,
where a deficiency of the alkali metal was desired, the zeolites were
vacuum hot-pressed (see Section 5.2.3) in the form of cylinders 1.77 cm in
diameter and about 3 cm long. A hole was drilled into one end to form a
closed end tube. This tube was then packed with the desired alkali metal.
Although no quantitative measurements were made it is estimated that a
tenfold volume excess of zeolite was used in these cases. When an excess
of alkali metal was desired, zeolite membranes of the order of 0.1 cm thick
were used with an estimated two-to fivefold volume excess of the alkali
metal. After vacuum sealing, the ampoules were placed in a muffle furnace
held at $425^{\circ}C$. In most cases the compatibility tests ran for 72 hours. A
thin film of the alkali metal formed on the sides of the ampoules and pre-
vented visual observation during the course of the test. (The vapor pres-
sure of sodium is approximately 1 mm at these temperatures.) However, from
the densities of the materials involved, it is expected that in those cases
where sodium was in excess, the zeolite was completely covered with the
molten metal. At the end of the tests, the ampoules were opened and the
excess alkali removed by reaction with alcohol. In most cases visual exami-
nation was used to determine changes in the materials. In addition to
separator materials, other materials to be used in cell construction were
subjected to compatibility test with the alkali metals.

Molten lithium was found to severely attack recrystallized alumina by destroying its structural integrity. In addition, some etching of the glass container by lithium distilled from the sample was noted. Molten lithium was found to completely degrade a pellet formed by vacuum-hot pressing of a Type X xeolite in the lithium ion form (LiX). This particular sample of LiX contained LiCl from the exchanging operation (Section 5.2.2). The presence of the LiCl would not be expected to materially affect the test results. In all cases all that remained of the zeolite pellet was a black sludge. Lithium is said to be one of the most corrosive of the liquid metals.[47] Because of the difficulties associated with handling liquid lithium and the time involved in developing the required technology, no further work was done on systems utilizing pure lithium anodes.

More extensive tests were run using molten sodium. The proposed cell configuration (Section 7.2) utilized such materials as alumina, Armco iron, or nickel. No apparent reaction was noted between these materials and molten sodium. It would appear that they would be suitable for use in a cell with a sodium anode.

Samples of sodium zeolites, Types A, X, and Y were prepared by vacuum hot pressing and exposed to molten sodium at 425°C for 72 hours as described above. In those cases where the sodium was in excess, the pellets were completely disintegrated leaving a dark sludge. When a deficiency of sodium was used as in the tests involving the zeolite tubes, the zeolite in immediate contact with the sodium was attacked. In addition to this attack, the zeolites appeared to be penetrated by the molten sodium. This was evidenced by a yellow coloration extending a few millimeters into the zeolite pellets. After exposure to molten sodium, zeolite pellets reacted with water to liberate hydrogen. The mechanism of this penetration is not known but it was possibly through pores or channels of the zeolite crystallite. It is these channels which give synthetic zeolites their molecular sieve properties. If penetration was by way of these pores, it might be eliminated or minimized by blocking the pores with a solid or liquid material. Therefore, a cylinder of NaX was vacuum impregnated with molten LiCl-KCl before

testing with sodium. However, this impregnation of the zeolite did not improve its compatibility with molten sodium.

Other separator compositions were checked for compatibility with molten sodium. These compositions include NaX bonded with H_3PO_4 (Z-14) and fired at 740°C or 850°C, NaX bonded with sodium silicate (Z-16) and fired at 700° or 780°, pure NaX fired at 940° (Z-17), a high sodium porcelain, a laminate of this porcelain on porous ZrO_2 and a sodium-alumino-phosphate material designated C-9. The composition and fabrication of these materials is described in Sections 5.1.1, 5.1.2, and 5.2.3. Similar results were found with the porcelain and with all zeolite samples -- disintegration of the pellet and formation of a dark powder. After exposure, the alumino-phosphate material was completely disintegrated leaving a dark sludge. Although the ceramic on zirconia appeared to be in one piece it was completely blackened and could not be handled without breakage.

A sample of a KX zeolite was completely disintegrated by molten potassium in a compatibility test. As a result of these compatibility tests, the use of molten alkali metals as anodes with separators of this type was dropped from consideration.

3.3 CONCLUSIONS

Calcium is not suitable as an anode in this application. It would be very difficult to maintain good electrical contact between a solid calcium anode and a solid zeolite separator especially when calcium was undergoing an anodic oxidation. The use of a molten salt anolyte would eliminate the contact problems. The logical choice for the molten salt is a LiCl-KCl eutectic mixture. This mixture will react with calcium to form a liquid calcium-lithium alloy. This liquid alloy is very corrosive and would be difficult to contain. The more common alkali metals (Li, Na, and K) are liquids at the desired operating temperatures. Thus good electrical contact could be maintained with the solid separator. Unfortunately the alkali metals completely disintegrated the proposed separator materials. The use of solid lithium-magnesium alloys with molten salt anolytes gave anodes

with a potential almost as negative as that of lithium itself. The lithium content of the solid alloys was low and thus the lower anode potential was obtained only at the expense of a much higher anode weight. Magnesium used with a molten LiCl-KCl eutectic appears to be the most suitable anode material to use with zeolite or porcelain type separators in cells to operate for extended times.

SECTION 4

CATHODE STUDIES

The purpose of this portion of the experimental program was the measurement of the potentials with current drain of selected materials that would give the most energetic cathodes. All the results described in this section were obtained by half cell measurements. Results obtained with cathodes which were a part of a complete cell are given in Section 6.

Cathode materials tested included the chlorides of copper (II), copper (I), silver (I), bismuth (III), iron (III) and compounds of chromium (VI) and vanadium (V). These materials were tested as either pure salts or as solutions in other molten salts. In some cases the materials were tested in the presence of the reaction products of the proposed anodes.

4.1 EXPERIMENTAL

4.1.1 EQUIPMENT

Figures 3, 4, and 5 are block diagrams of the equipment used for polarization measurements on cathode materials as well as for cell testing.

a. Furnace

Hevi-Duty Electric Multiple Unit Furnace type MU-3018, 115-230 volts, 2575 watts. Two of the four heating units were disconnected as shown in the schematic wiring diagram (Figure 4) so that only the upper half of the vertical tube type furnace was heated.
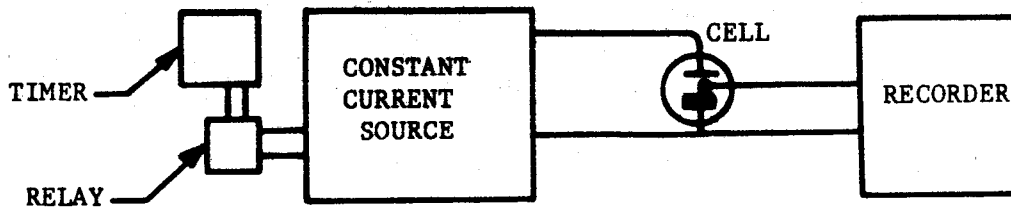
FIGURE 3. BLOCK DIAGRAM OF APPARATUS FOR POLARIZATION STUDIES
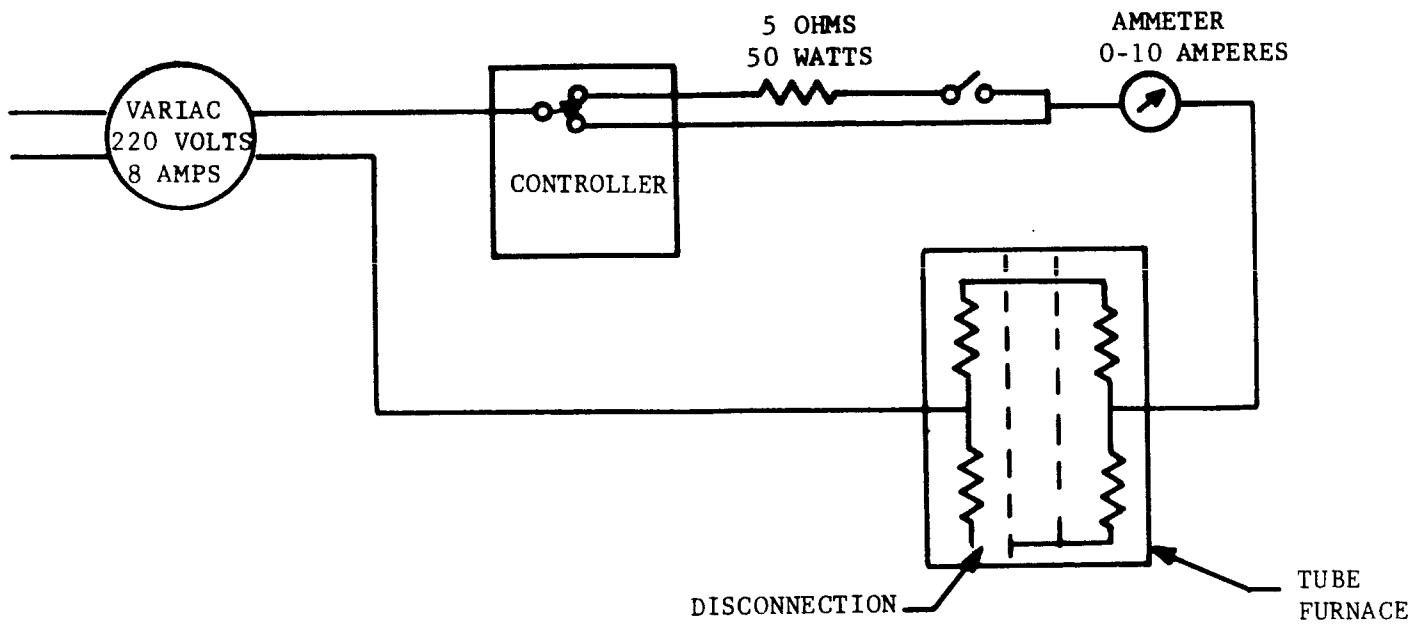
R08713

FIGURE 4. BLOCK DIAGRAM OF CELL HEATING APPARATUS

-33-
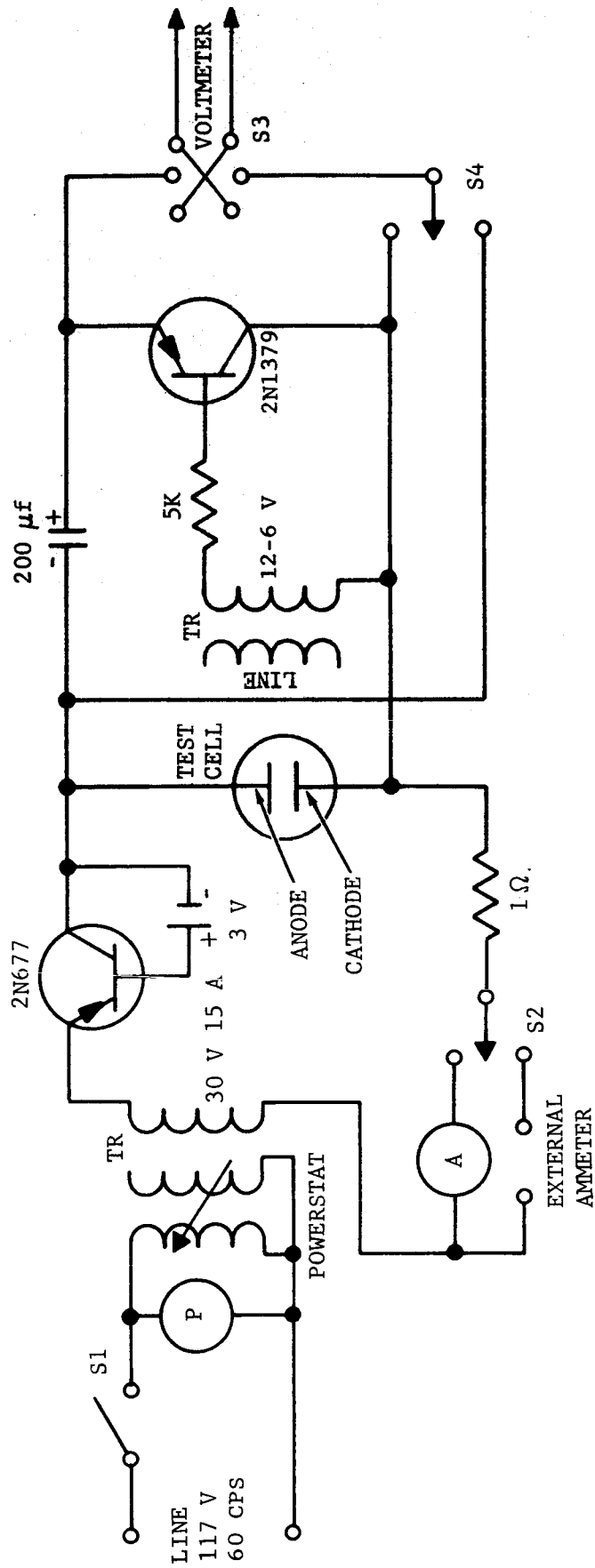
FIGURE 5. COMMUTATOR DISCHARGE CIRCUIT

R12318

-34-

b. Controller

Bristol Series 536 Free-Vane Electronic Indicating Controller. The
Bristol Company, Waterbury 20, Connecticut.

c. Recorder

Sargent Recorder Model MR. The potentiometric ranges (1.25-2500 mV)
were used wherever possible. When higher voltage ranges were required a
Hewlett-Packard VTVM Model 412A was used between the signal source and the
recorder input. This procedure insured an input resistance $>10^8$ ohms to
avoid polarization of the reference electrode.

d. Constant Current Sources

Harrison Laboratories Model 6201A. The power supply was operated in the
constant current mode with an external programming resistor. The
programming resistor was switched either manually or automatically with a
cycling timer to change the current drains through the cell. The arrange-
ment is shown in Figure 3.

In cell testing or whenever d.c. resistances were desired, a sine wave
transistorized commutator[49] was used. This instrument was a modification
of the well-known Kordesch-Marko bridge.[50] A circuit diagram of the
instrument as constructed for use in our Laboratories is given in Figure 5.
This particular circuit permitted direct measurements of either the IR drop
in the cell or the cell voltage corrected for IR drop depending on the
position of switch S_4. In actual operation this switch was a single pole
double throw relay activated periodically by a commercial timer.
(Industrial Timer Corporation, Timer Assembly CM-8, Gear Assembly A-12).

A block diagram of the experimental arrangement used to automatically
record cell performance is given in Figure 6. In operation the timer at
fixed intervals actuated the relay R. The contacts of this relay were
switch S_4. This switched the output of the commutator between the two
measured quantities; the IR free cell voltage and the IR drop. These two
quantities were measured on a potentiometric recorder (Sargent, Model MR)
which had a range of up to 2.5 volts. The cell current passed through
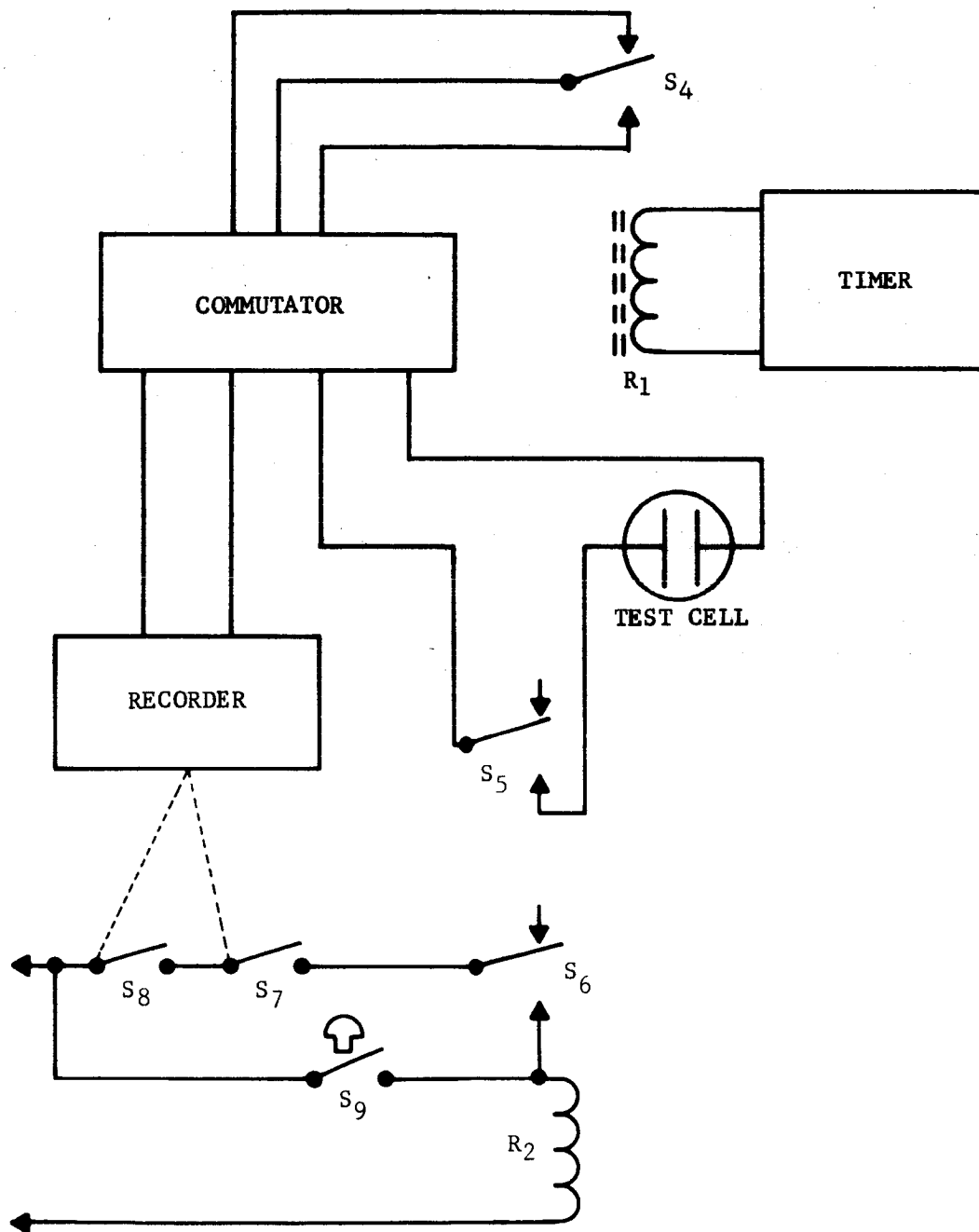
FIGURE 6. EXPERIMENTAL ARRANGEMENT FOR RECORDING CELL PERFORMANCE

R12317

switch S_7, which in turn was controlled by the latching relay R_2. In series with the coil of this latching relay were three switches; S_5, which was one set of relay contacts and S_7 and S_8 which were controlled by the position of the recorder pen. These latter two switches were adjusted so that S_7 was open when the pen was above a certain point on the scale and S_8 was open when the pen was below a certain point on the scale. At the intermediate positions both switches were closed. Switch S_9 was of the momentary close, push button type. It would effectively bypass all the other switches in the circuit of the relay coil.

In operation, S_9 was closed for a short period of time. This closed the circuit for the cell current through S_5 as well as the contacts of the latching switch S_6. In the meantime the pen of the recorder shifted to some position between the two previously set extremes and closed both S_6 and S_7. This provided an alternate path for power to the coil of R_2. This alternate path kept R_2 actuated even when S_9 was released. R_2 remained actuated until either S_6 or S_7 was opened by the recorder pen. This type of operation was adopted to permit automatic recording of data over long time periods without possible damage to the equipment if the cell voltage should drop to zero (S_8 opened) or the IR drop reach a high value (S_7 opened).

4.1.2 ELECTROLYTIC CELLS

A wide variety of cells for cathode or complete cell testing were constructed. The type of cell used was dictated by the design and purpose of the experiment as well as the components to be used.

A schematic diagram of the first cell, designated cell A, used in the experiments is shown in Figure 7. All of the glass parts were Pyrex. The cell container was a test tube 300 by 38 mm in outside diameter. Within the cell and under a dry, oxygen-free, argon atmosphere, a LiCl-KCl eutectic mixture and the cathode depolarizer to be tested were compartmented by two small tubes with fritted glass bottoms which acted as

INERT
GAS

INERT GAS BLANKET

THERMOCOUPLE

AUXILIARY
ELECTRODE

REFERENCE ELECTRODE

INDICATOR ELECTRODE

LiCl-KCl
EUTECTIC
MIXTURE

CATHODE DEPOLARIZER

GLASS FRIT

GLASS FRIT
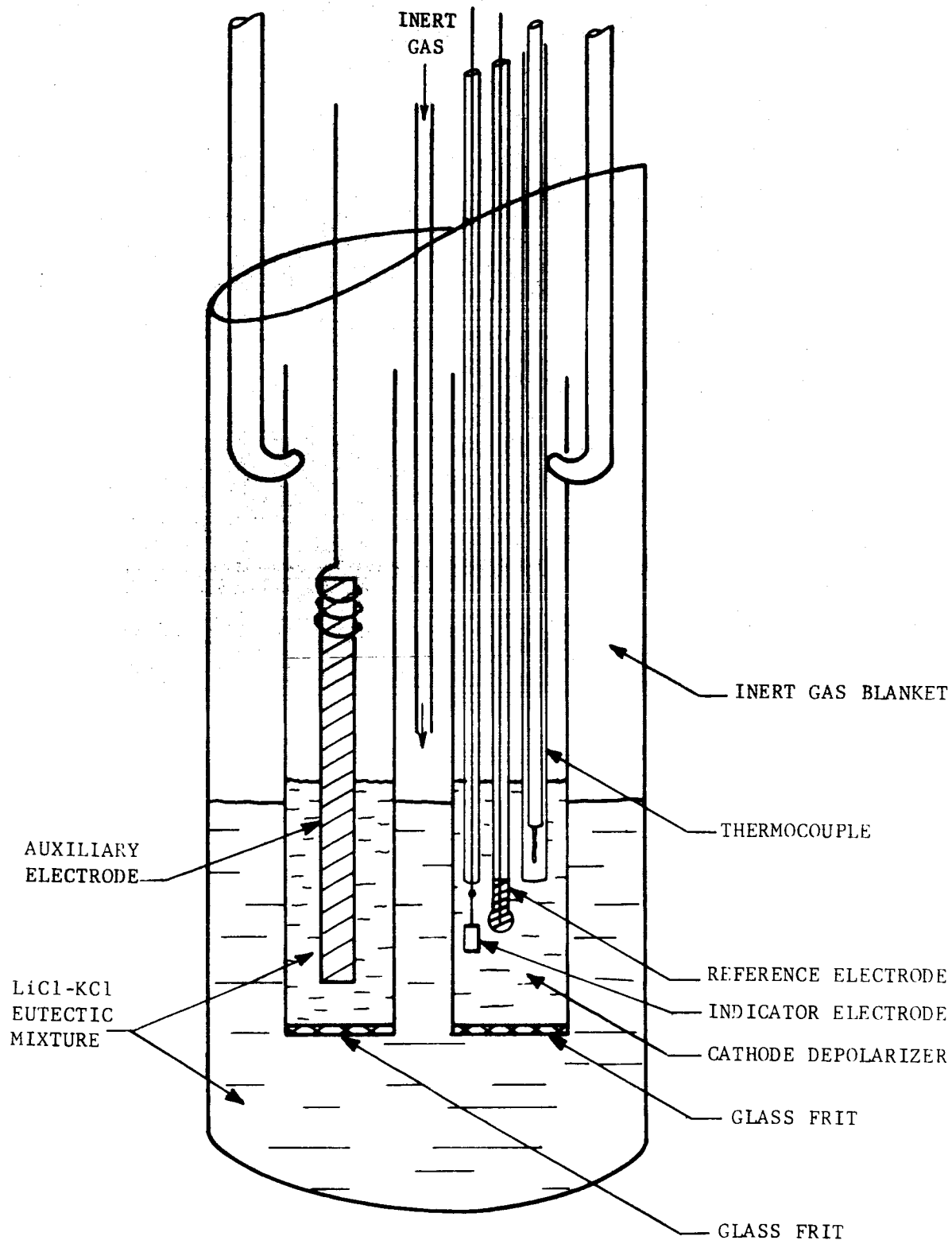
R08712

FIGURE 7.   ELECTROLYTIC CELL A

-38-

salt bridges.

A spectrographically pure graphite rod in one tube was used as the auxiliary electrode. The indicator electrode was a foil, a wire, or a rod of the electrode material under test. The indicator electrode, the reference electrode, and the thermocouple were placed in the tube containing the cathode material.

Substantial diffusion of the eutectic mixture into the cathode material compartment was the probable cause of the steady drifts of cathode potentials repeatedly observed using this experimental setup. The cell could not be used for the testing of volatile cathode materials.

In cell B, components were contained within a Pyrex H-shaped apparatus (Figure 8). The auxiliary electrode was compartmented from the rest of the cell using a Pyrex tube with a fritted glass bottom which was inserted in one arm of the cell. The other arm contained the indicator electrode, the reference electrode, and a thermocouple.

The auxiliary electrode compartment contained a small amount of LiCl-KCl eutectic. The main compartment contained the cathode material to be tested. The diffusion of the eutectic mixture into the catholyte was slow. However, the setup was found unsuitable for testing volatile cathode depolarizers such as bismuth trichloride.

In cell C, shown in Figure 9, the cathode material was contained in a Pyrex tube 260 by 12.7 mm in inside diameter. The indicator electrode was a gold wire 0.63 mm in diameter projecting 16.7 mm from the closed end of a Pyrex tuve 270 by 3.2 mm in outside diameter. The total projected area of the gold electrode was 1/3 cm^2.

The auxiliary electrode was a spectrographic graphite rod 3.2 mm in diameter and 30 cm long. The density of the material was 1.9 g/cm^3. The rod was inserted in a Pyrex tubing 290 by 6 mm in outside diameter closed at the lower end and provided with side openings cut near the closed end with a diamond wheel. The reference electrode was identical in design with
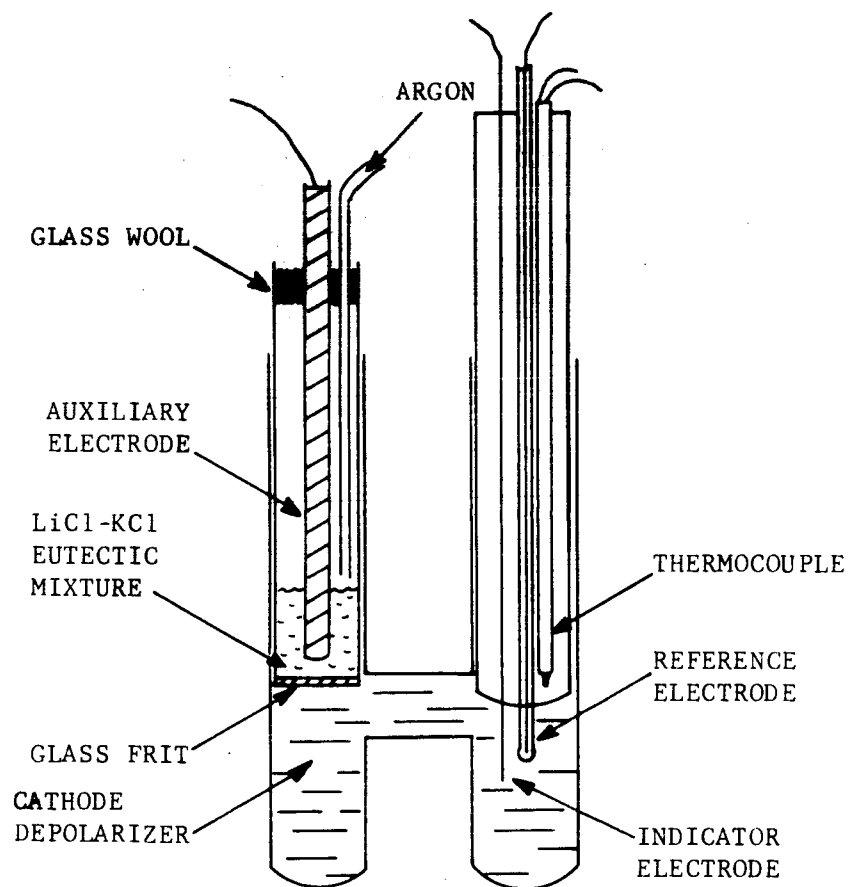
FIGURE 8.   ELECTROLYTIC CELL B

-40-

GRAPHITE
AUXILARY
ELECTRODE

CELL CONTAINER

THERMOCOUPLE

INDICATOR ELECTRODE

REFERENCE
ELECTRODE

ELECTRODE SHEATH
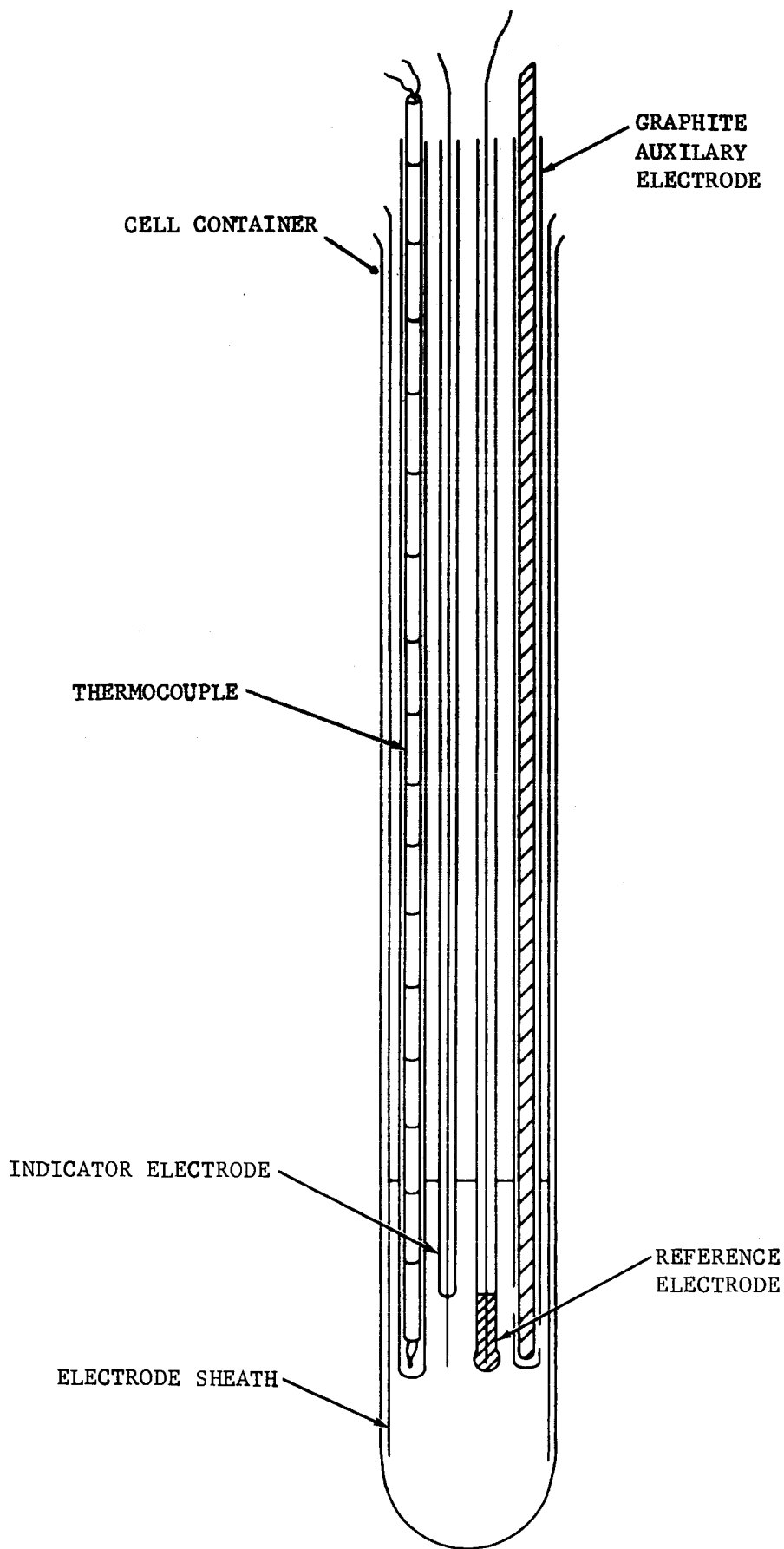
FIGURE 9.   ELECTROLYTIC CELL C.

that described below in Section 4.1.3.

The thermocouple was of the ISA Type K (chromel-alumel junction). The wires, 0.32 mm in diameter, were inserted in short sections of two holes, round section refractory insulator 2.4 mm in diameter. The thermocouple sheath was made of Pyrex tubing 280 by 4.2 mm in outside diameter.

The electrodes and the thermocouple were fitted snugly in a Pyrex tubing 270 by 12.7 mm in outside diameter. The electrode assembly could be inserted with little friction in the cell container. This cell was found satisfactory for experiments with volatile electrolytes.

For cathode studies in which sodium ions were coulometrically added during the test, cell D shown in Figure 10 was used. The cell container was a Pyrex tube 240 mm by 30 mm in outside diameter. Within the cell the cathode depolarizer was compartmented with a ceramic tube 170 mm long, 10.5 mm in outside diameter and 9 mm in inside diameter. The ceramic material was prepared as described by Labrie.[13] This material is discussed in Section 5.1.1.

The indicator electrode was a wire of the material tested 0.63 mm in diameter projecting 16.7 mm from the closed lower end of a Pyrex tube 250 by 3.2 mm in diameter. The projected area of the electrode was 1/3 cm^2.

The auxiliary electrode was a spectrographically pure graphite rod 0.63 cm in diameter and 30 cm long projecting from the neds of a Pyrex sheath by about 2 cm. The density of the graphite was 1.9 g/cm^3.

The Ag - 0.13m AgCl reference electrode was as described in Section 4.1.3.

The indicator electrode and the reference electrode were inserted in the ceramic tube containing the cathode depolarizer. The auxiliary electrode and a thermocouple of the ISA Type K (chromel-alumel junction) were placed in the outside compartment containing a molten binary salt mixture.

The cell was found very satisfactory for the study of the effect of diluents such as sodium ions which were coulometrically added to the cathode depolarizer by ionic conduction through the ceramic.

INERT
GAS

GLASS WOOL

INERT GAS BLANKET

CERAMIC TUBE

AUXILIARY
ELECTRODE

REFERENCE ELECTRODE

CATHODE DEPOLARIZER

THERMOCOUPLE

ANOLYTE

INDICATING ELECTRODE
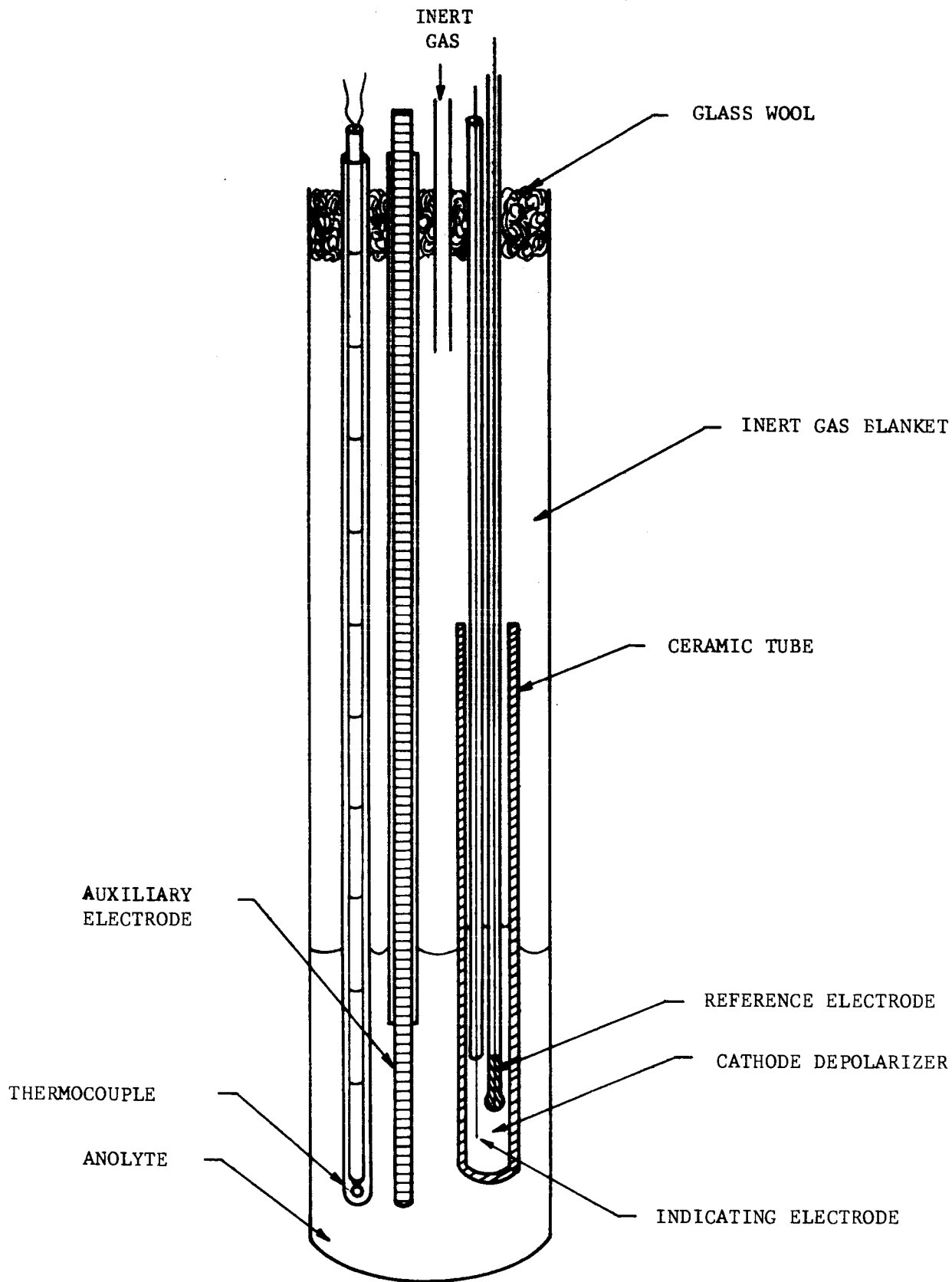
R10255

FIGURE 10.   ELECTROLYTIC CELL D

Additional experimental arrangements used for cell discharges and resistivity measurements are described in Section 6.

4.1.3 REFERENCE ELECTRODE

The reference electroce system may be represented as follows:

$$\text{Ag} \Big/ \begin{array}{c} \text{AgCl} \ (0.13\underline{m}) \\ \text{KCl-LiCl} \ (55\text{-}45 \ \text{W/W}) \end{array} \Big/\!\!\Big/ \text{glass} \tag{8}$$
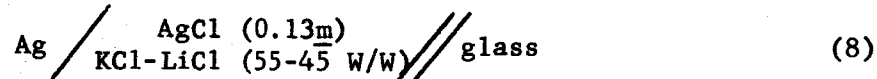
The half cell was constructed from 3.2 mm outside diameter Pyrex tubing about 300 mm long, closed, and slightly blown at one end to reduce the wall thickness. The tube was heated to 130°C, vented with dry inert gas, then placed in a dry-box where a few milligrams of the premixed powder of AgCl and KCl-LiCl eutectic mixture was dropped to the bottom of the tube and the silver wire was inserted.

Potentials given in this report are usually with respect to a reference electrcde which is $1\underline{m}$ in AgCl. To convert the measured potentials to the $1\underline{m}$ reference, 0.127 volts was subtracted from the measured potentials. For comparison a Pt-$1\underline{m}$ Pt(II) electrode has a potential of +0.727 volts vs. the Ag-$1\underline{m}$ AgCl electrode.

This electrode could not be used in the study of ferric chloride which melts and boils at temperatures below the melting point of the solvent in the Ag-AgCl reference electrode. However, the potential of the Au-FeCl$_3$ system at 290°C could be obtained indirectly with respect to Ag-AgCl electrode as follows:

The voltage of the system

$$\text{Au} \Big/ \text{FeCl}_3 \Big/\!\!\Big/ \text{glass} \Big/\!\!\Big/ \text{BiCl}_3 \Big/ \text{Au} \tag{9}$$
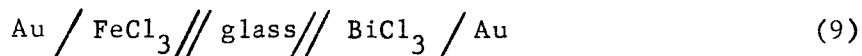
was measured at 290°C. The voltage of the system

$$\text{Au} \Big/ \text{BiCl}_3 \Big/\!\!\Big/ \text{glass} \Big/\!\!\Big/ \begin{array}{c} \text{AgCl}(0.13\underline{m}) \\ \text{KCl-LiCl} \ (55\text{-}45 \ \text{W/W}) \end{array} \Big/ \text{Ag} \tag{10}$$
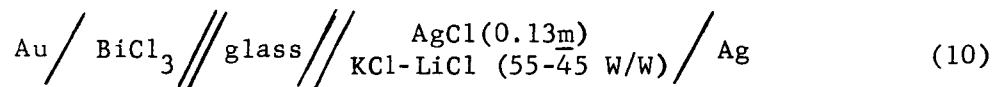
was determined at a temperature range between 330° and $390^\circ C$.* A linear voltage-temperature relationship was observed in this range. Thus, assuming the linearity extending to $290^\circ C$, the voltage at the latter temperature was obtained by graphical extrapolation of the straight line. The potential of the $Au-FeCl_3$ half-cell with respect to Ag-AgCl reference electrode at $290^\circ C$ can then be obtained by adding algebraically the voltages of the two systems.

4.1.4 CHEMICALS

The following chemicals were obtained as the commercially available anhydrous materials. They were vacuum desiccated and kept in a dry box before use.

a. **Cathode Depolarizers**

Cupric chloride, from Baker & Adamson; purity 99.0%.

Cuprous chloride, from J. T. Baker; purity 92.5% (polarographic analysis showed the presence of approximately 7% $CuCl_2$.)

Bismuth trichloride, from J. T. Baker; purity 99.7%.

Silver chloride, from J. T. Baker; purity 99.0%.

Ferric chloride, sublimed powder from Matheson, Coleman and Bell.

Potassium chromate, from J. T. Baker; purity 99.6%.

Potassium dichromate, from Mallinckrodt Chemical Works; purity 99.5%.

Vanadium pentoxide, from J. T. Baker; purity 100.0%.

b. **Cathode "Diluents"**

Calcium chloride, from J. T. Baker; purity 96.6%.

Bismuth metal, from J. T. Baker; purity 100.0%.

c. **Solvent**

The eutectic mixture of 45 weight percent lithium chloride/55 weight percent potassium chloride was used as the solvent for potassium chromate

---

* Although the lower limit of the temperature range investigated was below the melting point of the solvent in the reference electrode, the recording of the potential remained steady and no break in the linearity of the temperature-potential relationship was observed.

and as an anolyte. Chlorine was used to remove water from the LiCl-KCl
eutectic.[15]

4.1.5 PROCEDURE

The evaluation of cathode materials was performed by measuring the open
circuit potential and the polarized potentials at current densities of
0.015 amp/cm^2 and 0.150 amp/cm^2 of cathode area as a function of time. The
potentials were measured using an Ag-0.13$\underline{m}$ AgCl in LiCl-KCl electrode as
described in Section 4.1.3.

Certain cathodes were also tested in the presence of diluents. These
diluents were the oxidation products of the anode. Initially calcium was
the proposed anode. In these cases the diluent was added as $CaCl_2$. When
lithium was the proposed anode, LiCl was added as the diluent. Attempts to
coulometrically add Li^+ by electrolytic transfer across a ceramic membrane
were unsuccessful. However, Na^+ could be added in this manner.

4.2 RESULTS

4.2.1 BISMUTH (III)

The experimental results for bismuth trichloride as the pure molten salt
and mixed with calcium chloride are summarized in Figure 11. The
potential scale given in this figure is with respect to an Ag-0.13$\underline{m}$ AgCl
electrode which was used as a working reference electrode. To convert
these potentials to the Ag-1$\underline{m}$ AgCl scale, 0.127 volt must be subtracted
from those values given in the figure.

Pure molten $BiCl_3$ at 380°C gave an initial open circuit potential of +0.84
volt (vs. Ag-1$\underline{m}$ AgCl) on a gold electrode. After the initial current
passage, the open circuit potential was found to be +0.78 volt. Significant
changes in the initial open circuit potentials were observed with many of
the systems studied. This change could be explained by recognizing that
before the initial current drain there was no reduced form of the cathode
depolarizer present in the system. Consequently, the potential determining
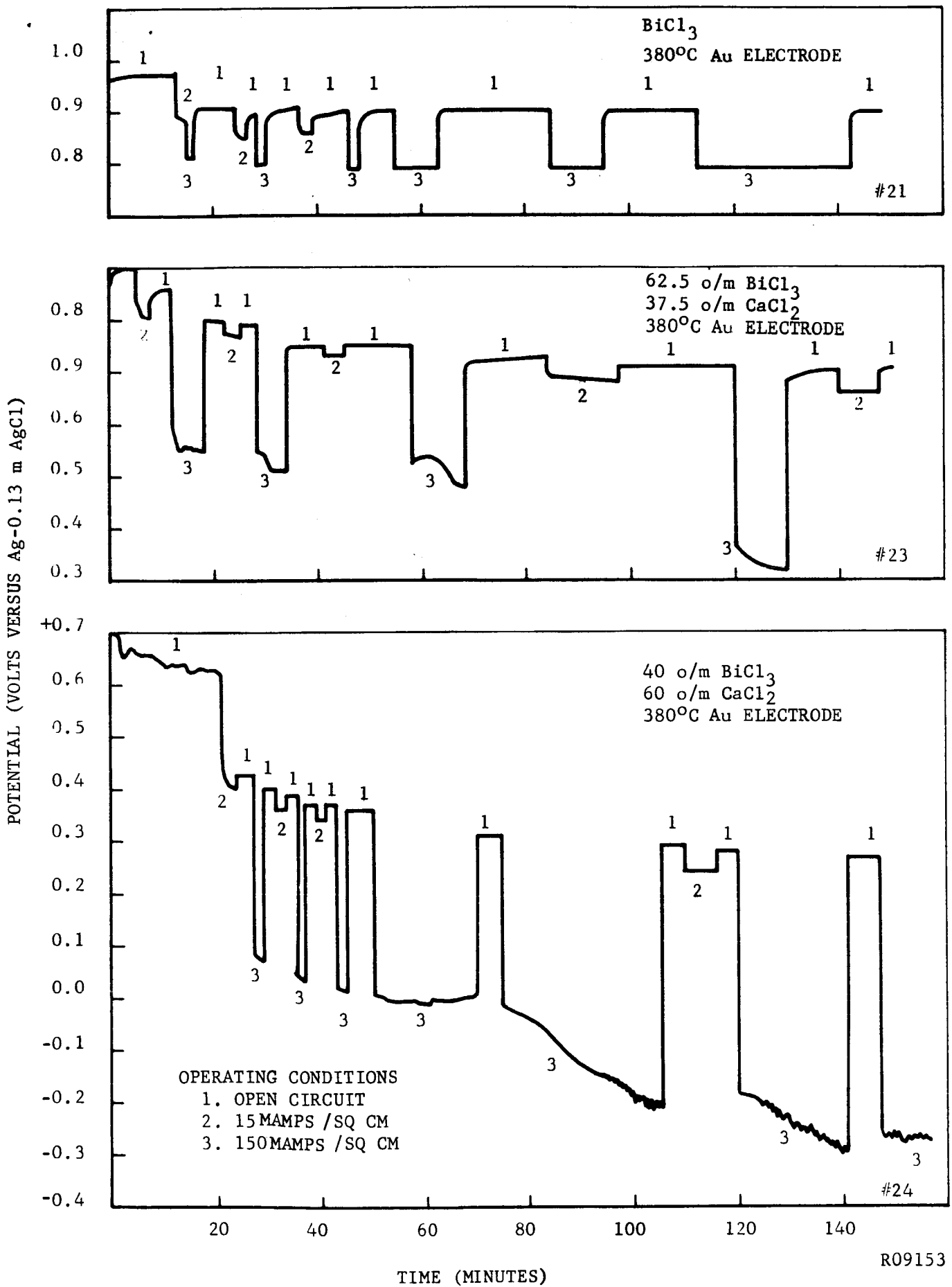
FIGURE 11. $BiCl_3$ REDUCTION. EFFECT OF DILUENTS

R09153

-47-

couple was very poorly defined and the system was not well poised. Upon current drain, the reduced form of the cathode depolarizer was present and the potential of the system became stabilized. In the pure molten $BiCl_3$ system, the average polarizations were about 45 and 110 millivolts at current densities of 0.015 and 0.150 amps/sq cm, respectively. The manner in which the potential changed when the current drain changed and the experimental setup suggested that a considerable portion of the observed polarization was due to IR drop in the electrolyte between the indicator and reference electrodes.

Figure 11 also shows the effect of various concentrations of calcium chloride "diluent" upon the performance of the $BiCl_3$ system. Compositions are given in mole percent. In addition to larger IR drops, considerable polarization was apparent, particularly at 0.150 amps/sq cm. These observations can be partially explained by the insolubility of $CaCl_2$ in molten $BiCl_3$ at these temperatures. Although a complete phase diagram for the $BiCl_3$-$CaCl_2$ system was not available, the phase diagram for $AgCl$-$CaCl_2$ and $CuCl$-$CaCl_2$ (Figure 12) would suggest that only about 15 to 20 mole percent of $CaCl_2$ would be soluble.

The phase diagram for the Bi-$BiCl_3$ system (Figure 12) shows that the reduction product of $BiCl_3$ at these temperatures would be expected to form a single liquid phase with $BiCl_3$ until approximately one-third of the $BiCl_3$ was reduced. This single liquid phase was probably a solution of $BiCl$ in $BiCl_3$. The $BiCl$ was either formed directly by the two electron reduction of $BiCl_3$:

$$BiCl_3 + 2e \longrightarrow BiCl + 2Cl^- \tag{11}$$
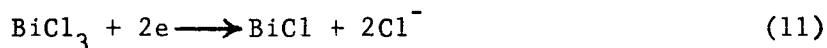
or by a three electron reduction of $BiCl_3$

$$BiCl_3 + 3e \longrightarrow Bi + 3Cl^- \tag{12}$$

followed by reaction of the Bi with excess $BiCl_3$

$$2Bi + BiCl_3 \longrightarrow 3BiCl \tag{13}$$

Bi-BiCl₃
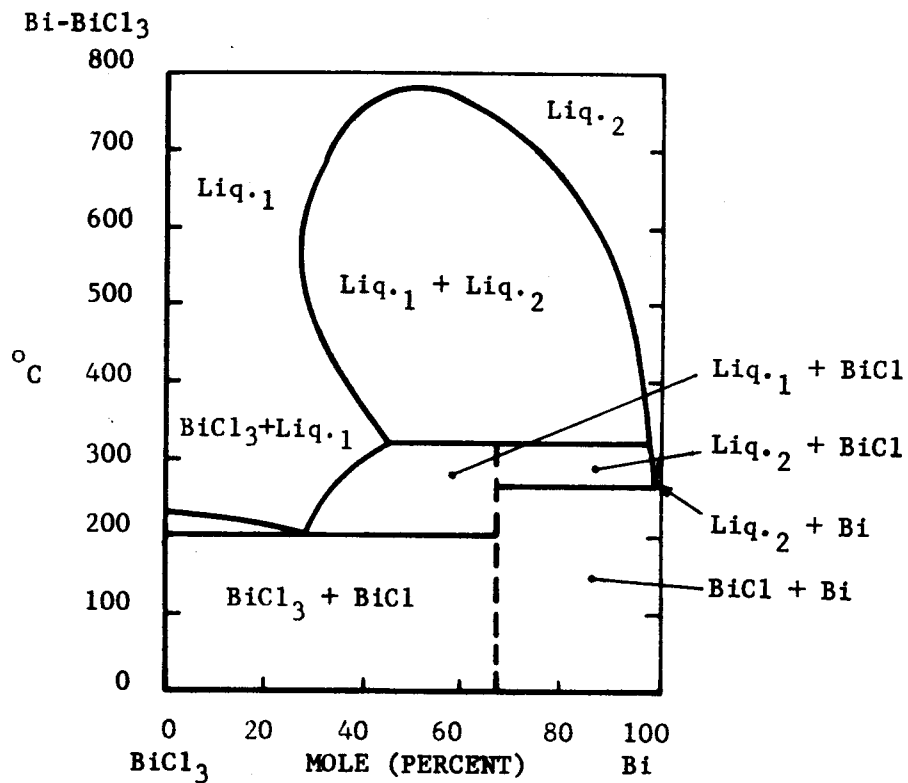
S. J. Yosim, A. J. Darnell, W. G. Gehman
and S. W. Mayer, J. Phys. Chem., 63, 231 (1959).

CuCl-CaCl₂
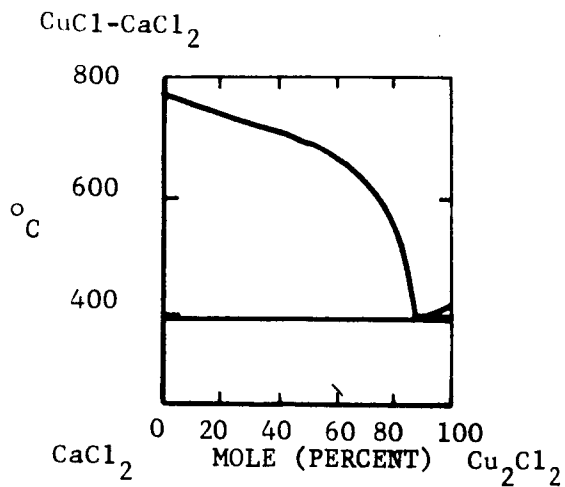
Otto Menge, Z. anorg. Chem., 72,
209 (1911).

AgCl-CaCl₂
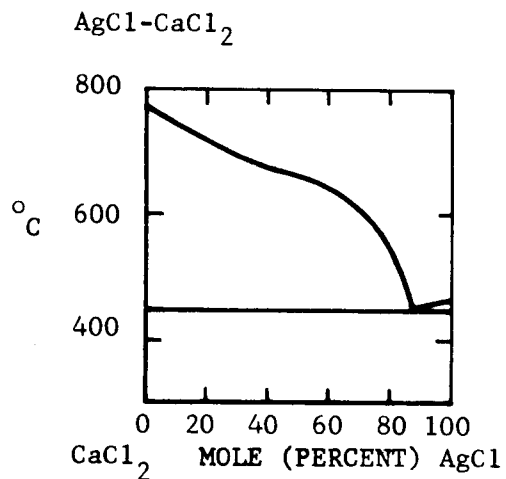
Otto Menge, Z. anorg. Chem., 72,
204 (1911).

RO9155

FIGURE 12.   PHASE DIAGRAM[51]

Regardless of the manner in which the reaction occurred, the formation of a soluble reduction product would be expected to affect the potential of the system (Nernst equation). Figure 13 shows the effect of both $CaCl_2$ and Bi metal upon the $BiCl_3$ system with W and Au electrodes. The compositions were chosen on the basis of the following assumptions:

(1) An initial three-fold excess of $BiCl_3$

(2) A three electron reduction for $BiCl_3$

(3) Metallic Bi and $CaCl_2$ appear in equivalent amounts

The results can also be summarized as follows:

Depolarizing Solution	Tempera- ture (^{o}C)	Electrode Material	Open Circuit Potential	Polarization at 0.015 amp/cm^2	0.150 amp/cm^2
$BiCl_3$	425	Tungsten	+ 0.92 V	0.03 V	0.1 V
$BiCl_3$ 2 equiv.		Tungsten	+ 0.40 V	0.01 V	0.1 V
$CaCl_2$ 1 equiv.	425				
Bi 1 equiv.		Gold	+ 0.46 V	0.015 V	0.1 V

Examination of the gold electrodes after tests showed extensive degradation of the gold. Gold and metallic Bi are known to form liquid alloys at these temperatures.[59] It is possible that the stability of the liquid Au-Bi alloy would promote the reaction

$$BiCl + Au \longrightarrow Bi + AuCl \tag{14}$$

and produce the metallic Bi necessary for alloy formation. Thus, it appeared that the poorer performance of these systems was due to a degradation of the gold electrode by alloy formation with a corresponding increase in current density.

No degradation was noted with a tungsten electrode even at 425°C (Figure 13). Polarization was slight and appeared to be essentially of a resistive nature. The shift of the electrode potential in the negative direction when Bi was added to the system was quite apparent. (Compare Figures 11 and 13.)
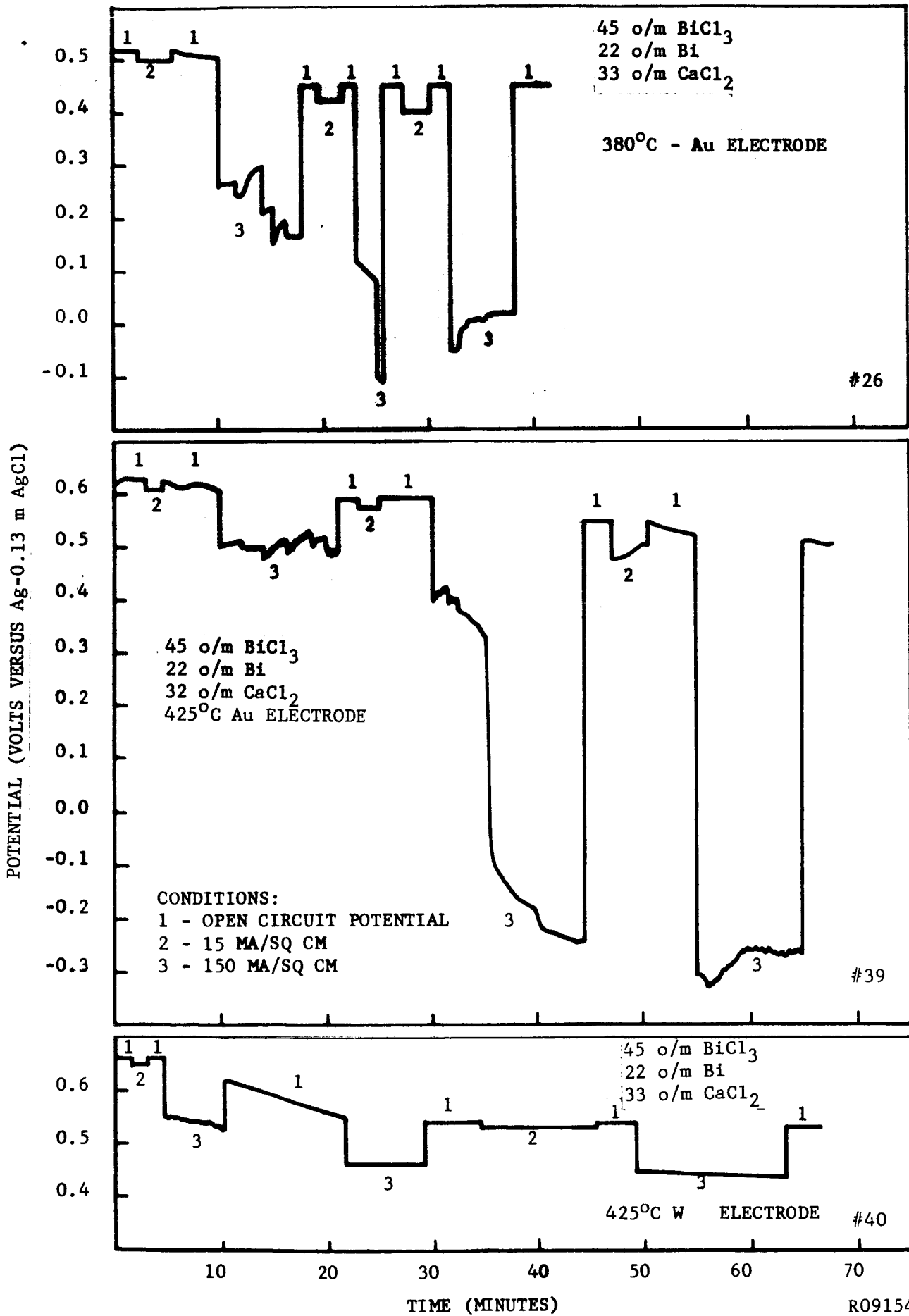
FIGURE 13. $BiCl_3$ REDUCTION. EFFECT OF DILUENT, TEMPERATURE, AND ELECTRODE

-51-

With all cells containing $CaCl_2$, some solid material was present at the operating temperature. This solid material was probably undissolved $CaCl_2$. With the ternary system ($BiCl_3$-Bi-$CaCl_2$), solid material was observed at temperatures as high as $640°C$. Upon cooling of these mixtures, more solid material was formed and at $182°C$ an inflection appeared in the cooling curve and the mixture became completely solid.

Two experiments were performed with Graphite/$AlCl_3$·NaCl/Ceramic//$BiCl_3$ cells using Cell D shown in Figure 10. At the time of these tests, sodium was the proposed anode. Thus the effect of Na^+ on the reduction of $BiCl_3$ was desired. Since Na^+ can be transferred across the ceramic, NaCl was used in the anode compartment. To reduce the melting point of the system, $AlCl_3$ was also added. The cells were operated at a temperature of $380°C$. Based on a 2-electron reduction to BiCl and cycling current densities of 0.150 amp/cm^2 of cathode area for 6 minutes and 0.015 amp/cm^2 for 54 minutes every hour for 72 hours, an amount of $BiCl_3$ 50% in excess of the theoretical amount was used. The first test was concluded after 72 hours while the second test was allowed to continue until substantial polarization and instability in the system was noted. This occurred after 115 hours. Figures 14 and 15 show the results of these tests. The relatively high potential differences between low and high current drains shown in Figure 14 were caused by a large IR drop between the indicator electrode and the reference electrode which had been inadvertently placed too far from the cathode. This difficulty was corrected in the test indicated in Figure 15. It appeared from the performance of the second cell that directly or indirectly, a 3-electron reduction of Bi^{+++} to $Bi°$ had occurred. This was substantiated by the presence of bismuth metal in the cathode compartment of the cell at the conclusion of the experiment. Had a two electron reduction occurred, all of the $BiCl_3$ would have been consumed in 108 hours. In the test, instability in the system was noted only after 115 hours. Based on a 2-electron reduction of $BiCl_3$ to BiCl, the utilization efficiency of 115 hours was 106%. Based on a 3-electron reduction, the efficiency was 71%.
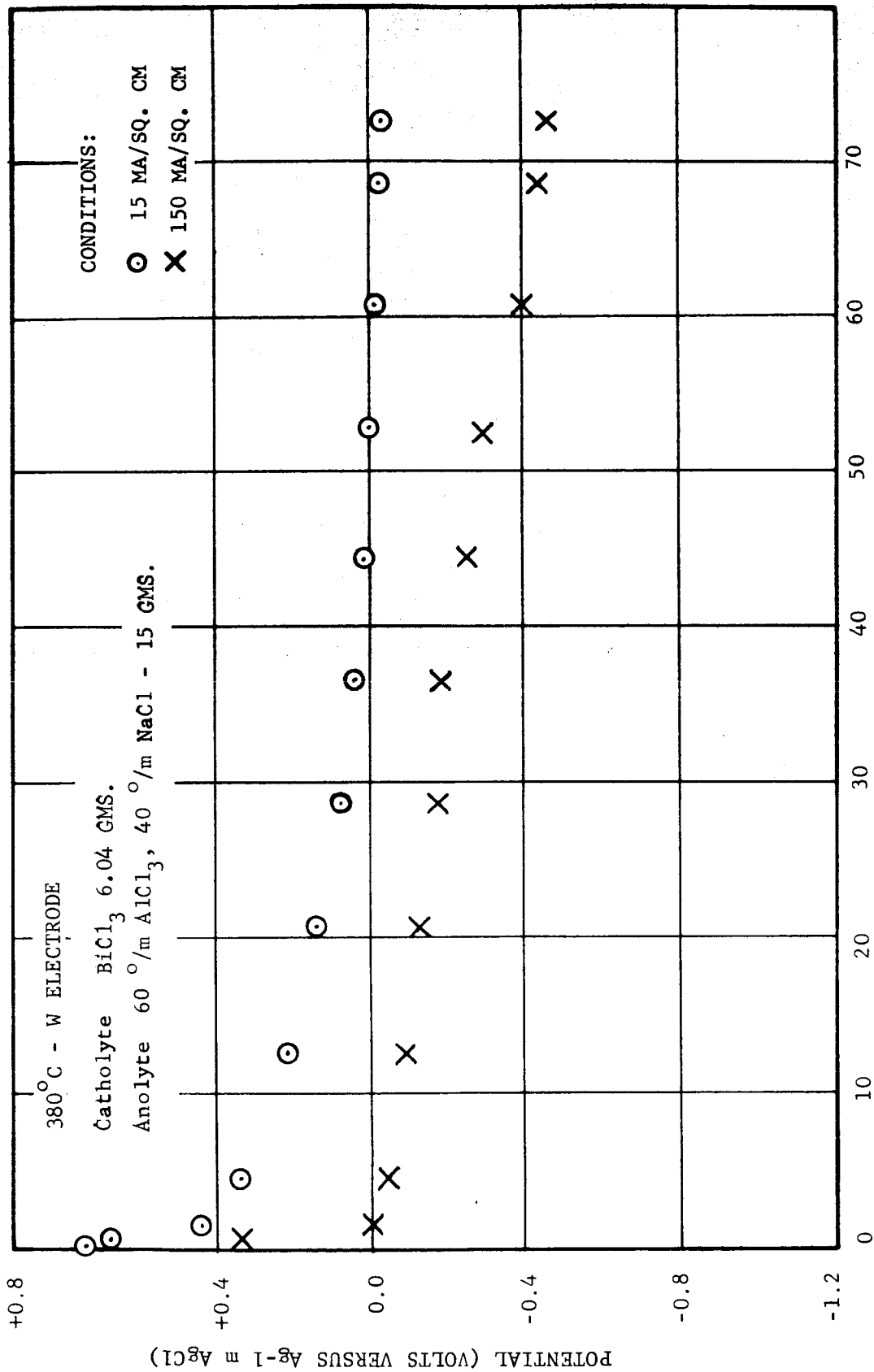
FIGURE 14. $BiCl_3$ REDUCTION EFFECT OF DILUENT-COULOMETRIC ADDITION OF Na^+. 72 HOUR TEST

R10259

-53-
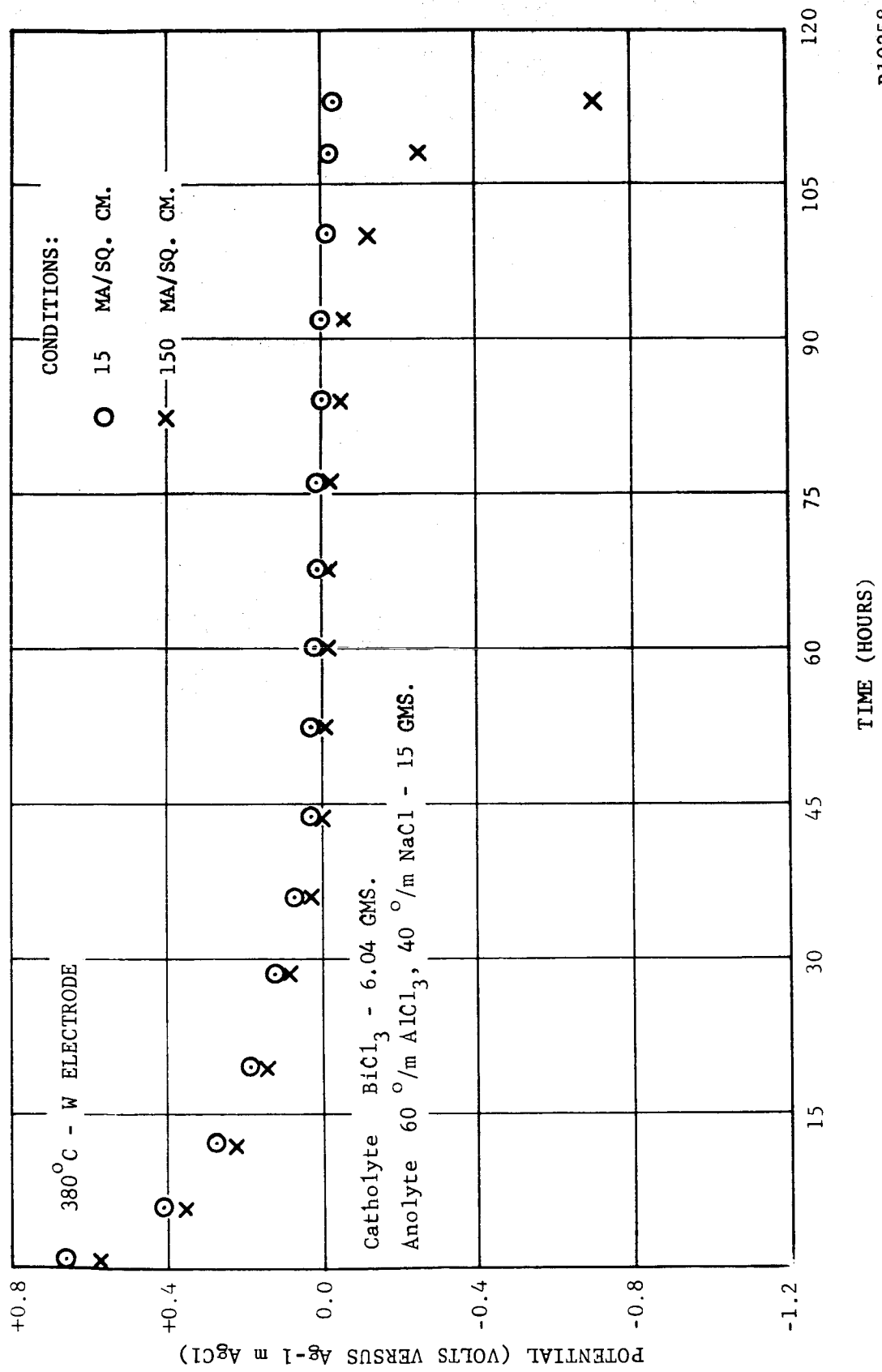
FIGURE 15. BiCl₃ REDUCTION. EFFECT OF DILUENT-COULOMETRIC ADDITION OF Na⁺. 115 HOUR TEST

No attempts were made to analyze for bismuth in the anolyte. It was expected that such an analysis would be negative for the following reasons: (1) the porcelain membranes in themselves were essentially nonporous,[52] (2) no cracks were found in the membrane after the tests, (3) this porcelain does not undergo ion exchange with multivalent ion,[14] and (4) the electrolytic movement of cations would be from the anode compartment to the cathode compartment. In addition to electrochemical testing, the compatibility of molten $BiCl_3$ with materials of the proposed cell was determined. The procedure for these tests was the same as given in Section 3.2. Bismuth trichloride was tested with sodium zeolites Type A, X, and Y, Al_2O_3, Armco iron, and nickel. No apparent reaction was noted with the zeolites or the Al_2O_3. A reaction was noted with the iron and nickel. $BiCl_3$ was a strong oxidizing agent and reacted according to the reactions

$$2Bi^{3+} + 3 \text{ Ni} \longrightarrow 2 \text{ Bi} + 3 \text{ Ni}^{2+} \tag{15}$$

$$2 \text{ Bi}^{3+} + 3 \text{ Fe} \longrightarrow 2 \text{ Bi} + 3Fe^{2+} \tag{16}$$
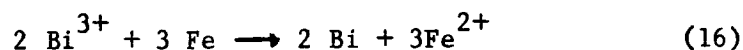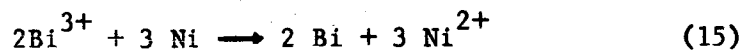
The resulting metallic Bi was very soluble in molten $BiCl_3$. The phase diagram for the $BiCl_3$-Bi system (Figure 12) showed that at these temperatures the solubility of Bi in $BiCl_3$ was about 30 mole per cent. Thus, the Bi plated on the Ni or Fe immediately dissolved in $BiCl_3$ and thus left a fresh surface of Ni or Fe for further reaction. Even when the solution became saturated with BiCl and metallic Bi remained, the presence of a liquid metal in the cathode compartment could lead to electrical shorting. It was this reaction of $BiCl_3$ with Ni and Fe which eliminated this material as a suitable cathode for this application. Since W could not be fabricated into flexible containers, it was not further considered as a suitable cathode collector. A flexible container was necessary to accommodate the volume changes which occur during cell discharge. (See Section 7.1.)

4.2.2 CHROMIUM (VI)

Pure molten potassium dichromate and a 6.65 mole percent solution of potassium chromate in LiCl-KCl eutectic mixture gave open circuit potentials of +0.76 volt and +0.42 volt, respectively, on gold at $450^{\circ}C$. Under current drain, the polarization increased rapidly to negative potential values. Potential-time curves for these systems at low current densities are shown in Figure 16 and 17. The extensive polarization is quite apparent. A dark green deposit was found on the electrodes in both experiments. A portion of the polarization appeared to be due to the very high resistance of this film.

Chromium trioxide, CrO_3, was unsuitable as a cathode in the presence of LiCl-KCl. A volatile reaction product, tentatively identified as chromyl chloride, CrO_2Cl_2, was formed.

4.2.3 COPPER (I)

The interpretation of test results with cuprous chloride half cell was complicated by two factors

(1) Cuprous chloride, even the so-called reagent grades, contained 5-10% of $CuCl_2$ as an impurity.

(2) In tests under current drain, cupric ions were formed by the electrochemical reaction in the anode section of the cell.

The presence of Cu(II) in the cell could give rise to potential due to the Cu(II)-Cu(I) system rather than the desired Cu(I)-Cu(O) system. This effect was seen in the variation of open circuit potentials with electrode material and in pronounced potential shifts of half cells under current drain.

The open circuit potential of molten CuCl at 450° was +1.10 and +1.15 volts on gold and tungsten electrodes, respectively. On copper electrodes the potential was +0.51 volts. The difference was attributed to the reaction

$$Cu(II) + Cu(O) \longrightarrow 2\ Cu(I) \tag{17}$$

-56-
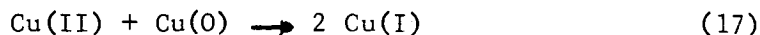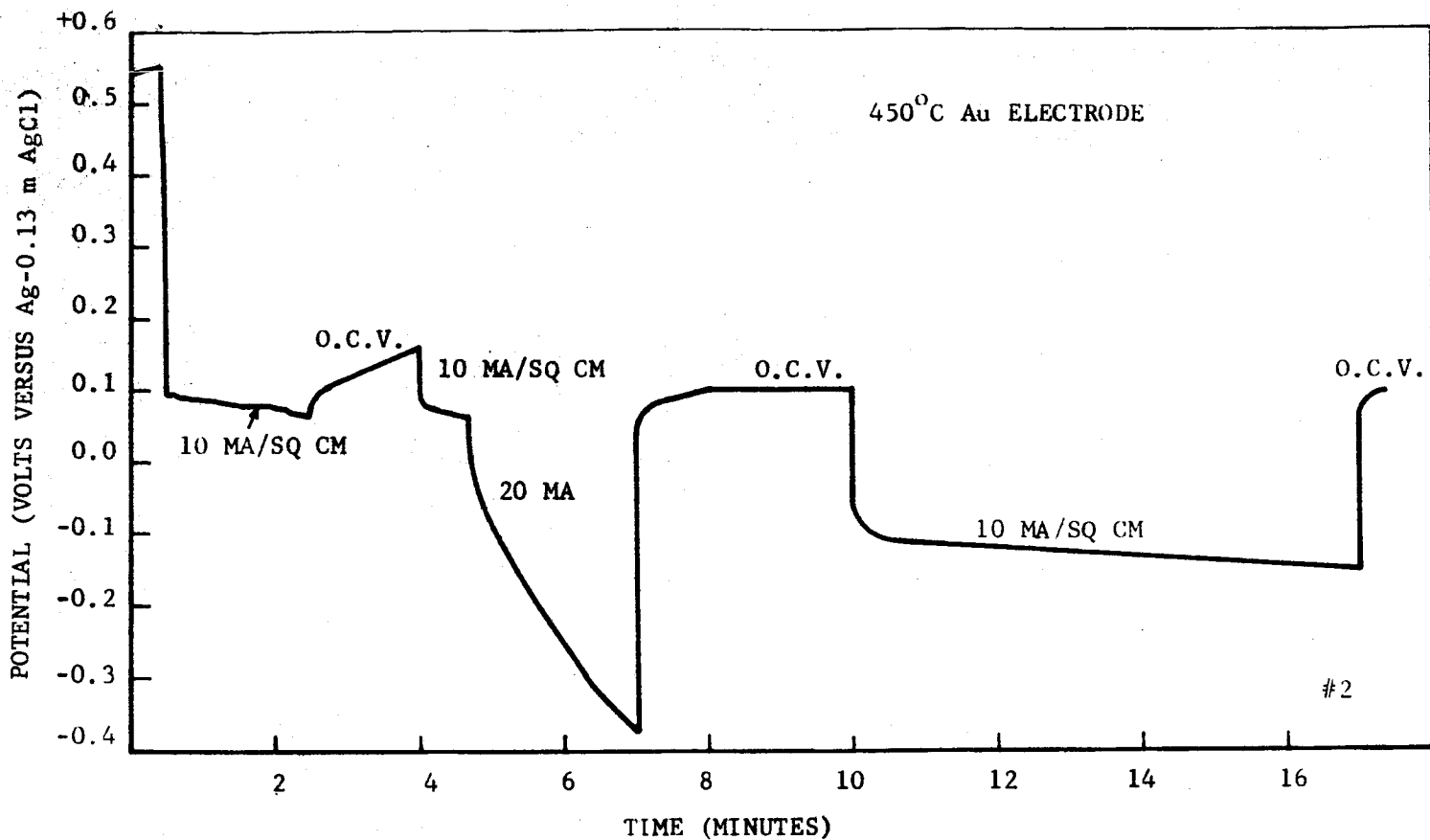
FIGURE 16. REDUCTION OF 6.65 MOLE PERCENT $K_2Cr_2O_7$ IN LiCl-KCl
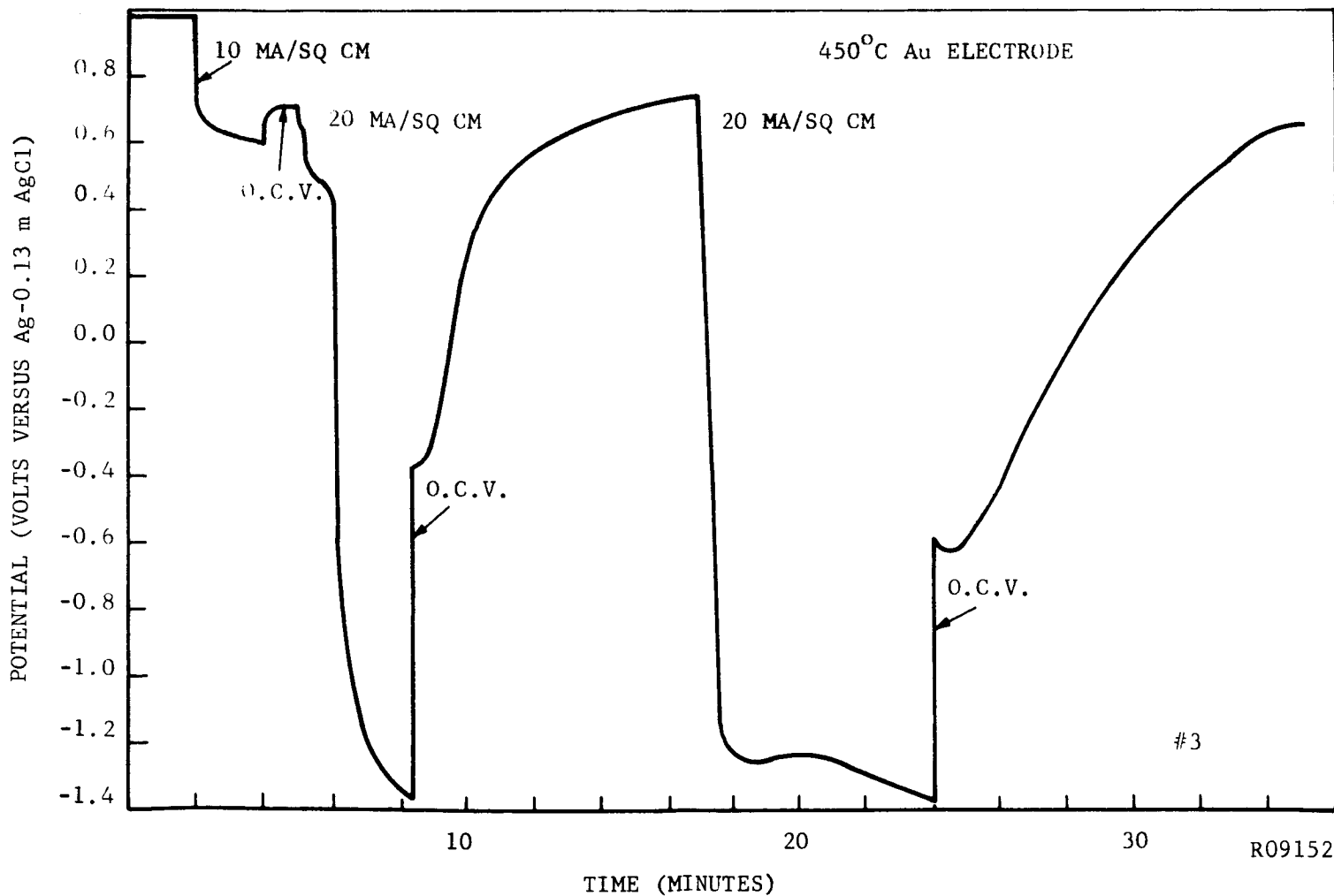
FIGURE 17. REDUCTION OF MOLTEN $K_2Cr_2O_7$

-57-

on the copper electrode which materially reduced the Cu(II) concentration in the vicinity of the electrode. No such reaction occurred with the tungsten or gold electrodes. The shift of the electrode potential with the cathodic reduction of the Cu(II) impurity is seen in Figure 18. These results were obtained with a gold electrode. Little polarization other than IR drop was noted. The slight decrease in potential with time was probably due to dilution of the CuCl by molten KCl-LiCl. The electrolysis cell shown in Figure 7 was used to obtain these curves.

The effect of LiCl as a diluent on the performance of the Cu(I) system was measured. A mixture composed of equimolar concentrations of CuCl and LiCl gave the following results on a tungsten electrode:

Temperature	450°C.	500°C.
Initial Open Circuit Potential	+0.37V	+0.37V
Potential at 0.015 amp/cm^2	-	-0.19V
Potential at 0.150 amp/cm^2	-0.15V	-0.21V

In an effort to prevent excessive dilution of the cathode by materials of the anode compartment and to eliminate effect of anodically generated Cu(II), a half cell utilizing a ceramic barrier between the anode and cathode section was constructed. This cell design is shown in Figure 10.

In the initial experiments, a LiCl-KCl eutectic mixture was used in the anode compartment of the cell. The objective of this test was to transfer coulometrically lithium and/or potassium ions through the ceramic to the cathode compartment and evaluate the effect of this diluent on the depolarizing properties of the cathode material. The cathode of the Graphite/ LiCl-KCl/Ceramic/CuCl/W system gave an initial open circuit potential of +1.14 volt at 450°C. The ceramic separator cracked within 10 minutes of
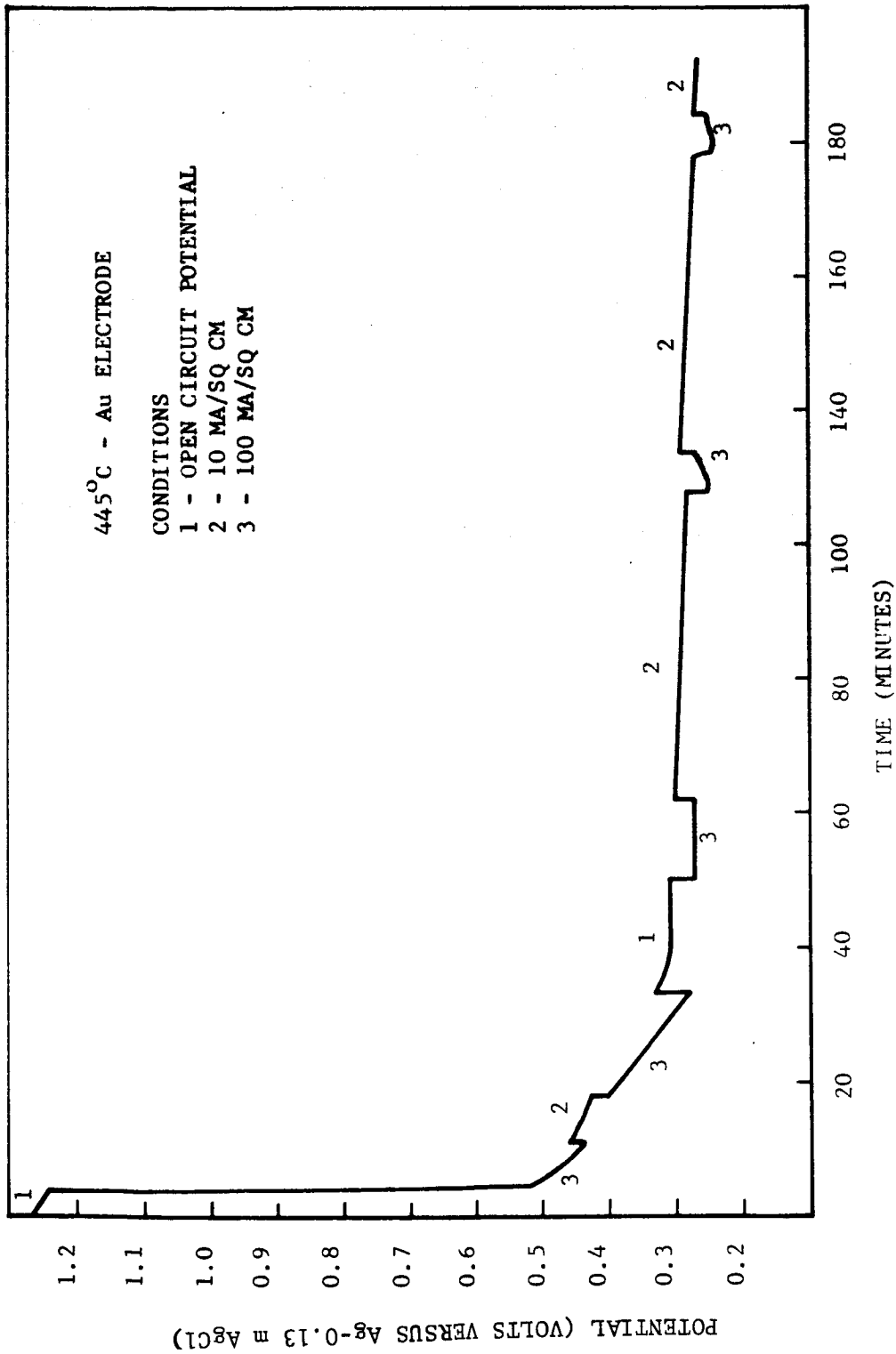
FIGURE 18. CuCl REDUCTION

445°C – Au ELECTRODE

CONDITIONS
1 – OPEN CIRCUIT POTENTIAL
2 – 10 MA/SQ CM
3 – 100 MA/SQ CM

TIME (MINUTES)

POTENTIAL (VOLTS VERSUS Ag-0.13 m AgCl)

the start of the test. Dilution of the cathode depolarizer with the LiCl-KCl eutectic mixture ensued prematurely. To ascertain that the failure of the ceramic tube was caused by ionic stress rather than thermal shock, an identical experimental setup was heated gently to 450°C. and allowed to remain on open circuit for about 1/2 hour before applying any current. A break of the ceramic occurred only after a current of 5 ma for 8 minutes followed by a current drain of 50 ma for about 5 minutes was passed through the cell. Apparently the ceramic was not able to exchange sodium ions with lithium and/or potassium ions at the rates determined by the current used in the experiment.

No apparent physical stress or weakening of the ceramic was observed at the conclusion of a 72 hour test with the same experimental arrangement using molten $AlCl_3$-NaCl as anolyte. The cell was run at 450° in alternate periods of 54 minutes at low current drain (0.015 amp/cm^2 of cathode area) and six minutes at high current drain (0.150 amp/cm^2). The results of the test are shown in Figure 19. It must be noted that the graph shows plottings of a single run and represents sequent potentials at high and low current drains.

Assuming Faraday's Law was obeyed and a coulometric transfer of sodium ions into the cathode compartment of the cell occurred, one-third of the initial amount of CuCl was left in the cathode compartment and the equivalent ratio between the remaining CuCl and NaCl was 1 to 2 at the conclusion of the 72 hour test (67% utilization of the CuCl).

Additional electrochemical experiments with a cuprous chloride cathode were performed with complete cells. These results are described in Sections 6.1 and 6.2.

Compatibility tests were run between cuprous chloride and NaX, NaY, and NaA zeolites, Armco iron, nickel, and Al_2O_3. No reaction was noted with the zeolites. In the tests involving CuCl, a black residue was noted at the
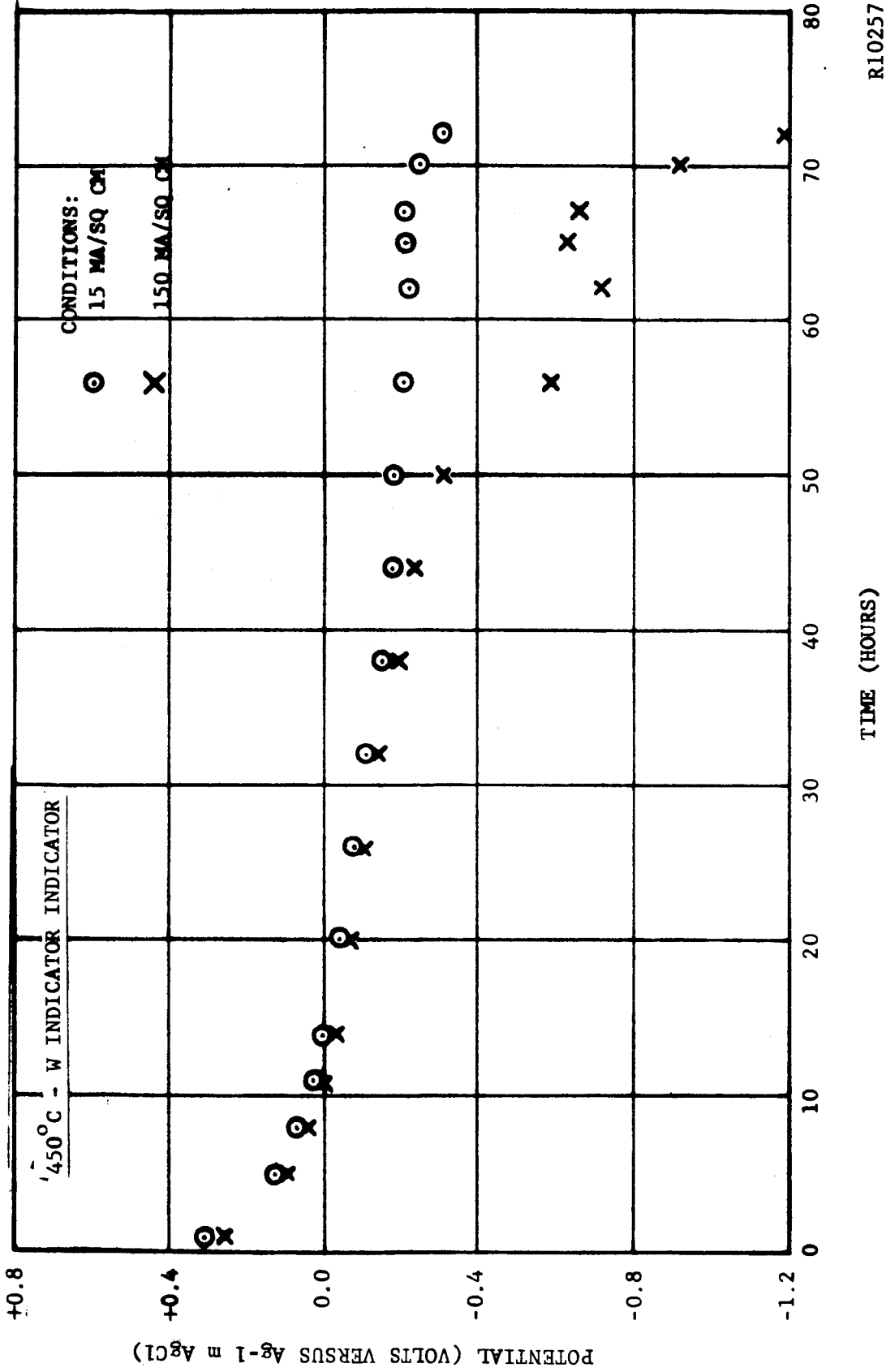
FIGURE 19. CuCl REDUCTION - EFFECT OF COULOMETRIC ADDITION OF Na$^+$
72 HOUR TEST

end of the test period. However, there are reports that CuCl does turn dark in the presence of light. This could be due to a photo-decomposition of CuCl to form finely divided copper,

$$CuCl \longrightarrow Cu + 1/2 \, Cl_2 \qquad (18)$$

similar to the photo-decomposition of AgCl.

Molten CuCl did not react with Ni or Al_2O_3. It did react with Armco iron to form an adherent coating of metallic copper. The reaction was probably

$$2Cu^+ + Fe \longrightarrow 2Cu + Fe^+ \qquad (19)$$
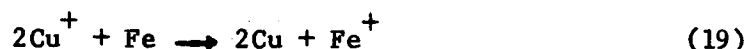
Cu, unlike Bi, has a very low solubility in its salts and a protective layer of metallic copper was formed on the iron surface.

In anticipation of fabrication of prototype cells, the compatibilities of some of the proposed components with CuCl were determined. Samples of pellets of NaX 0.24mm thick bonded with $Na_2Si_2O_5$, Kovar A (composition 29% Ni, 17% Co, 0.3% Mn, bal. Fe) and an Au-Cu brazing alloy (Incoro 60) were sealed in ampoules containing a mixture of CuCl with 10 mole per cent KCl. The addition of KCl was made to lower the melting point of the cathode depolarizer as explained in Section 6.1. After 72 hours at 425°C., the samples were examined. The zeolite pellets were fragile; even before treatment one of the samples cracked. The Kovar sample in contact with CuCl-KCl showed a weight gain of 14% due to a grainy but apparently protective deposit of Cu. No measurements were made upon the sample of brazing alloy in contact with CuCl-KCl since it broke into several small pieces, all of which could not be recovered. No further experiments on the alloy could be completed because of the small amount of sample available.

4.2.4 COPPER (II)

Copper (II) was used as a cathode in two forms cupric chloride and cupric oxide. Molten $CuCl_2$ is a very strong oxidizing agent. It was the strongest oxidizing agent found in this study. No lengthy experiments were carried

out with molten cupric chloride chloride since practically all the electrode materials tested deteriorated within a short time in the melt. Initially using the cell shown in Figure 7, open circuit potentials of +0.88 volt and +1.32 volts were measured on gold and graphite, respectively. It appeared that some dilution of the molten $CuCl_2$ with LiCl-KCl eutectic mixture occurred during these experiments. Using a latter cell design (Figure 9), open circuit potentials were +1.39 volts on gold, +1.45 volts on graphite, and +1.39 volts on tungsten at $525^{\circ}C$. Initially, very little polarization was observed at 0.015 and 0.150 amp/cm^2. No extensive polarization experiments could be conducted because of the deterioration of the electrodes.

The gold electrodes dissolved completely within ten minutes following their immersion in the molten salt. The tungsten electrodes were found satisfactory for tests lasting up to several hours although substantial dissolution of the metal occurred. A spectroscopic graphite rod having a density of 1.90 g/cm^3 was found to have expanded and softened as a result of about one hour immersion in $CuCl_2$ melt.

Gold electrodes were also used in solutions composed of $CuCl_2$ and LiCl-KCl eutectic mixture. The dissolution of gold was not significantly reduced in these solutions in spite of the reduction in electrochemical activity which is shown in Table IX.

Some effort was expended to find a suitable cathode material for use in $CuCl_2$ melt. The selected electrode materials include tantalum, tungsten, pyrolytic graphite, boron carbide and "Glassy Carbon". The results were as follows:

1. A tantalum wire 1.25 mm mils in diameter completely dissolved within 15 hours in the melt at $525^{\circ}C$.

2. A tungsten wire 0.63 mm in diameter partially dissolved under the same conditions.

3. A sample of pyrolytic graphite held in molten $CuCl_2$ at $540^{\circ}C$. for 15 hours expanded in the direction perpendicular to the plane of deposition.

-63-

TABLE IX

CHARACTERISTICS OF $CuCl_2$ CATHODES

Cathode Composition	Temperature (^{o}C)	Electrode Material	Open Circuit Potential vs. Ag-1mAgCl Ref. Electrode	Polarization at	
				0.015 amp/cm^2	0.15^o amp/cm^2
$CuCl_2$	525	Tungsten	+ 1.39V	- -	0.2V
$CuCl_2$	525	Graphite	+ 1.44V	- -	- -
$CuCl_2$	525	Gold	+ 1.39V	- -	0.03V
50 ^{o}/m $CuCl_2$ 50 ^{o}/m LiCl-KCl	450	Gold	+ 0.88V	0.01V	0.05V
25 ^{o}/m $CuCl_2$ 75 ^{o}/m LiCl-KCl	450	Gold	+ 0.78V	0.01V	0.12V

4. A rod section of "Glassy Carbon" (from the Tokai Electrode Mfg. Co. in Tokyo, Japan) dissolved to about 2/3 of its initial size in $CuCl_2$ melt at 540° for 72 hours. The remaining part of the rod section retained the glossy appearance and strength observed before treatment.

5. Boron Carbide (supplied by the Norton Company) was found unattacked following immersion in the melt at 540°C. for 72 hours.

The specific resistivities of boron carbide and "Glassy Carbon", determined in the temperature range between 25° and 525°C. by means of a four point probe, are given in Table X. The sample of boron carbide used in the experiment was a 6.3mm rod having the following composition:

$$
\begin{array}{ll}
B & - - - - - - 76.5\% \text{ min.} \\
C & - - - - - - 20\text{-}22\% \text{ min.} \\
B_2O_3 & - - - - - - 0.2\% \text{ min.} \\
Fe & - - - - - - 0.5\% \text{ max.} \\
Al & - - - - - - 0.2\% \text{ max.} \\
Ca & - - - - - - 0.1\% \text{ max.} \\
Mg & - - - - - - 0.05\% \text{ max.}
\end{array}
$$

TABLE X

SPECIFIC RESISTIVITY OF BORON CARBIDE AND "GLASSY CARBON"

Boron Carbide		"Glassy Carbon"	
Temperature °C	Specific Resistivity ohm-cm	Temperature °C	Specific Resistivity ohm-cm
25	0.398	27	4.900×10^{-3}
100	0.204	114	4.754×10^{-3}
150	0.143	202	4.626×10^{-3}
197	0.105	292	4.501×10^{-3}
300	0.061	396	4.382×10^{-3}
400	0.040	524	4.186×10^{-3}
525	0.022		

Because of the difficulties associated with finding suitable materials to contain the highly oxidizing $CuCl_2$ no further tests were run using this depolarizer.

4.2.5   IRON (III)

Pure ferric chloride quickly deteriorated both the gold indicator electrode and the graphite auxiliary electrode although the metal chloride did not appear to have melted at the operating temperature of the cell (290°C.). The Au-$BiCl_3$ half cell was used as the reference electrode and the potential obtained was converted with respect to Ag-AgCl in LiCl-KCl as described in Section 4.1.3. An open circuit potential of +1.13 volts was thus obtained. No current could be passed through the cell because of the very high cell resistance. This high resistance was attributed to the presence of unmelted solids in the cell.

The oxidizing power of ferric chloride was reduced by dilution with either the LiCl-KCl eutectic or a mixture of the eutectic and $CaCl_2$. The results at 450° of these dilutions upon the open circuit potential and upon the polarization of the electrode with current drain could be summarized as:

| Mixture, Mole % | Electrode | Open Circuit Potential, vs 1m AgCl | Polarization at | |
			15 mamps/cm^2	150 mamps/cm^2
18.2 FeCl$_3$; 81.8 LiCl-KCl	Au	+0.70V	0.03V	0.10V
8.5 FeCl$_3$; 13 CaCl$_2$; 78.5 LiCl-KCl	Au	+0.65V	0.05V	1.3V
50 FeCl$_3$; 50 LiCl-KCl	W	+0.73V	0.010-0.015V	1.2V

Experimental curves for these systems are given in Figure 20. Compositions are given in mole percent. The potential scale given in this figure is with respect to an Ag-0.13m AgCl electrode which was used as a reference electrode. To convert these potentials to the Ag-1m AgCl scale, 0.127 volt must be subtracted from those given in the figure. The large polarization observed at
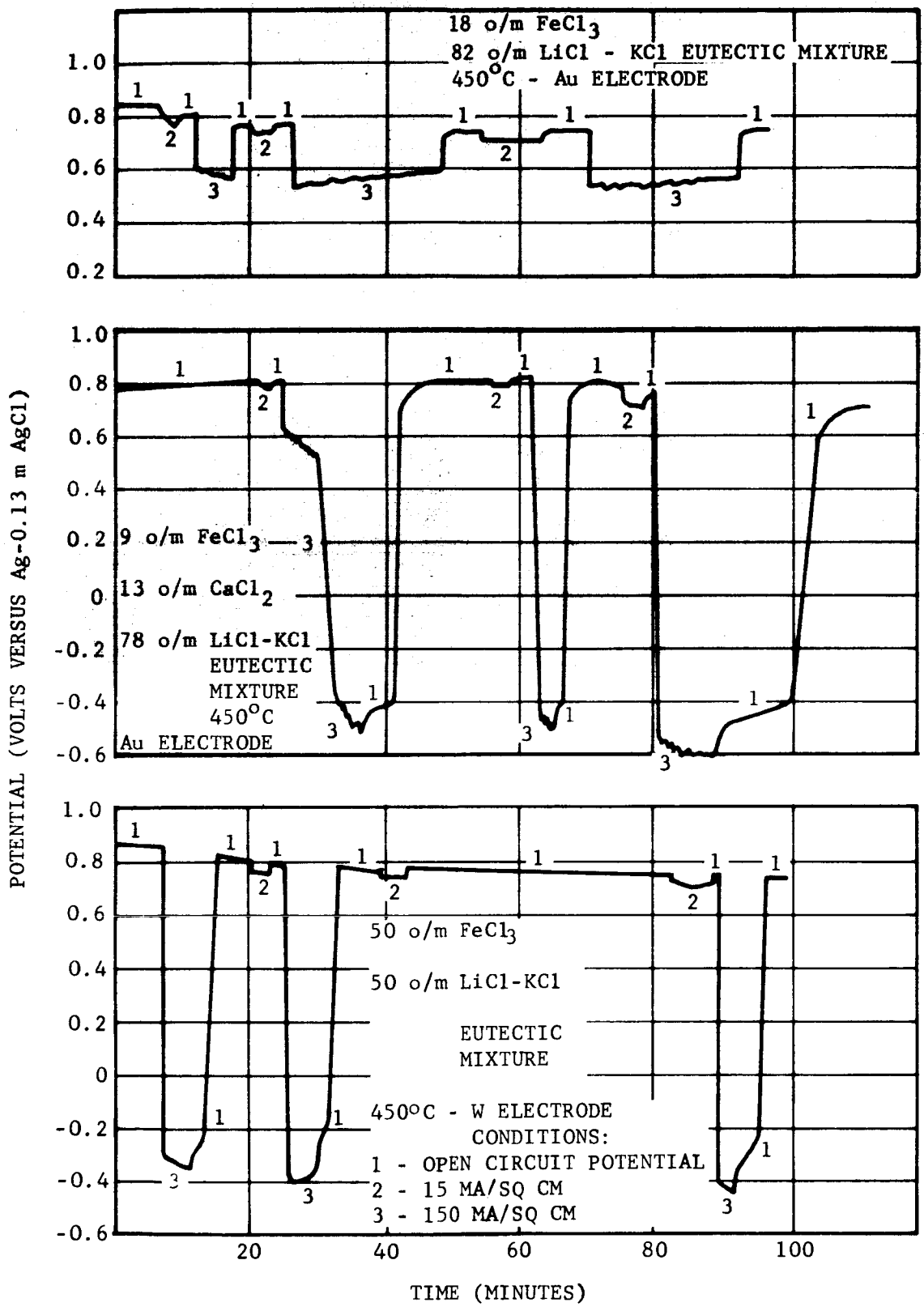
FIGURE 20. FeCl$_3$ REDUCTION. EFFECT OF DILUENT AND ELECTRODE

the higher current drain was attributed to the local depletion of ferric ions in the vicinity of the indicator electrode resulting in transition from the Fe(III)-Fe(II) system to the Fe(II)-Fe(0) system.

4.2.6 SILVER (I)

Pure molten silver chloride gave an open circuit potential of +0.21 volt on a Pt electrode at 480°C. Little polarization was observed at current densities of 0.015 and 0.150 amps/sq.cm. A slow decrease in potential with time was probably due to dilution of the AgCl with LiCl-KCl. Electrolytic cell A had been used for these measurements. A mixture of 67 mole percent AgCl and 33 mole percent $CaCl_2$ (1 to 1 equivalent ratio) gave a steady state open circuit potential of +0.32 volt on an Au electrode. Experimental curves for these systems are given in Figure 21. As would be expected from the phase diagram for the AgCl-$CaCl_2$ system (Figure 12), the mixture of AgCl and $CaCl_2$ contained a solution of $CaCl_2$ in AgCl and some undissolved $CaCl_2$.

A solution of 85 mole percent AgCl and 15 mole percent $CaCl_2$ which is completely liquid at 500° gave an open circuit potential of +0.31 volts on a gold electrode. After an initial voltage drop, the polarization was less than 30 mv at 0.150 amp/cm^2 of cathode area. The potential-time curve for this system is shown in Figure 21.

4.2.7 VANADIUM (V)

Vanadium pentoxide, V_2O_5, was soluble in molten LiCl-KCl. In addition to its solubility, it was a very strong oxidizing agent and reacted with molten chlorides liberating chlorine. It has also been reported[53] that less than one electron is involved in the reduction of each V_2O_5 molecule to form an insoluble lithium vanadium bronze.

4.3 SUMMARY AND CONCLUSIONS

Chromium (VI) compounds either reacted with chloride electrolytes or formed insoluble films with high resistances upon reduction. V_2O_5 reacted with
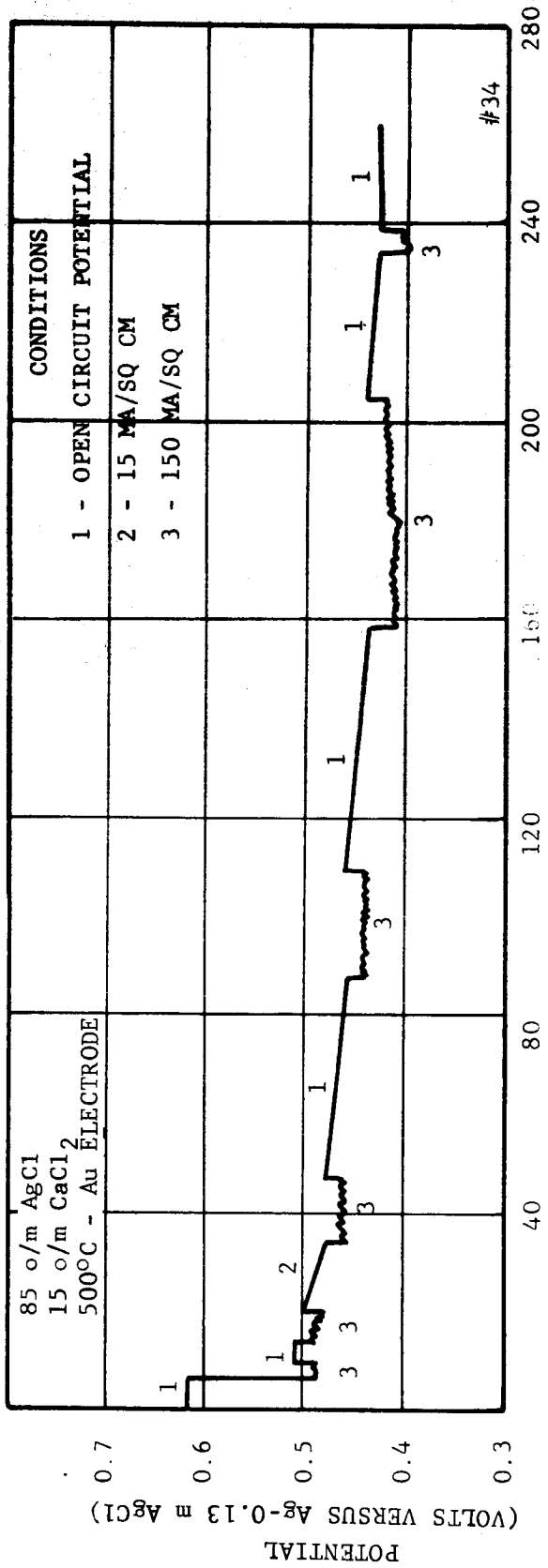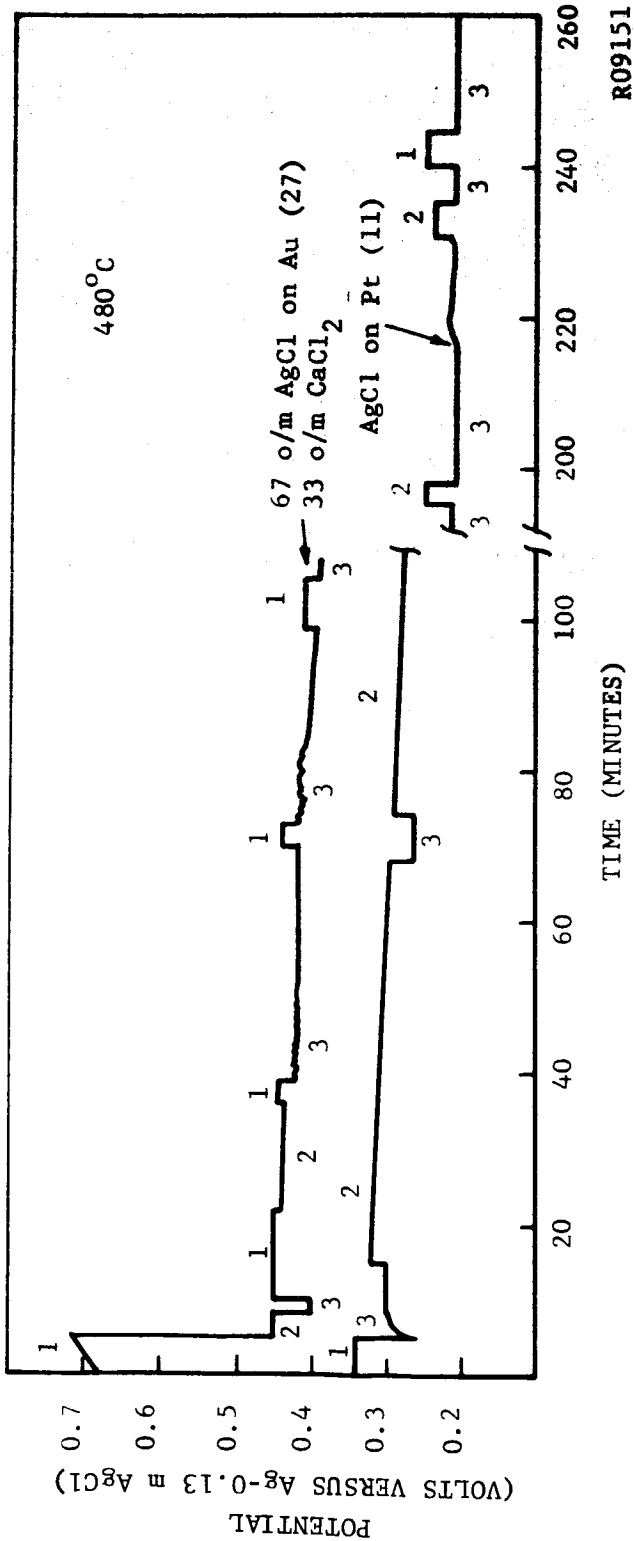
FIGURE 21. AgCl REDUCTION

-69-

molten chlorides and in addition appeared to have a very high equivalent weight (small number of electrons per V_2O_5 molecule).

All of the pure molten chlorides, with the exception of ferric chloride, showed very little polarization under current drain. Ferric chloride was unable to support high current drains without shifting to a reduction reaction which yielded metallic iron as the product. This reaction occurred at much lower potentials.

Mixing some of these chlorides with equivalent amount of by-products assumed to contaminate the cathode material during normal cell discharge caused substantial open circuit potential shifts toward negative values, and rapidly increasing polarization under current drains. Some of these mixtures were more or less in the solid phase at the operating temperature of the cell and therefore resistance as well as concentration polarization would be expected.

Silver chloride showed good electrochemical performance but its equivalent weight was too high. Cupric chloride was the strongest oxidizing agent studied as a possible cathode material. Its extreme reactivity with practical electrode materials and proposed cell cases eliminated it from further consideration for long discharge times. Although bismuth trichloride shows excellent electrochemical properties, the formation of soluble or liquid reduction products would make its utilization very difficult. Since no solid reaction product is formed to protect the current collector, the collector must be made of a very noble metal to prevent its reaction with $BiCl_3$. This collector must also have flexibility to accommodate volume changes which occur during discharge. The formation of a liquid reaction product could, depending upon the orientation of the cell, partially or completely block the ionic path between the anode and cathode.

On the basis of the experimental work, cuprous chloride was selected as the

most promising cathode depolarizer for further study in complete cells.
This selection was based upon the following points:

a. There was essentially no polarization[54] in the cathodic deposition of solid copper from pure molten cuprous chloride at current densities up to 0.5 A/cm^2.

b. Oxidation products of anode materials such as lithium, sodium, and potassium could be added coulometrically (ionic transfer across the separator) to CuCl in relatively large quantities before freezing of the catholyte occurred. Thus, CuCl remained molten at 425°C. with up to approximately 38 mole percent of LiCl, 35 mole percent of NaCl and 55 mole percent of KCl.[51]

c. The omission of an electrolyte in the cathode compartment increased the energy density of test cells.

d. Practical materials such as nickel or Armco iron could be used to contain molten CuCl and act as a current collector without being deteriorated by the salt.

e. A solid reduction product, metallic copper, formed in the cathode compartment of the cells. This was the ultimate reason for the disqualification of $BiCl_3$ as a cathode depolarizer. The final reduction product of this salt was bismuth metal which was molten at the operating temperature of the cell. Depending upon the orientation of the cells in space, the molten inert metal could partially or completely obstruct the ionic path between anode and cathode compartments.

SECTION 5

SEPARATORS

For this report a separator was defined as any material which was used as a barrier between the anode and cathode compartments of the cell. It included porous materials as well as solid ionic conductors. The zeolite materials included any separator which used a synthetic zeolite as a starting material.

5.1 NONZEOLITE MATERIALS

5.1.1 PORCELAINS

High sodium porcelain tubes approximately 170mm long, 10.5mm O.D., and 9mm I.D. were slip cast and sintered for cathode depolarizer investigations. The composition, raw materials, and material processing technique were the same as those described by R. J. Labrie[13] of the National Bureau of Standards. The sintered composition may be expressed as:

	Wt.%
SiO_2	53.1
Al_2O_3	35.4
Na_2O	9.6
K_2O	0.2
TiO_2, Fe_2O_3, MgO, CaO	1.7

In addition, 1.27cm diameter membranes were also slip cast and sintered for cation exchange investigations. These materials are generally referred to as NBS porcelain.

In the initial experiments in which the oxidation products of the anode were coulometrically added to the cathode depolarizer, the high sodium porcelain was used as the separator. When lithium ions were to be transferred, it was first necessary to exchange the sodium ions of the porcelain for lithium ions. This exchange was performed by immersing the porcelain tubes in molten lithium nitrate at 285^OC for eight days. The melt was replenished every other day with a fresh batch. Following this treatment the tubes were rinsed with water and vacuum dried at 300^OC. Two of these tubes were again filled with lithium nitrate melt and partially immersed in more of the melt at 300^OC. By means of graphite electrodes inserted in the tubes, current drains of 50 ma and 100 ma were passed through the ceramic for one hour in alternate periods of about 10 minutes. No visible evidence of stress was observed on the ceramic. The tubes were again rinsed and dried then given the same galvanic treatment using LiCl-KCl eutectic mixture, in place of $LiNO_3$, at 450^OC. The ceramic tubes showed marked crazing throughout the area that was immersed in the eutectic mixture. This was probably caused by stresses from uneven exchange with lithium ions and potassium ions in the ceramic.

Replacement of sodium ions with lithium ions was also performed with NBS porcelain pellets as follows. A pellet of this porcelain was sealed on AV30 tube (alumina) with a Pyroceram 45 glass seal. The alumina tube was partially filled with lithium nitrate melt and immersed in more of the melt at 290 ± 2^OC. A second but unsealed pellet of the same material was also immersed in $LiNO_3$ melt. After 24 hours of impregnation, tungsten electrodes were placed in the melts, inside and outside the alumina tube, and the resistance of the sealed membrane at 290° was evaluated as a function of time with an AC Conductivity Bridge at 1000 cps. The results are given in Table XI.

TABLE XI

RESISTIVITY OF LITHIUM EXCHANGED PORCELAIN AT 290°C

Time	Resistance (ohms)	Resistivity (ohm-cm)
24 hours	40.5	729
32 hours	30.5	549
46 hours	27.4	493
78 hours	26.0	468
118 hours	25.6	461

The membranes were found slightly crazed but strong and uncracked. The bonding of the membrane to the alumina tube appeared unaffected by the treatment. However, as previously mentioned, when the lithium nitrate was replaced with the LiCl-KCl eutectic mixture, current flow through the porcelain caused extensive crazing.

5.1.2 SODIUM ALUMINATES

During the course of this program, the compatibility of the zeolites with molten metals was found to be poor. This was generally attributed to an attack on the silicate. In an attempt to retain sodium as an anode material, an investigation of sodium aluminates containing P_2O_5 as a sintering aid was initiated. It was hoped that these compositions, having no silica, would exhibit greater resistance to attack by molten sodium. Table XII indicates the compositions selected for sintering evaluations. These compositions were selected on the basis of a K_2O, Al_2O_3, P_2O_5 phase diagram describing stable crystalline and noncrystalline areas by Z. N. Syritskaya.[55] Composition C-9, made with 67 $NaPO_3$ and 33 Al_2O_3 (weight %) to yield a theoretical composition of 33.3 Na_2O, 33.3 Al_2O_3, and 33.3 P_2O_5 (mole %) was polycrystalline, nonhydroscopic, and structurally sound after sintering at 700°C for 16 hours. Subsequent liquid sodium compatibility tests were negative (Section 3.2). Further development was discontinued when the cell research was focused on the use of lithium-magnesium alloy anode materials in preference to sodium.

The aluminate compositions were prepared by mixing the raw materials in methanol with a mortar and pestle followed by a 15 minute calcine at 700°C. The calcined material was subsequently ground in methanol, dried, and granulated with 2% polyvinyl alcohol (PVA) for dry pressing and sintering.

TABLE XII

COMPOSITIONS OF SODIUM ALUMINATES

No.	Mole %		
	Na_2O	Al_2O_3	P_2O_5
C-5	50.0	46.2	3.8
C-7	50.0	43.4	6.6
C-8	40.0	40.0	20.0
C-9	33.3	33.3	33.3
C-10	10.0	22.5	67.5
C-11	20.0	20.0	60.0

5.1.3 POROUS SEPARATORS

Two materials were used as porous separators. These were a porous alumina referred to as AL-300 and a sintered glass frit. The material, AL-300, was a raw alumina material in block form supplied by Western Gold and Platinum Company, Belmont, California. Discs machined from AL-300 were sintered at 1400°C/16 hours and 1500°C/2½ hours. Their respective porosities of 39 and 15% show the latitude one may have for the development of porous materials. High temperatures will completely vitrify the material. AL-300 also exhibited excellent strength at 10-15 mils. The use of AL-300 as a separator in complete cells is described in Section 6.1.

In addition to use as a separator, the AL-300 alumina was also considered for use as a porous backing to give the required mechanical strength to thin zeolite membranes. This application is described in Section 5.4.

A porous glass disc was used as a separator in the cell tests described in Section 6.3. These are commercially available as filter discs. The fine

porosity grade has a nominal maximum pore diameter of 4 to 5.5 microns. Their thickness was 0.12 cm.

5.2   ZEOLITE MATERIALS

5.2.1   PREPARATION OF CRYSTALLINE ZEOLITES

The Type A and Type X zeolite powders are commercially available in both the Na^+ and Ca^{++} forms. These commercially available A and X zeolites were used as the starting material for the studies with A and X zeolites. Type Y zeolite is not readily available and was therefore synthesized by crystallization from aluminosilicate gels. This preparation was as follows.

Dissolve 5.0 grams of $NaAlO_2$ (Matheson, Coleman, and Bell, Technical, CB941) and 22.0 grams of NaOH (Baker Analyzed Reagent, 3726) in 89.5 ml of distilled water. Allow this solution to cool somewhat (actual temperature did not appear to be critical). Weight out 125 grams of colloidal SiO_2 (Matheson, Coleman, and Bell, Practical, 30% SiO_2 by weight, P7694) and mix with $NaAlO_2$-NaOH solution in a Waring type blender until homogeneous.

Place the resultant paste in a 500 ml Erlenmeyer flask. Equip the flask with a reflux condenser and heat on a water bath for approximately 24 hours. During this period, the homogeneous gel recrystallizes into an easily separable solid phase. The solid phase is removed by vacuum filtration and washed with distilled water until the pH of the filtrate drops to about 10.5. Four 50 ml portions of distilled water are usually sufficient. Occasionally this method of preparation produced a batch in which the washings remain at pH 12. This material was always found to be amorphous to X-rays.

After filtering and washing, the solid is air dried overnight or for several hours at $100^{\circ}C$. The zeolite can be activated (water removed from the pores) by vacuum drying at approximately $350^{\circ}C$. This preparation yields about 8 grams of the air dried but unactivated zeolite.

X-ray diffraction patterns indicated that the sodium form of type Y zeolite could be prepared. Several attempts to directly synthesize the lithium and potassium forms of type Y yielded a material which was amorphous to X-rays. The lithium form of type Y was therefore prepared by exchanging NaY with an aqueous solution of LiCl. Similarly, other cation forms of Type A and X zeolited were prepared by ion exchange of the sodium forms with the appropriate cation.

5.2.2 ION EXCHANGE STUDIES AND X-RAY DIFFRACTION PATTERNS

A variety of ion exchanging procedures were used depending on the purpose of the experiment and upon the nature of the zeolites and the cations involved. In addition to cation species for use in the proposed system, a variety of cation species for a study on a completely solid state battery were prepared. This solid state battery is described in Appendix A.

The initial experiments were designed to determine the rate and extent of ion exchange which could be obtained with zeolites. In these experiments a weighed portion of anhydrous Type A zeolite in the Na^+ form (NaA) was equilibrated with distilled water and air dried. The weight of the zeolite was found to increase 20.8 percent due to absorbed water. Exactly 0.1 equivalent of the hydrated zeolite was treated with 100 ml of a 1.0 $\underline{N}$ solution of $AgNO_3$ slightly acidified with HNO_3. At 15 minute intervals, the Ag^+ in solution was analyzed polarographically. No further decrease in the Ag^+ concentration was noted after the first 15 minute period. For the exchange reaction

$$NaA + Ag^+ \rightleftarrows AgA + Na^+ \tag{20}$$

the apparent exchange constant, K'_{ex}, defined as

$$K'_{ex} = \frac{(Ag^+A)(Na^+)}{(Na^+A)(Ag^+)} \tag{21}$$

was 88.7 for the single exchange. This corresponded to a 90.4 percent exchange. A second treatment with $AgNO_3$ showed that the zeolite was 101

percent exchanged. After filtering and washing with distilled water until no trace of Ag^+ was detected in the filtrate, the zeolite was air dried. This white powder was then activated at $350^\circ C$ under vacuum. The activated zeolite, now AgA, was bright orange.

A similar procedure was used in an attempt to prepare CuA_2. In this case a very finely divided, light blue powder was obtained. Upon vacuum activation, the sample turned black. A reddish brown gas was noted when the cold trap cooled with liquid nitrogen was allowed to warm to room temperature. X-ray diffraction patterns showed the presence of CuO and a large amount of amorphous material. CuA_2 was obtained by exchanging with a one normal solution of $Cu(NO_3)_2 \cdot 3H_2O$ in 95% ethanol. A filterable blue solid was obtained. In the drying of this material, the temperature was kept below $150^\circ C$. At approximately $200^\circ C$, the blue solid was converted to a brown or black material which was shown by x-ray diffraction to be a mixture of an amorphous material and CuO. Even in CuA_2 dried at $< 150^\circ$, some loss of zeolite structure was noted. These results indicate the profound effect of the cation type upon the stability of the zeolite. NaA can be heated above 900° before loss of structure occurs.

The majority of the exchanging reactions were carried on with one of the following procedures.

A suspension of 0.1 equivalent of zeolite (based on replaceable cations) in the sodium form in 100 ml of a solution containing 0.1 equivalent of the exchanging cation was maintained at room temperature for approximately 0.5 hours by magnetic stirring. The solid was then removed by vacuum filtration. The suspension and filtration of zeolite was repeated until it had been exposed to a total of at least 0.3 equivalents of exchanging cations. After the final filtration, the zeolite was washed with a small portion of distilled water before drying at $100^\circ C$ in air and activating in vacuum at $350^\circ C$.

It was soon noted that the Teflon covered stirring bar was being abraded by this process and that the zeolite was being contaminated by material from

the magnetic stirring bar. The procedure was modified by using a stream of air bubbling through the suspension instead of the magnetic stirring.

To achieve a greater degree of exchange a percolating procedure was devised. The zeolite to be exchanged was placed in a glass tube similar to a chromatographic column. Vacuum was applied at the base of the tube and a solution of the exchanging cation was allowed to percolate through the zeolite. The column was maintained at approximately 80°C. As in the preceding process, the zeolite was treated with a three-fold excess of exchanging cation.

Generally, one normal aqueous solutions of the exchanging cations as nitrates or chlorides were used. Small amounts of acids were used to prevent hydrolysis of some of the salts. Type A and Type X zeolites are quite sensitive to acids and therefore the pH of the exchanging solutions was kept as high as possible.

Samples of NaA, LiA, KA, AgA, CaA_2, NaX, LiX, AgX, CaX_2, CuX_2, NaY and LiY were prepared by these methods and submitted for x-ray diffraction studies. X-ray diffraction patterns were used in this study to determine if the various methods of preparation of Type Y zeolites were successful and to determine if the zeolite crystal structure was preserved with cation exchange and activation. In addition, the effect of the cation upon the spacing of the crystal planes was determined.

Powder diffraction patterns were taken on a Norelco Phillip Spectrometer using filtered CuK_{α} radiation. The results for the three types of zeolite containing various cations are given in Tables XIII, XIV, and XV. The Miller indices (h, k, l) were assigned from the relation

$$m = h^2 + k^2 + l^2 \qquad (22)$$

where m was determined by the slide rule method from the d-spacings.[56] Using this method it was found that the Type A zeolites had a simple cubic structure with a unit cell length of approximately 12.3 $\overset{o}{A}$; Type X zeolite had a face centered cubic structure with a unit cell length of 25.0 $\overset{o}{A}$; and

TABLE XIII

X-RAY DIFFRACTION DATA – d SPACINGS FOR TYPE A ZEOLITES

d, Å

m	h,k,l	NaA Lit.	NaA Obs	LiA Obs	KA Obs	AgA Obs	CaA$_2$ Lit.	CaA$_2$ Obs	CuA$_2$ Obs
1	100	12.294	12.39	12.18	12.30	12.30	12.243	12.35	12.27
2	110	8.706	8.70	8.53	8.70	8.75	8.664	8.70	8.66
3	111	7.109	7.12	6.96	7.13	7.08	7.075	7.10	6.96
4	200	-	-	-	6.19	6.15	6.121	6.16	6.17
5	210	5.508	5.50	5.39	5.50	5.50	5.478	5.50	5.47
6	211	5.031	5.03	-	5.12	-	5.002	-	5.01
8	220	4.357	4.35	4.27	-	4.33	-	-	4.33
9	221,300	4.107	4.09	4.01	4.09	4.08	4.084	4.09	4.07
10	310	-	3.86	3.80	3.90	3.87	3.875	-	3.88
11	311	3.714	3.69	3.63	3.70	3.69	3.696	3.70	3.69
12	222	-	-	-	3.55	3.545	3.539	-	3.56
13	320	3.417	3.40	3.34	3.40	3.411	3.398	3.40	3.40
14	321	3.293	3.28	3.21	3.29	3.300	3.276	3.28	3.27
16	400	-	-	-	3.08	-	-	3.18	3.05
17	410,322	2.987	2.98	2.92	2.98	3.076	2.972	2.99	2.966
18	411,330	2.904	2.89	2.84	2.90	2.976	2.888	2.90	2.880
19	331	-	-	-	-	2.891	-	-	2.810
20	420	2.754	2.74	2.69	2.75	2.740	2.741	2.74	2.740
21	421	2.688	2.69	2.63	2.69	2.680	2.676	-	2.665
22	332	2.626	2.62	2.57	2.62	2.619	2.614	2.62	2.608

TABLE XIV

X-RAY DIFFRACTION DATA - d SPACINGS FOR TYPE X ZEOLITE

d, Å

m	h,k,l	NaX Lit.	NaX Obs	LiX Lit.	LiX Obs	AgX Lit.	AgX Obs	CaX_2 Lit.	CaX_2 Obs	CuX_2 Obs
3	111	14.47	14.48	14.37	14.25	14.37	14.60	14.37	14.48	14.24
8	220	8.85	8.84	8.79	8.75	8.82	8.84	8.79	8.84	8.58
11	311	7.54	7.54	7.49	7.49	7.54	7.56	7.51	7.56	-
12	222	-	-	-	-	-	-	-	-	6.92
16	400	-	-	-	-	6.23	6.25	-	-	-
19	331	5.73	5.73	5.70	5.68	-	-	5.71	5.71	5.60
27	333,511	4.81	4.81	4.79	4.77	4.80	4.79	4.79	4.79	4.70
32	440	4.42	4.41	4.40	4.37	4.41	4.40	4.40	4.39	-
35	531	4.23	4.22	4.21	-	4.22	4.21	-	-	4.07
36	600	-	-	-	-	-	-	-	-	-
40	620	3.946	3.93	3.931	3.91	-	-	3.936	3.92	-
43	533	3.808	3.80	3.794	3.76	3.805	3.79	3.800	3.79	-
44	622	3.765	-	3.749	-	3.760	3.75	3.754	-	-
48	444	3.609	-	3.590	3.56	3.603	3.587	3.593	3.58	3.46
51	551,711	3.500	-	3.482	3.46	3.494	3.490	3.486	3.48	3.28
56	642	3.338	3.33	3.324	3.30	3.335	3.324	3.328	3.31	-
59	553,731	3.253	3.25	3.239	3.21	3.250	3.241	3.241	3.22	-
67	733	3.051	3.04	3.040	3.02	-	-	3.041	3.025	-
68	-	-	-	-	-	3.027	3.02	-	-	-
72	660,822	2.944	2.94	2.933	2.92	2.941	2.928	2.934	2.919	-
75	555,751	2.885	2.88	2.874	2.86	2.882	2.865	2.875	2.864	-
80	840	2.794	2.79	2.782	2.76	2.792	2.778	2.783	2.764	-
83	753,911	2.743	2.74	2.730	2.70	2.739	2.720	2.732	2.720	-
88	664	2.663	2.66	2.653	2.63	2.662	2.650	2.653	2.642	-
91	931	2.620	2.61	2.609	-	2.617	2.605	2.610	2.597	-
96	-	2.550	2.55	2.542	-	2.549	2.538	-	-	-

TABLE XV

X-RAY DIFFRACTION DATA -d SPACINGS FOR TYPE Y ZEOLITES

| | | d, Å | | |
| | | NaY | | LiY |
m	h,k,l	Lit.	Obs.	Obs.
3	111	14.3	14.4	14.36
8	220	8.73-.80	8.75	8.84
11	311	7.45-.50	7.46	7.53
12	222	-	-	-
16	400	-	-	-
19	331	5.67-.71	5.68	5.68
27	333,511	4.75-.79	4.74	4.76
32	440	4.37-.46	4.36	4.37
35	531	-	-	-
36	600	-	-	-
40	620	3.90-.93	3.90	3.90
43	533	3.77-.79	3.76	3.76
44	622	-	-	-
48	444	3.57-.59	3.56	3.56
51	551,711	3.46-.48	3.45	3.45
56	642	3.30-.33	3.30	3.30
59	553,731	3.22-.24	3.21	3.21
67	733	3.02-.04	3.02	3.01
72	660,822	2.90-.93	2.91	2.91
75	555,751	2.85-.87	2.85	2.85
80	840	2.76-.78	2.74	2.76
83	753,911	2.71-.73	2.71	2.70
88	664	2.63-.65	2.63	2.63
91	931	2.59-.61	2.59	2.58
96	844	2.52-.54	2.53	-

Type Y had a face centered cubic structure with a unit cell length of 24.7 $\overset{\circ}{A}$. Values of d-spacings as reported in the literature are given for comparison. The spacings for the Type A material are taken from reference[18], for the Type X from reference[34], and for the Type Y from reference[35]. All materials, with the exception of CuA_2 and CuX_2, were vacuum activated at $350^{\circ}C$ before determining the diffraction patterns. CuA_2 and CuX_2 were temperature sensitive and therefore were activated at $150^{\circ}C$. The peaks for the CuX_2 zeolite were present on the top of a high background level, indicating some structure degradation of the zeolite had occurred.

The diffraction patterns show that the synthetic crystalline zeolites can be prepared in various cation forms by ion exchange with some changes in the crystal parameters.

In latter investigations it became apparent that some of the exchanged zeolites, particularly the LiX were contaminated with the exchanging salt. Thus the LiX actually was a mixture of LiX and LiCl. To prepare LiX uncontaminated by LiCl, the exchanged zeolite was carefully washed by repeated suspension in distilled water and filtered until no chloride ion was detected in the filtrate using the silver nitrate test. At this point a sample of the washed zeolite was dissolved in nitric acid and again tested with silver nitrate. Only a trace of chloride ion was found. These tests indicate that both the external and internal surfaces of the zeolite crystallites were essentially free of exchanging salts. To distinguish these two samples, the zeolite containing no LiCl was designated LiX-PJ.

During the latter portions of this program extensive cracking of rigidly fixed zeolite membranes was observed in cell tests. A proposed reason for this cracking was a change in the dimensions of the zeolite unit cell upon replacement of the cations. This could give a significant volume change (see Appendix B for the calculated volume changes in going from an NaX to a partially exchanged LiX). To further examine this phenomenon, samples of NaX were subjected to various types of ion exchange procedures, and the resulting zeolites analyzed by chemical means to determine their cation

composition and by x-ray diffraction to determine their crystal parameters.

Samples of NaX were subjected to aqueous ion exchange with solutions of LiCl and with solutions having the same salt composition as the LiCl-KCl eutectic. The samples resulting from these exchanges were designated LiX-PJ and LiKX (aqueous), respectively. An exchanged zeolite, designated LiKX (fused), was prepared by dispersing one part by weight of NaX zeolite in ten parts of LiCl-KCl eutectic mixture at 400°C for 18 hours. The exchanged zeolite was separated from the eutectic melt by vacuum filtration through a glass frit. A specially devised heating arrangement was used to prevent freezing of the eutectic melt during the slow process of filtration. The zeolite samples exchanged in aqueous solutions and in fused salt were dispersed in distilled water and filtrated several times until no chloride ion was detected in the filtrate using the silver nitrate test. At this point, samples of the washed zeolite were dissolved in nitric acid and again tested with silver nitrate. Only a trace of chloride ion was found in the acid solutions of the aqueous and fused salt exchanged zeolites. The zeolite samples were then dehydrated in vacuum at 350°C.

To determine the extent of exchange, the alkali metal content of the various zeolites was determined by flame photometry. A 0.500 gram sample of finely ground zeolite was placed in a platinum dish, moistened with water, and treated with three separate 5 ml portions of 48 percent hydrofluoric acid, evaporating to near dryness after each addition. 10 ml of 18M sulfuric acid were added and the mixture was heated just to strong fumes of SO_3. The residue was taken up in 10 to 15 ml of water and transferred to a Vycor test tube. The solution was evaporated to fumes and heated while delivering a slow stream of air from a quartz tube above the solution until all the sulfuric acid was removed. The residue was dissolved in 0.7N sulfuric acid solution. Standard solutions of the appropriate cation were prepared with appropriate additions to compensate for the interfering effects of acidity and aluminum concentration as suggested by Brumbaugh and Fanus.[57] The results of the flame photometry analysis are given in Table XVI in terms of the weight percent of the

alkali metals found and in terms of the mole percent of total cations. The results show that the cation composition of the zeolite does depend upon the conditions of exchange.

TABLE XVI

ANALYSIS OF ALKALI METAL CATIONS IN EXCHANGED ZEOLITES

		LiX-PJ	LiKX (aqueous)	LiKX (fused)
Percent Ion Exchange		71.5	77.7	83.4
Percent by Weight in Samples				
	Na	3.74	3.04	2.61
	Li	2.83	1.23	2.54
	K	--	10.98	7.57
Mole Percent of Total Cations*				
	Na	28.5	22.4	16.9
	Li	71.5	30.0	54.3
	K	--	47.6	28.8

* Assuming no other cation is present in the samples.

To determine the effect of pretreatment upon the crystal parameters, various samples of zeolite were subjected to x-ray diffraction analysis. These samples were NaX exposed to air and thus containing absorbed water, NaX vacuum dried to remove absorbed water, a sample of LiX prepared by exchange of NaX with an aqueous solution of LiCl (LiX-PJ), a sample of NaX exchanged with an aqueous solution having the same salt concentration as the eutectic (LiKX-aq), and a sample of NaX exchanged with the molten eutectic (LiKX-fused). The length of the unit cell, a_o, was calculated from the crystal spacings using the relation

$$a_o = (h^2 + k^2 + l^2)^{\frac{1}{2}} d_{hkl} \qquad (23)$$

where d_{hkl} is the spacing for the crystal plane having the Miller indices h, k, and l. The average length with its standard deviation for the unit cells is shown in Table XVII. The average cell length was determined from a minimum of ten "d" spacings.

TABLE XVII

UNIT CELL LENGTH FOR TYPE X ZEOLITES

Zeolite	a_o in $\overset{o}{A}$
NaX-air equilibrated	24.959 $\pm$ 0.096
NaX-vacuum dried	24.983 $\pm$ 0.038
LiX-PJ	24.601 $\pm$ 0.104
LiKX-aqueous	24.782 $\pm$ 0.121
LiKX-fused	24.555 $\pm$ 0.092

The unit cell lengths were compared by the statistical "t" test. The "t" test is a statistical method of comparing the averages of two series of measurements and of determining whether or not there is a significant difference between these averages. The test gives a measure for these averages and ascertains the chance of occurrence of various values of this measure when there is no difference between the averages. This measure, called "t", is the ratio of the difference between the averages to the standard deviation of this difference. Tables are available showing the chances that various limiting values of "t" would be exceeded if both series of measurements were the same. Various confidence limits can be chosen in the use of this test. The confidence limit is usually defined as the probability that when the two measurements are the same, the measured value of "t" will be less than or equal to the limiting value. In using the "t" test, a measured value of "t" below the critical or limiting values listed in the table indicates that the existence of a difference is "not proved". On the other hand, if the limiting value is exceeded this is considered to be evidence that a difference does exist. The complement of the confidence limit then gives the probability that the critical value of "t" could be exceeded even when the two results are the same.

The values of the experimental "t" for the differences in unit cell lengths between the various zeolites are given in Table XVIII along with the critical values of "t" for the 95% and 99% confidence limit. When the experimental value of "t" was less than the critical value, no difference

TABLE XVIII

STATISTICAL ANALYSIS OF UNIT CELL DIFFERENCES

Zeolites Compared	Experimental "t"
NaX-air equilibrated and NaX-vacuum dried	0.735
NaX (dry) and LiKX-fused	13.61
LiX-PJ and LiKX-fused	1.052
LiKX-fused and LiKX-aqueous	4.72

Critical value of "t" for 95% confidence level is 2.101

Critical value of "t" for 99% confidence level is 2.878

between the unit cell lengths was indicated; and when the experimental "t" exceeded the critical value, a significant difference was indicated. The statistical analysis showed that there was a significant difference in the unit cell length between dry NaX and the exchange zeolite, but that there was no significant difference with the various exchanging methods. However, the various methods of exchange did give different chemical compositions as discussed above.

5.2.3 FABRICATION PROCEDURES

A variety of fabrication procedures was developed for zeolite membranes. Some of these procedures were developed so as to preserve the zeolite structure while in other cases the principal objective was to form strong membranes with a low resistance. As the program progressed, various bonding techniques were developed for specific objectives or materials. Because of previous experience, initial efforts were directed toward vacuum, hot pressing. To obtain additional strength in thin membranes with large cross-sectional areas, bonding techniques using phosphoric acid or sodium silicate were investigated. The use of these materials as sintering aids usually resulted in some loss of zeolite structure. When the emphasis shifted to the use of lithium exchanged zeolites, self sintering processes were developed. The lithium zeolite sintered at temperatures

considerably below those of the sodium zeolites. Even at the lower sintering temperatures, the lithium zeolites showed some structural degradation. To maintain the maximum zeolite structure, hot pressing techniques at lower temperatures were developed. Each of these techniques is described below.

a. **Vacuum, Hot Pressing**

The vacuum hot pressing technique was developed as a method of fabricating reasonably strong zeolite pellets without additional bonding agent and with a maximum of retained zeolite structure. A stainless steel vacuum chamber containing a heated Carbolloy die was used. This die was used to prepare either pure zeolite pellets or zeolite pellets with gold foil electrodes pressed onto their surfaces. The foil electrodes were used as contacts for a.c. resistance measurements. A sketch of the chamber is given in Figure 22. The chamber could be evacuated to a pressure of a few microns while heating the sample. The vacuum heating dehydrated the zeolite powders before compacting. Dehydration was very important since the zeolites could lose their crystallinity if they were pressed while fully hydrated. The typical compacting procedure was to place the powdered zeolite and the foil electrodes where desired in the carbolloy die in the chamber. The chamber was evacuated and heated to 150-200°C for approximately one hour. A pressure of 700 to 2000 kgm/cm^2 was then used to form coherent, dense, and structurally intact compacts. Densities close to 90 percent of the single crystal value have been obtained by this method.[20]

b. **Bonding and Sintering**

Additional bonding and sintering procedures were developed for three types of zeolite materials; sodium Type A, (NaA), sodium Type X (NaX), and lithium exchanged NaX (LiX-PJ). Three bonding techniques were investigated; (1) zeolite plus sintering aids, i.e. sodium silicate and phosphoric acid; (2) hot pressing; and (3) self sintering. The main problem associated with the sintering of zeolite is the relatively low transformation temperature of 700-800°C at which the zeolite structure begins to deteriorate. Due to this problem, x-ray diffraction analysis was used as the primary means of establishing sintering limits in conjunction

PRESSURE

THERMOCOUPLE WELL

HEATER
LEAD

VACUUM LINE

HEATER LEAD

CYLINDRICAL
HEATER

CYLINDRICAL
HEATER

ZEOLITE COMPACT

GOLD LEAF
ELECTRODES
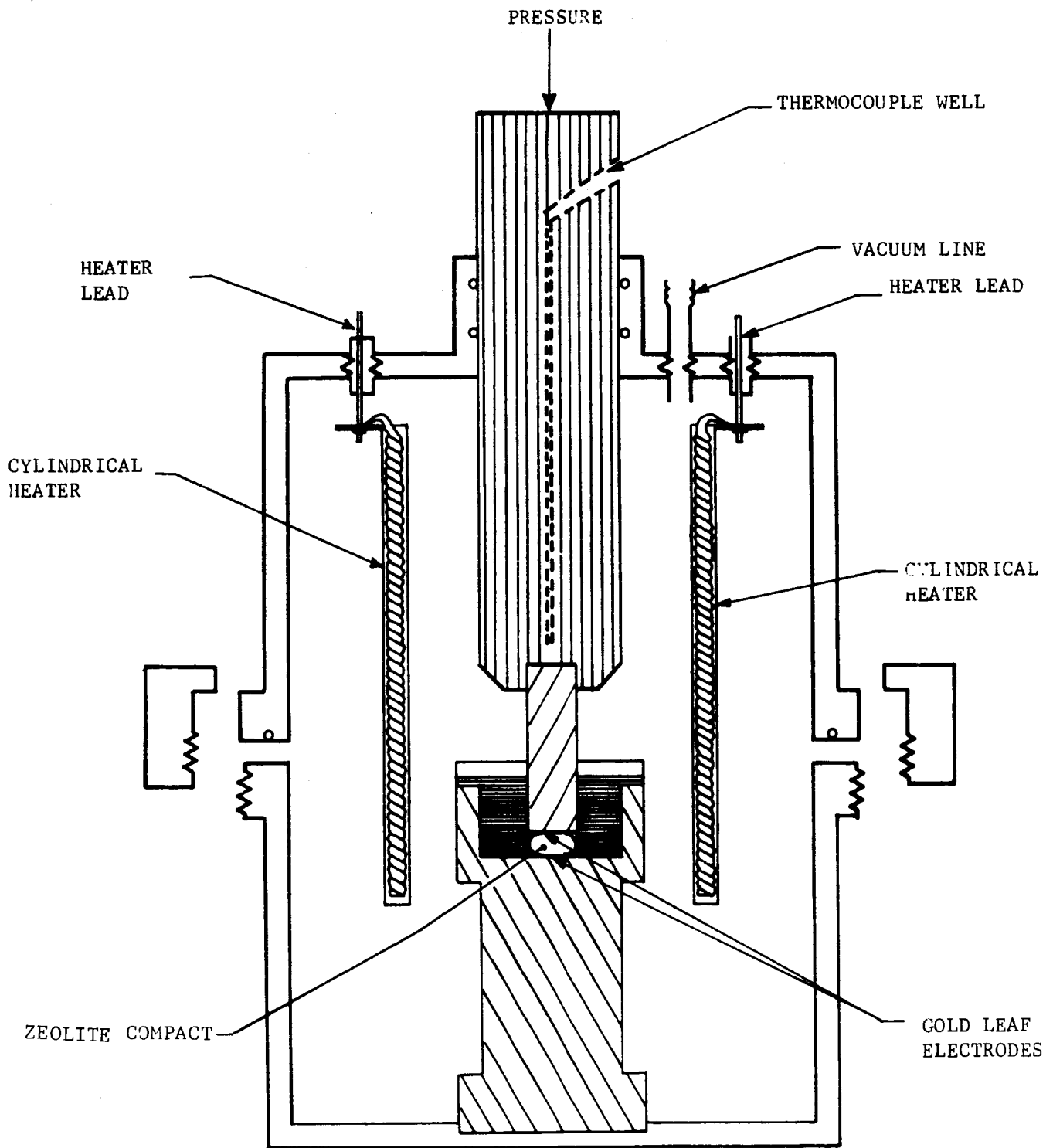
R08714

FIGURE 22. CHAMBER FOR VACUUM, HOT-PRESSING

with sufficient structural integrity for the ultimate development of 0.25-0.40 mm thick membranes. Additional characterization of the raw materials and sintered zeolites was obtained by differential thermal analysis, thermogravimetric analysis, and dilatometry.

Highlights of the fabrication results are as follows:

Type NaA zeolite containing 18% phosphoric acid sintered at 740°C for 45 minutes exhibited a retained zeolite crystal structure and good strength. Type NaX zeolite containing 18% phosphoric acid sintered for 30 minutes at 740°C also exhibited similar properties. A 21% addition of sodium silicate to NaX followed by sintering at 700°C for 30 minutes resulted in good zeolite membranes. Lithium exchanged NaX, designated LiX-PJ, hot pressed at 344 kgms/cm^2 at 700°C for two hours had an excellent zeolite structure and strength. Additions of 18% phosphoric acid to LiX-PJ zeolite caused deterioration of the zeolite structure and was difficult to control. LiX-PJ was the only zeolite investigated in which the zeolite structure could be retained during self sintering. However, at least partial decomposition of the zeolite structure appeared to be necessary to the sintering mechanism.

(1) Experimental Procedure

(a) Pressing and Sintering

The zeolite powder was first saturated with distilled water followed by the appropriate addition of sodium silicate or phosphoric acid. The material was then granulated by hand in a glass drying dish as it was intermittently dried in an oven (80°C) or over a hot plate. The bonding of the material during granulation formed particles that were readily separated into a minus 80 plus 200 mesh fraction for dry pression. Additions of an organic binder (polyvinyl alcohol, PVA) to promote granulation resulted in poor sintered strength and was abandoned. Following final drying at 80°C, the powder was pressed in a 1.27 cm diameter Meehenite die with heat treated drill rod punches. No lubricant or antisticking additions were required. Sintering times and temperatures were initially based on DTA (differential thermal analysis) and TGA

(thermogravimetric analysis) of the raw zeolite and sintering compositions. X-ray analysis was the final criteria for verifying the structure of the sintered zeolite. Sintering was performed in a tube furnace operated between 700°C and 800°C. The samples were preheated on a refractory slab in the entrance of the tube to approximately 300°C for ten minutes and then pushed into the firing zone for a specified time. The samples were withdrawn from the hot zone and cooled in the entrance for 5 minutes before removing to room temperature. The fired discs were inspected for scratch hardness and shrinkage. Those samples exhibiting good strength were then submitted for x-ray diffraction. Optimum times, temperature, and compositions relationships were established crystallo-graphically by this means to ensure the maintenance of the zeolite structure. Additional sintering experiments were conducted on the most promising compositions to increase their fired densities, the objectives being to reduce the intergranular pore volume to a closed pore condition, thus leaving the molecular pore of the zeolite as the principal connecting pore system. Density measurements were made by the volume displacement method in water on saturated specimens. This technique allowed comparison to published data[18] utilizing the same procedure.

(b) Hot Pressing

Hot pressing of the lithium exchanged zeolite was initiated in order to derive a "pure" zeolite for cell research free from the unknown preturbations of the binder materials. Also, hot pressing appeared to be the obvious approach for attaining high strength with a maximum of retained zeolite crystal structure, particularly with the temperature sensitive lithium exchanged zeolite.

Zeolite pellets 1.27 cm in diameter by 0.16 cm thick were hot pressed in alumina dies mounted in a small tube furnace contained between the platens of a manual hydraulic press. A wash of -325 mesh Al_2O_3 was applied to the alumina punch faces to facilitate ejection of the pellet. The pressed pellets were subsequently lapped to remove traced of the wash before x-ray analysis.

(2) Results

(a) Type A Zeolites

Initial DTA data indicated that NaA began a transformation at 770°C. In the presence of phosphoric acid the first perceptible transformation occurred at 850°C. TGA data showed dehydration and activation were complete at 400°C. Both analyses were run at a temperature rise of 10°C/minute.

Table XIX shows compositions containing phosphoric acid and sodium silicate. Samples Z-2, 3, and 4 were initial exploratory compositions made for sintering observations and x-ray analysis. Table XX, X-ray Diffraction Data, confirmed the DTA information in showing that the sodium silicate materials, Z-3, readily transformed at 810°C, while the phosphoric acid materials, Z-5, retained their structure at 800°C. Table XX also shows the complete disintegration of the raw zeolite, NaA, when heated to 880°C. This material was taken from a DTA run. The first column headed NaA contains the diffraction data obtained on the powder as received. Table XX is representative of the data obtained; the intensities, though not indicated, varied with hydration as described in the literature.[18]

Following the preliminary evaluations of Z-2, 3, and 4, two series of compositions were prepared to determine the effects of concentration on strength, crystal structure, and sinterability. Z-7, 8, and 10 yielded good structures and strength in 0.38 mm, 1.27 cm diameter discs that survived drops of 1 meter. Sintering at 740°C for 30 minutes resulted in little detectable distortion of the zeolite lattice parameters for compositions containing either 10% phosphoric acid or 21% sodium silicate; Z-8 containing 10% phosphoric acid appeared to be stronger than Z-10 containing 21% sodium silicate.

Sintering results shown in Table XXI indicate the relative shrinkage and scratch resistance of the compositions sintered at 700, 740, and 780°C for 30 minutes, respectively. Z-8 appeared to contain about the minimum amount of phosphoric acid for acceptable sintering. Z-10 and Z-11 were both well

TABLE XIX

SINTERING COMPOSITIONS FOR TYPE A ZEOLITES

Number	Wt. % Zeolite	Wt. % Binder	Binder
Z-2	90	10	H_3PO_4
Z-3	80	20	$Na_2O \cdot 2SiO_2$
Z-4	70	30	H_3PO_4
Z-5	80	18 + 2 PVA	H_3PO_4
Z-6	69	31	H_3PO_4
Z-7	82	18	H_3PO_4
Z-8	90	10	H_3PO_4
Z-9	95	5	H_3PO_4
Z-10	79	21	$Na_2O \cdot 2SiO_2$
Z-11	89	11	$Na_2O \cdot 2SiO_2$
Z-12	94	6	$Na_2O \cdot 2SiO_2$
Z-13	96.5	3.5	$Na_2O \cdot 2SiO_2$

Materials added as:

Phosphoric Acid - 85% H_3PO_4

Sodium Silicate - N Brand 41% $Na_2O \cdot 2SiO_2$

PVA - Polyvinyl Alcohol - 2% Aqueous Solution

TABLE XX

TYPICAL X-RAY DIFFRACTION DATA OF SINTERED TYPE A ZEOLITES

h,k,l	NaA	NaA (880°/10°C/min)	Z-3 (810°/10min)	Z-5 (800°/10min)	Z-7 (700°/30min)	Z-8 (740°/30min)	Z-10 (740°/30min)
100	12.23	-	11.93	12.44	12.35	12.26	12.26
110	8.66	-	8.49	8.75	8.70	8.65	8.66
111	7.04	-	6.96	7.13	7.09	7.04	7.07
210	5.48	-	5.39	5.51	5.48	5.48	5.48
211	4.99	-	-	5.02	5.00	4.98	5.00
220	4.34	-	-	4.34	4.32	4.33	4.33
221	4.09	4.17	{ 4.13 / 4.04	4.09	4.09	4.09	4.09
311	3170	3.60	3.67	3.70	3.70	3.70	3.70
320	3.40	3.31	3.37	3.41	3.41	3.40	3.40
321	3.28	3.26	3.25	3.28	3.28	3.27	3.28
410	2.99	3.02	2.99	2.98	2.98	2.97	2.98
411	2.89	-	2.96	2.89	2.90	2.90	2.89
420	2.76	-	-	2.75	2.75	2.74	2.74
421	2.68	-	-	2.68	2.68	2.68	2.68
332	2.62	2.55	2.59	2.61	2.61	2.61	2.61
422	2.49	2.49	2.54	2.50	2.51	2.50	2.50
430	2.45	-	-	2.45	2.45	2.45	2.45
511	2.37	2.35	-	2.35	2.35	2.35	2.36
520	2.28	-	-	-	-	-	-
521	2.24	-	-	-	2.24	2.24	-

TABLE XXI

SINTERING RESULTS TYPE A ZEOLITE

	Sintered Diameter, Inches		
Composition	700°C/30 Min.	740°C/30 Min.	780°C/30 Min.
Z-6	.458 h	.446 h	.430 h
Z-7	.475 h	.470 h	.460 h
Z-8	.487 s	.485 h	.480 h
Z-9	.494 c	.489 c	.489 c
Z-10	.494 s	.485 h	.444 w
Z-11	.496 c	.489 s	.451 h
Z-12	.498 c	.494 c	.475 s
Z-13	.500 c	.495 c	.473 c

w - warped
h - hard
s - soft
c - chalky

TABLE XXV

SUMMARY OF TGA AND XRD DATA FOR TYPE X ZEOLITES

Material	Sinter, °C-Min.	$450°C \rightarrow RT$ % Wt.Gain	XRD and Remarks
Z-28	Raw	22.8	Clear defined peaks
	680-30	11.3	
	700-30	3.3	Peak splitting, noticeable "amorphous" swell beginning @ 18°-20°.
	690-30	6.8	Similar to 700-30, no large differences.
NaX	Raw	32.6	Sharp strong peaks.
	750-30	31.6	
	800-30	26.9	
	800-45	13.4	Marked reduction in peak intensities.
LiX-PJ	Raw	36.2	Sharp strong peaks.
	700-60	32.3	
	700-90	29.5	Sharp peaks, intensities slightly less than raw material.
	750-30	0	
	680-8 hours	26.8	
	680-15½ hours	0	"Amorphous" - one obscure peak.
	660-15½ hours	31.5	
	HP-14 700-1 hr.	28.7	Good x-ray - Pressed @ 7350 psi.
	HP-17 700-2¼ hrs.	33.2	Sharp x-ray - Pressed @ 4900 psi.
	HP-19 680-17 hrs.	24.0	Marked reduction in peak intensities - Pressed @ 4900 psi.

a rigid seal between the membrane and its supporting structure in cell fabrication.

Table XXV summarizes the TGA and XRD data for the Z-28 (phosphate bonded) LiX-PJ, NaX, and LiX-PJ zeolites. A typical TGA curve is shown in Figure 23. The weight loss varied with the sintering conditions and retained zeolite. The zero weight gains from $450^{\circ}C$ to room temperature shown in Table XXV represented "amorphous" XRD patterns. The weight gains reported in Table XXV and shown in Figure 23 were achieved in the ambient atmosphere of the laboratory.

The loss of the zeolite structure with various chemical and thermal treatments was also correlated with the density of the zeolite pellets. This density was determined from the weight and physical dimensions of the fabricated pellets. The correlation between the TGA and density results for representative pellets prepared by various bonding techniques is shown in Table XXVI. Although no attempt was made to analyze the results quantitatively, it is readily apparent that, in general, an increase in the severity of the thermal treatment either in terms of time or temperature caused a decrease in the zeolitic content and an increase in the density of the pellets.

It must be emphasized that the absence of zeolitic structure in a fabricated membrane as indicated by TGA or XRD does not necessarily imply a nonporous membrane. Thus, the porosity of Z-28 membranes (LiX-PJ with H_3PO_4 binder sintered at $700^{\circ}C$ for 15 minutes) was evaluated by weighing the membranes after each of the following operations:

(1) Vacuum drying at $350^{\circ}C$ for 1 hour.

(2) Brief immersion in distilled water and wiping off excess water.

(3) Air drying at room temperature for 3 hours.

(4) Vacuum drying at $350^{\circ}C$ for 19 hours.

Based upon the total amount of water absorbed, the average porosity was 43.4%. Relatively little water was retained after the room temperature

-101-

sintered at 780°C; however, Z-10 at 740°C was favored due to the onset of transformation in the sodium silicate compositions above 770°C.

Sintering experiments with Z-7 composition were conducted to determine the relationship between mechanical pores due to consolidation and the molecular pores of the zeolite structure. The density of NaA zeolite published by Linde[18] is 1.99 gm/cm^3, determined for a saturated structure. A similar measurement was made by the water displacement technique following a weight determination after 4 hours of boiling in water. The theoretical density was relatively constant at 85% over the sintering range of 700-760°C. The water absorption value was approximately 28% by weight for the same samples. Theoretical saturation has been reported to be 22.2%[18]; the difference was assumed to represent the consolidation porosity between grains.

(b) **Type X Zeolites**

The work performed on the Type A zeolites was translated to the development of bonded Type X materials. In Table XXII, Z-14 and Z-16 were the best compositions evaluated containing the NaX zeolite. The sintering limits were determined by the results of the x-ray diffraction, i.e. 740°C/30 minutes for composition No. Z-14 containing 18 weight % H_3PO_4 and 700°C/30 minutes for composition No. Z-16 containing 21 weight % sodium silicate.

With the introduction of the lithium-magnesium alloy anode and LiCl-KCl electrolyte in the cell research, the development of lithium exchanged zeolite membranes was initiated. Table XXIII describes experiments with the LiX-PJ prepared as described in Section 5.2.2. In these compositions, it was clearly evident that the sintering temperature was very critical near 700°C. Earlier, residues of the exchanging chlorides (original sample of LiX) were found to be very detrimental to good sintering behavior.

The low melting and transformation point of the lithium exchanged zeolite LiX was very sharp at approximately 700°C. In the absence of a binder, an amorphous transformation appeared to be rapidly nucleated after 1 to 2 hours

-96-

TABLE XXII

NaX MEMBRANE FABRICATION DATA

Number	Material	Binder, Wt%	Sinter, °C/Min.	Structure and Remarks
Z-14	NaX	H_3PO_4, 18	740/30	Zeolite
Z-14	NaX	H_3PO_4, 18	850/30	Distorted Zeolite & Glassy Phase
Z-15	NaX	H_3PO_4, 10	780/30	Zeolite
Z-16	NaX	$Na_2Si_2O_5$, 21	700/30	Zeolite
Z-16	NaX	$Na_2Si_2O_5$, 21	780/30	Distorted Zeolite & Glassy Phase
Z-17	NaX	None	940/30	Unidentified Crystals & Glass
Z-19	NaX	None	Calcine 950/30 Sinter 1280/2hrs.	Glass

TABLE XXIII

LiX-PJ MEMBRANE FABRICATION DATA

Number	Material	Binder, Wt%	Sinter, °C/min.	Dia., In.	Structure & Remarks
Li	LiX-PJ	None	700/30	.498	Diffraction pks. essentially same as raw material, soft
	LiX-PJ	None	800/30	.339	Amorphous x-ray, hard
	LiX-PJ	None	750/30	.368	Amorphous x-ray, hard
	LiX-PJ	None	690/overnite	.387	Amorphous x-ray, hard
	LiX-PJ	None	700/90	.474	Similar to 700/30, slight swell in background, medium
	LiX-PJ	None	690/180	.481	Soft
	LiX-PJ	None	700/120	.413	Sharp reduction in pk. intensity compared to 700/90, medium
	LiX-PJ	None	700/120	--	Amorphous x-ray, hard
Z-28	LiX-PJ	H_3PO_4, 18	Unfired		Weak diffraction, slight swell in background
	LiX-PJ	H_3PO_4, 18	680/30	.470	Weaker than unfired, higher swell, medium
	LiX-PJ	H_3PO_4, 18	690/30	.461	Similar to 680/30, hard
	LiX-PJ	H_3PO_4, 18	700/30	.453	Similar to 680/30, hard
	LiX-PJ	H_3PO_4, 18	700/15	.462	Hard
	LiX-PJ	H_3PO_4, 18	680/120	.455	Hard
	LiX-PJ	H_3PO_4, 18	680/90	.460	Similar to 690/30, hard

at 700°C. The unique properties of the exchanged zeolite offered the possibility of fabricating a binder free membrane. The main problem, of course, was to arrest the amorphous reaction sufficiently to develop bonding without loss of the zeolite structure. As shown in Table XXIII, LiX-PJ with no binder sintered at 700°C for 30 and 90 minutes retained good structure, but was soft to medium in hardness. Suitable structural integrity for the goals of this program require a "medium-hard" or "hard" scratch resistance.

The use of 18% H_3PO_4 as a binder provided satisfactory strength; however, there was a compromise in the apparent crystal structure with the loss of peak intensities and "amorphous" swelling of the diffractagram. The most satisfactory sintering condition for Z-28 was 700°C/15 minutes.

Table XXIV, LiX-PJ Hot Pressed Membrane Fabrication Data, shows the development of the hot press technique. As noted in Table XXIV, the transformation of LiX-PJ was also critical when hot pressed near 700°C. Excellent x-ray diffraction comparisons were obtained in samples HP-5, 6, and 10. In particular, it was difficult to differentiate the x-ray diffraction patterns of HP-10 and the starting materials. Suitable strength and crystal structures were attained at 344 kgms/cm^2 at 700°C/2 hours and at 515 kgms/cm^2 at 650°C/5½ hours. The best conditions for hot pressing crack free membranes were found to be at 344 kgm/cm^2 between 680° and 700°C. The conditions used in pressing sample HP-18 were preferred because a greater amount of retained zeolite structure was shown by x-ray diffraction.

(c) Reactivity, Crystal Structures, and Thermal Expansion Relationship of Type X Zeolites

The reactivity of a retained zeolite structure containing an "amorphous" phase and zeolite crystal could be directly related to moisture absorption from 450°C to room temperature in addition to x-ray diffraction peak intensities (Table XXV). In addition, this reactivity could also be correlated with large anomalies in the thermal coefficient of expansion. The latter factor contributed to the difficulties experienced in retaining

TABLE XXIV

LiX-PJ HOT PRESSED MEMBRANE FABRICATION DATA

Number	Material	Pressure, kgms/cm²	Sinter, °C-Time	Pressure Applied	Remarks
HP-1	LiX-PJ	172	600 - 55 min.	@ Sinter Temp.	Poor structural integrity, alignment problem, soft
HP-2	LiX-PJ	172	600 - 60 min.	@ Sinter Temp.	Poor structural integrity, reduced fill, soft.
HP-3	LiX-PJ	172	650 - 30 min.	@ Sinter Temp.	Poor structural integrity, soft
HP-4	LiX-PJ	344	650 - 120 min.	@ Sinter Temp.	Sticking in die, sample fractured, medium
HP-5	LiX-PJ	344	700 - 45 min.	@ Sinter Temp.	First good pellet, good x-ray diffraction, medium hard
HP-6	LiX-PJ	344	700 - 120 min.	@ 600°C.	Good pellet, medium hard
HP-7	LiX-PJ	344	720 - 90 min.	@ 650°C.	Glass, excessive shrinkage and cracking, medium hard
HP-8	LiX-PJ	515	700 - 45 min.	@ 650°C.	Good pellet, x-ray poor, mixed phases & amorphous swell
HP-9	LiX-PJ	515	680 - 60 min.	@ 650°C.	Similar to HP-8
HP-10	LiX-PJ	515	650 - 5½ hours.	@ 650°C.	Good pellet, x-ray data similar to raw material.
HP-11	LiX-PJ	515	670 - 3½ hours	@ Sinter Temp.	X-ray good, cracked.
HP-13	LiX-PJ	515	710	@ Room Temp.	To m.p. & heater off. cracked amorph. center
HP-14	LiX-PJ	515	700 - 55 min.	{ 172 @ Rm.Temp. / 515 @ Sint.Temp.	Good sample - cracked in TGA, x-ray good.
HP-15	LiX-PJ	515	676 - 2¼ hours		Sealed to AV-30 with 80/20 glass.
HP-16	LiX-PJ	515	695 - 2 hours	@ Room Temp.	Cracked in air.
HP-17	LiX-PJ	344	700 - 2¼ hours	@ Room Temp.	Ejected hot, cooled in furnace - cracked.
HP-18	LiX-PJ	344	700 - 2 hours	@ Sinter Temp.	Ejected cold - OK, sealed to quartz.
HP-19	LiX-PJ	344	680 - 17 hours	@ Sinter Temp.	Ejected hot - OK.
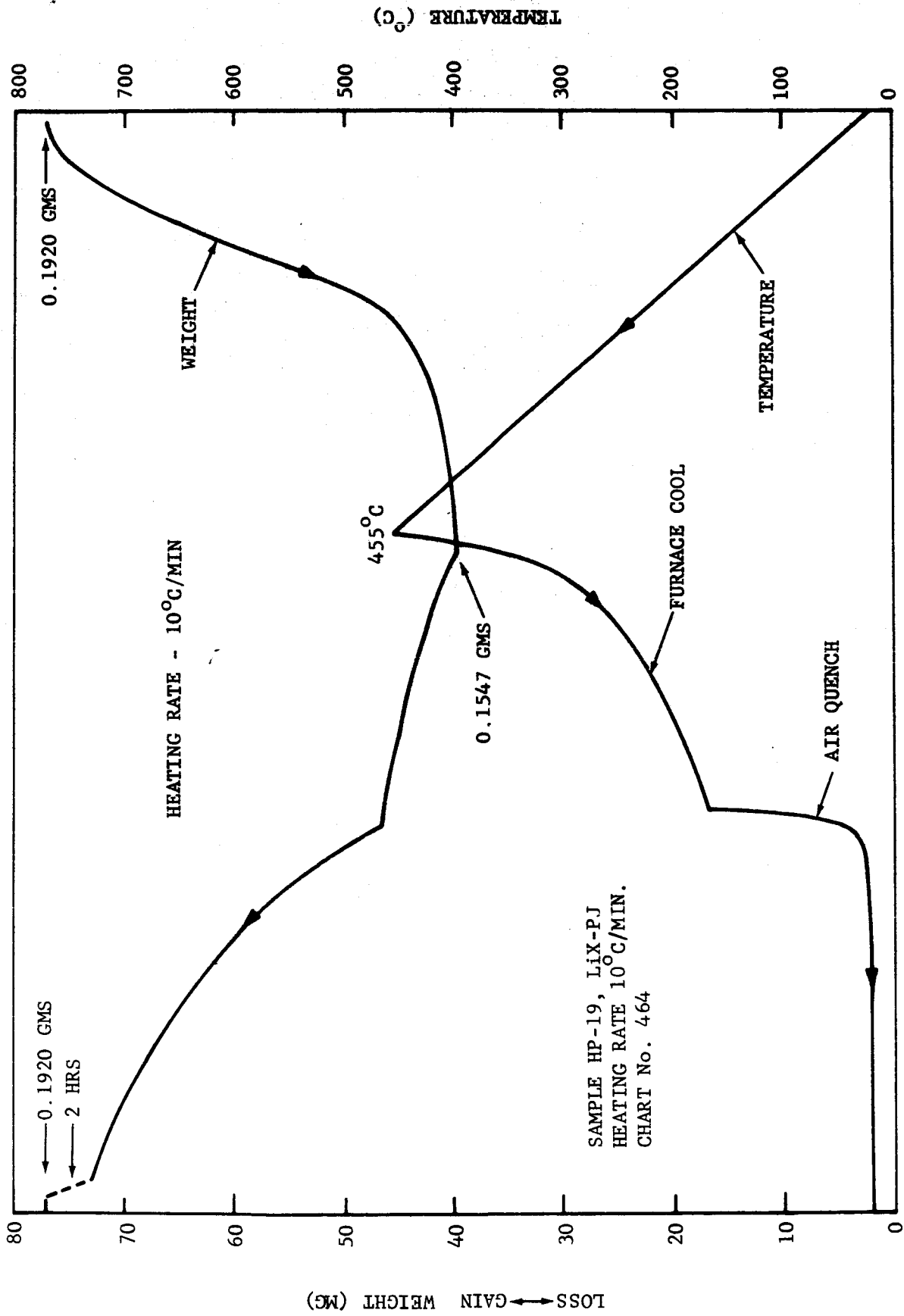
FIGURE 23. TGA CHART FOR LITHIUM ZEOLITE.

R13763

TEMPERATURE (°C)

WEIGHT

0.1920 GMS

HEATING RATE - 10°C/MIN

455°C

0.1547 GMS

TEMPERATURE

FURNACE COOL

AIR QUENCH

0.1920 GMS
2 HRS

SAMPLE HP-19, LiX-PJ
HEATING RATE 10°C/MIN.
CHART No. 464

LOSS ←→ GAIN   WEIGHT (MG)

TABLE XXVI

CORRELATION BETWEEN TGA AND DENSITY MEASUREMENTS FOR ZEOLITE MEMBRANES

Destination	Zeolite Material	Binder wt. %	Firing ^{o}C/time	TGA % H_2O	Density gm/ml
LiX-PJ	LiX-PJ	None	None	36.3	0.656
			660°/15h	31.6	0.711
			680°/8h	27.8	0.737
			680°/15h	0	1.226
			700°/30m	33.5	0.735
			700°/60m	32.7	0.691
			700°/90m	30.5	0.653
			700°/2h	29.7	0.719
			720°/50m	1.6	0.870
			750°/30m	0	1.879
Z-28	LiX-PJ	H_3PO_4/18	None	22.9	0.879
			680°/30m	11.9	0.968
			680°/45m	11.1	0.957
			680°/90m	5.9	1.053
			690°/30m	7.9	1.061
			700°/30m	4.9	1.074
Z-29	LiX-PJ	$Na_2Si_2O_5$/16	None	33.4	0.794
			620°/1h	2.4	0.931
Z-17	NaX	None	None	32.6	0.708
			750°/30m	31.6	0.737
			800°/30m	27.5	0.764
			800°/45m	13.4	0.877
Z-14	NaX	H_3PO_4/18	None	29.5	0.810
Z-15	NaX	H_3PO_4/10	None	32.9	0.801
			800°/30m	9.6	1.000
Z-16	NaX	$Na_2Si_2O_5$/21	None	28.1	0.842
			700°/30m	1.0	1.108

h = hours
m = minutes

drying period. Based upon the water retained after this period, the porosity associated with a zeolite structure was about 2.3%. This corresponds to a value of 2.6% weight gain when the results are presented in a manner similar to the TGA results of Tables XXV and XXVI. These results would seem to indicate that membrane treatments which destroy the zeolite structure do not necessarily lead to a nonporous material.

In order to determine the extent of thermal coefficient variations and associated seal problems, additional thermal expansion data were obtained on various zeolites and zeolite compositions developed in this program. A Leitz Dilatometer, Model NTV with a Mirror Galvanometer Attachment, was used for these measurements. A sketch of the dilatometer is shown in Figure 24. The sample was placed between the quartz sample holder and the quartz push rod. The thermal expansion of quartz is sufficiently low that it was negligible in comparison to the sample. Expansion and contraction of the sample caused a corresponding movement in the push rod. Movement of the push rod changed the angle of the mechanical mirror causing a deflection in the light beam proportional to the sample expansion or contraction. A thermocouple in the immediate vicinity of the sample was used to measure the sample temperature. The emf developed by the thermocouple rotated a mirror attached to a galvanometer coil. This galvanometer mirror caused a deflection of the light beam which was proportional to temperature and at right angles to the deflection caused by the sample expansion. The deflections of the light beam were recorded on a photographic film. The effects of melting and impregnation of the membrane material by the LiCl-KCl eutectic were also determined by placing a small amount of eutectic on the center of the dilatometer sample. Care was exercised to prevent the molten salt from reaching the juncture of the ends of the sample and the dilatometer push rods.

The most interesting point noted in the dilatometry investigation was the fact that the greater the amount of retained active zeolite, the greater the anomaly in the respective thermal coefficients of expansion. Typical results are shown in Figures 25 and 26. The starting point of each curve

SAMPLE

THERMOCOUPLE

FURNACE

SAMPLE
HOLDER

COOLING
COLLAR

LIGHT
SOURCE

PUSH
ROD

MECHANICAL
MIRROR
FOR
EXTENSION

LIGHT
BEAM

MIRROR
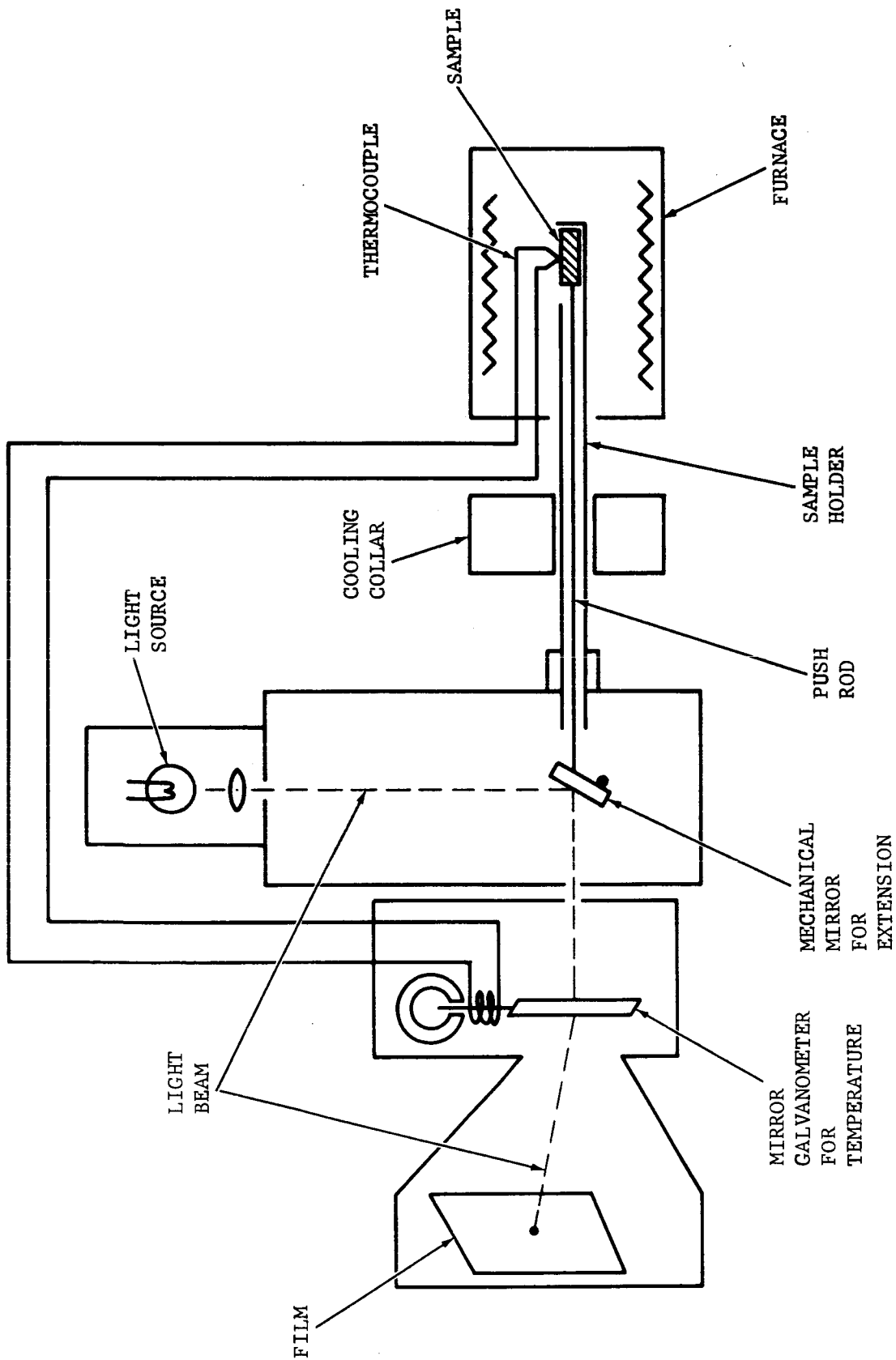GALVANOMETER
FOR
TEMPERATURE

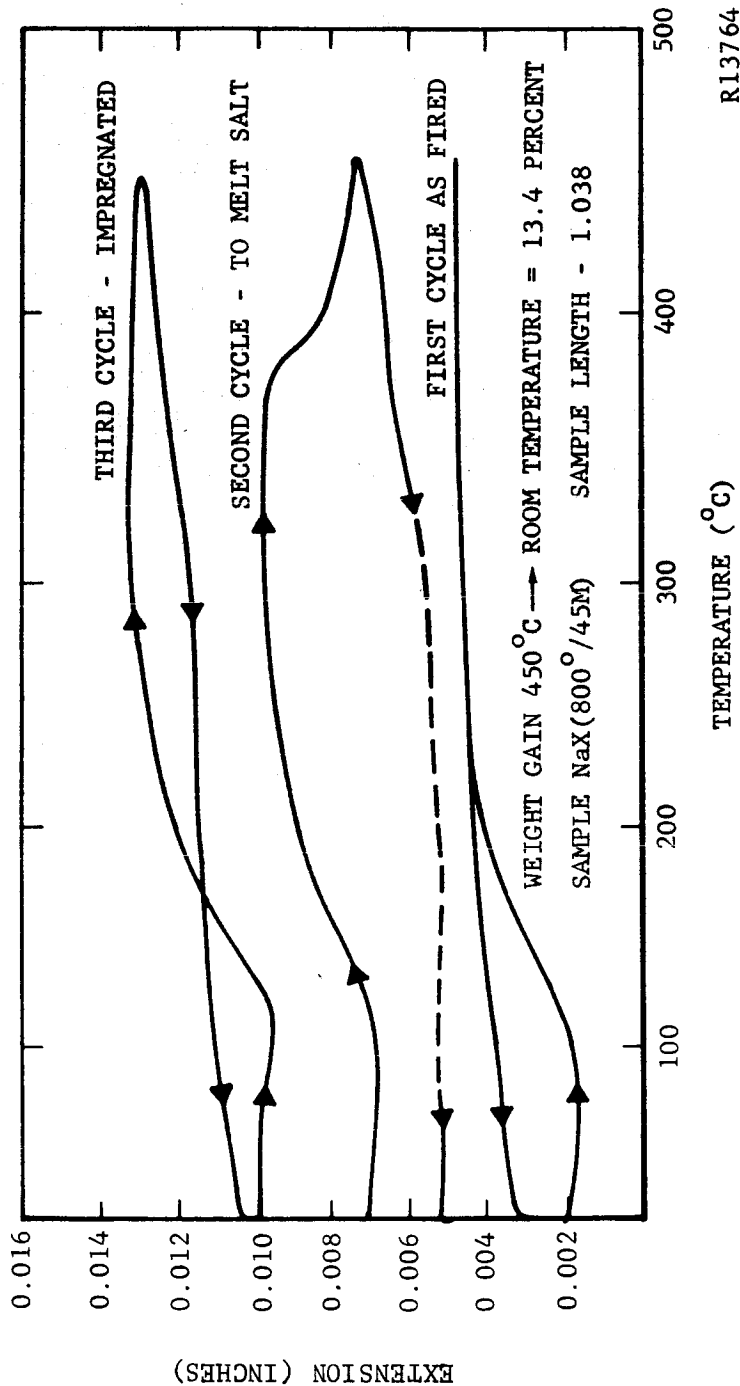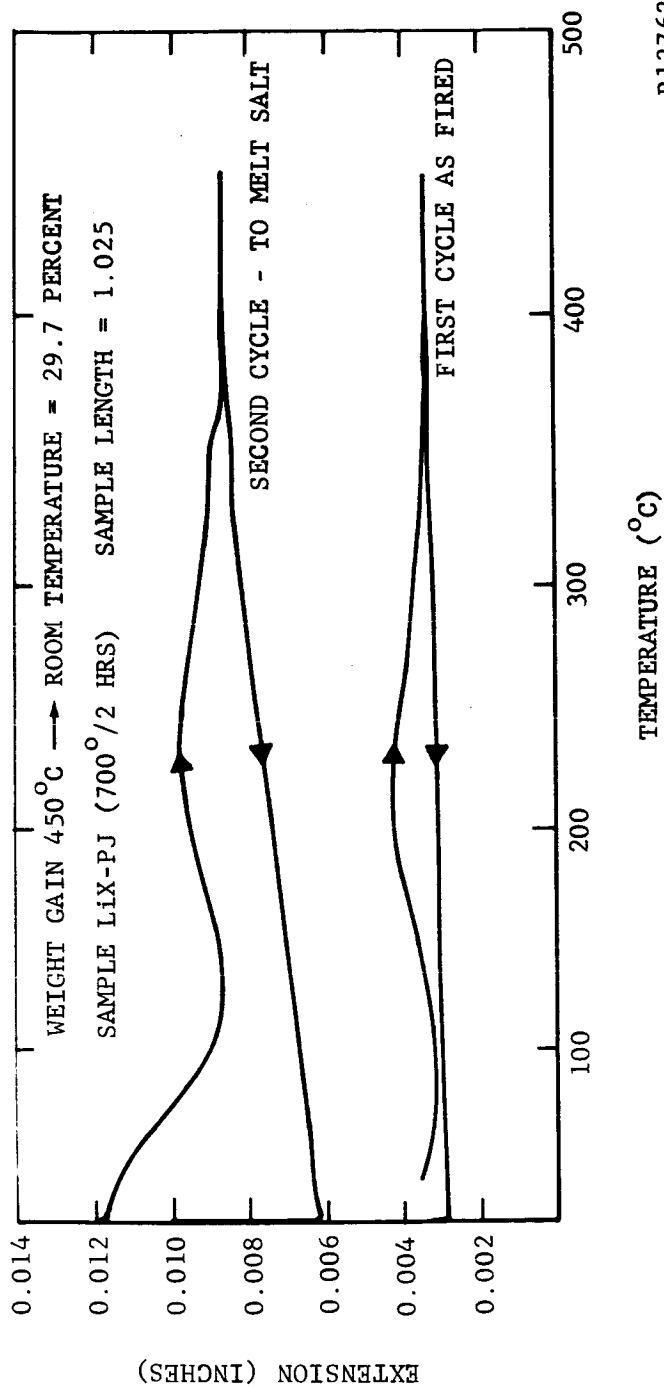FILM

FIGURE 24.   .:::   DILATOMETER

FIGURE 25. DILATOMETRY CHART FOR NaX.

FIGURE 26. DILATOMETRY CHART FOR LiX-PJ.

R13762

was shifted on the expansion axis to permit the recording of several curves for each sample. Initially no special precautions were taken to minimize moisture uptake by the samples prior to the dilatometry experiments. This point was particularly important with samples which had a large amount of zeolite structure. Under these conditions, it is expected that the return trace, i.e. when the sample is cooling, might be more characteristic of the expansion and contraction of the dehydrated samples. The initial shrinkages shown in the dilatometry curves were associated with moisture uptake and reactivity. The "amorphous" phase decreased this effect until the expansion line became eventually straight and assumed a linear expansion rate. The large shrinkage at the melting point of the eutectic shown in the second cycle for NaX in Figure 25 could account for the loss of rigid seal integrity during cell activation. Another key factor is shown in Figure 26 in which active LiX-PJ displayed very little thermal expansion. Because of its extremely low thermal expansion, rigid sealing of LiX-PJ materials would be limited to quartz or low expansion lithium-aluminum silicates. Both would require the additional development of a low expansion sealing glass. A second approach would require the use of flexible seals such as variations of the silicone elastomers, or inert gasket type seals utilizing inorganic fibers or soft noble metals.

5.2.4 ZEOLITE RESISTIVITIES

a. Methods

Zeolite resistivities were measured in the presence and the absence of fused salts. Measurements in the absence of fused salts were made with metal electrodes in intimate contact with the pellet. When the zeolite pellets were fabricated by vacuum, hot pressing, gold foil electrodes could be pressed onto the faces of the zeolite pellets during fabrication. In these cases, the fabrication method described in Section 5.2.3 was modified by placing thin gold foil electrodes on the top and the bottom of the powdered zeolite before heat and pressure were applied.

When other fabrication techniques were used, attempts to press foil elec-

trodes onto the surface of the fabricated pellets were unsuccessful because of poor contact and/or pellet breakage. The use of "conductive" paints and adhesives to form electrodes onto fabricated pellets was unsuccessful because of penetration of the paint or adhesive into some of the porous pellets.

For fabricated pellets attempts were made to achieve contact with the pellet with aluminum cr gold foil electrodes held against each side of the samples. To provide better contact between the foil and the pellets, pads of Fiberfrax, 2 mm thick, were used to back the metal foil. The Fiberfrax-backed foils were held against the pellets with the platinum contacts of the conductivity cell. Experimental results reported below indicated that incomplete contact with the surface of the pellet was giving rise to high resistance measurements. Only a limited amount of effort was expended on methods utilizing liquid metal contacts before this method was dropped in favor of evaporated gold electrodes.

Considerably better results were obtained with gold electrodes placed on the surface of the membrane by vacuum evaporation. Initially, some difficulty was encountered in the vacuum deposition of gold electrodes. The major problems were: (1) penetration of the gold into the samples, (2) lack of continuity in the evaporated gold film, and (3) breakage of many samples due to handling. The use of thicker membranes for conductivity measurements and improved vacuum depositing techniques led to very satisfactory results with this method.

For resistance measurements in the absence of fused salts the conductivity cell, shown schematically in Figure 27, was used. The conductivity cell was connected to a vacuum system capable of operation at pressure of $<10^{-6}$ mm of Hg. The interior of the cell was made of quartz to permit measurements at temperatures up to $1000^{o}C$.

In operation the zeolite pellet with its metal contacts was placed in the conductivity cell. The sample was completely dehydrated in the cell by slowly heating to $400^{o}C$ while holding the pressure at 10^{-5} to 10^{-6} mm.
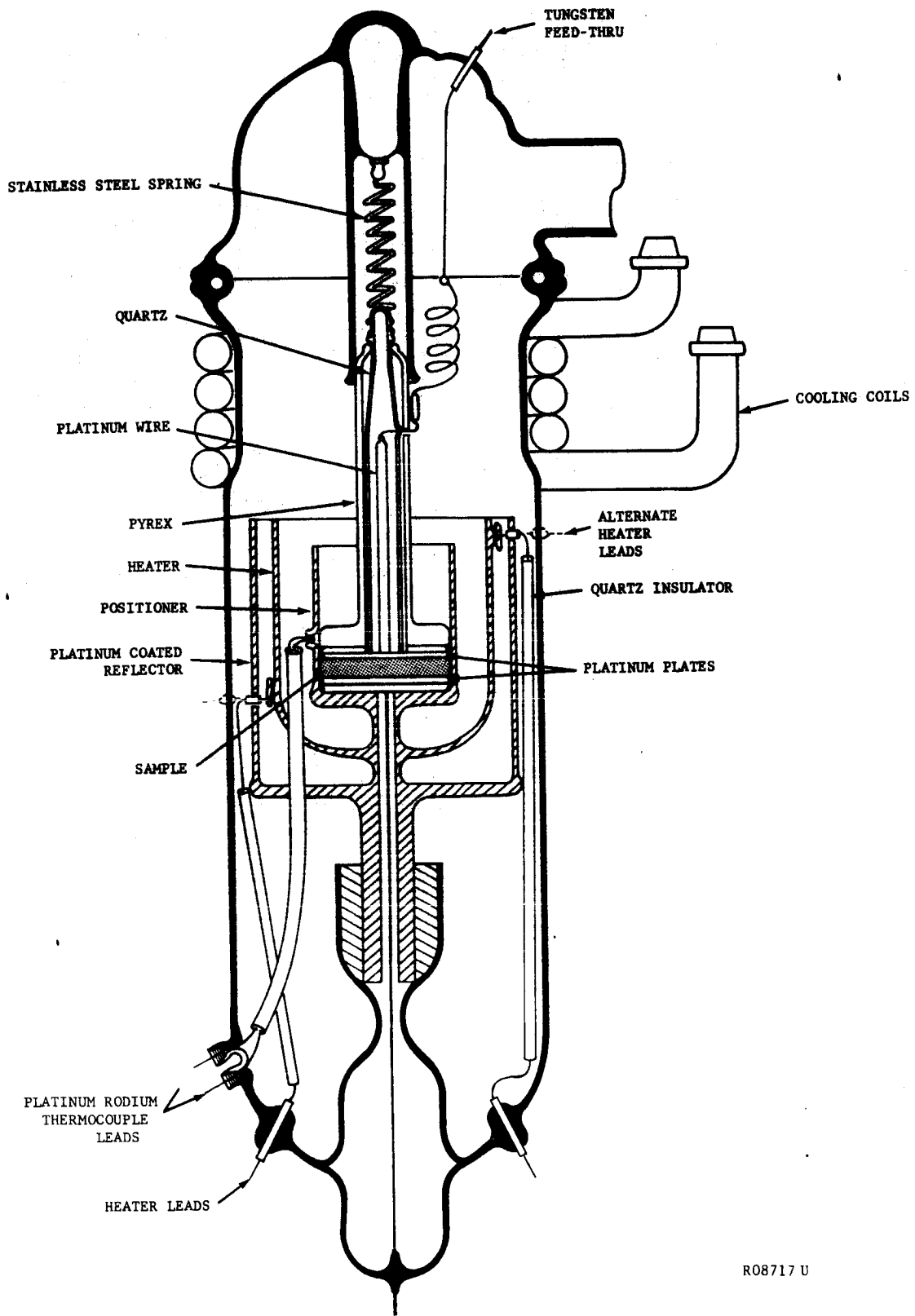
FIGURE 27. CONDUCTIVITY CELL

Resistance measurements were made at 1000 cps using an Electro-Measurement, Inc. Impedance Bridge Model 250-DA. When required for sharper balance, an external capacitor was connected across the "C" terminals of the bridge. This external capacitor was a Cornell-Dublier Model CDB3 variable in 0.0001 mfd. steps from 0.0001 to 10 mfd. A Hewlett-Packard VTVM, Model 400D or a Tektronix Oscilloscope, Type 502A was used as the external detector. Use of the equipment in this manner resulted in measurements of the sample as an equivalent circuit composed of a resistor and a capacitor in parallel.

For measurements of the resistance of the pellets in the presence of fused salts, cells of the type shown in Figure 28 were used. Cells of this type required that the pellet be sealed or attached to the support tube. In Figure 28A, molten bismuth metal and the LiCl-KCl eutectic were used in both compartments of the cell. The liquid metal ensured a uniform metallic contact on both sides of the zeolite membrane. The membrane was allowed to soak in the eutectic melt for about one hour and then was lowered into the bismuth pool. Tungsten electrodes were placed in contact with the molten bismuth in both compartments. The resistance of the cell was measured with a conductivity bridge (Industrial Instruments, Inc. Model RC21632) operating at 1000 cps.

In later tests where only the resistivity of the membranes was desired or where the progress of salt penetration was to be followed from resistance measurement, the cell shown in Figure 28B was used. This cell consisted of a Vycor test tube containing Pyrex or alumina tubes supporting pellets of the membrane materials under test. The tubes were filled with the eutectic melt and immersed in more of the melt at $415^{o}C$. By means of tungsten electrodes immersed in the electrolytes, inside and outside the inner tube, the resistance across the pellet was measured with the conductivity bridge. The impregnation was performed under vacuum. Resistance measurements were made at atmospheric pressure.

In an effort to eliminate many of the problems associated with seals
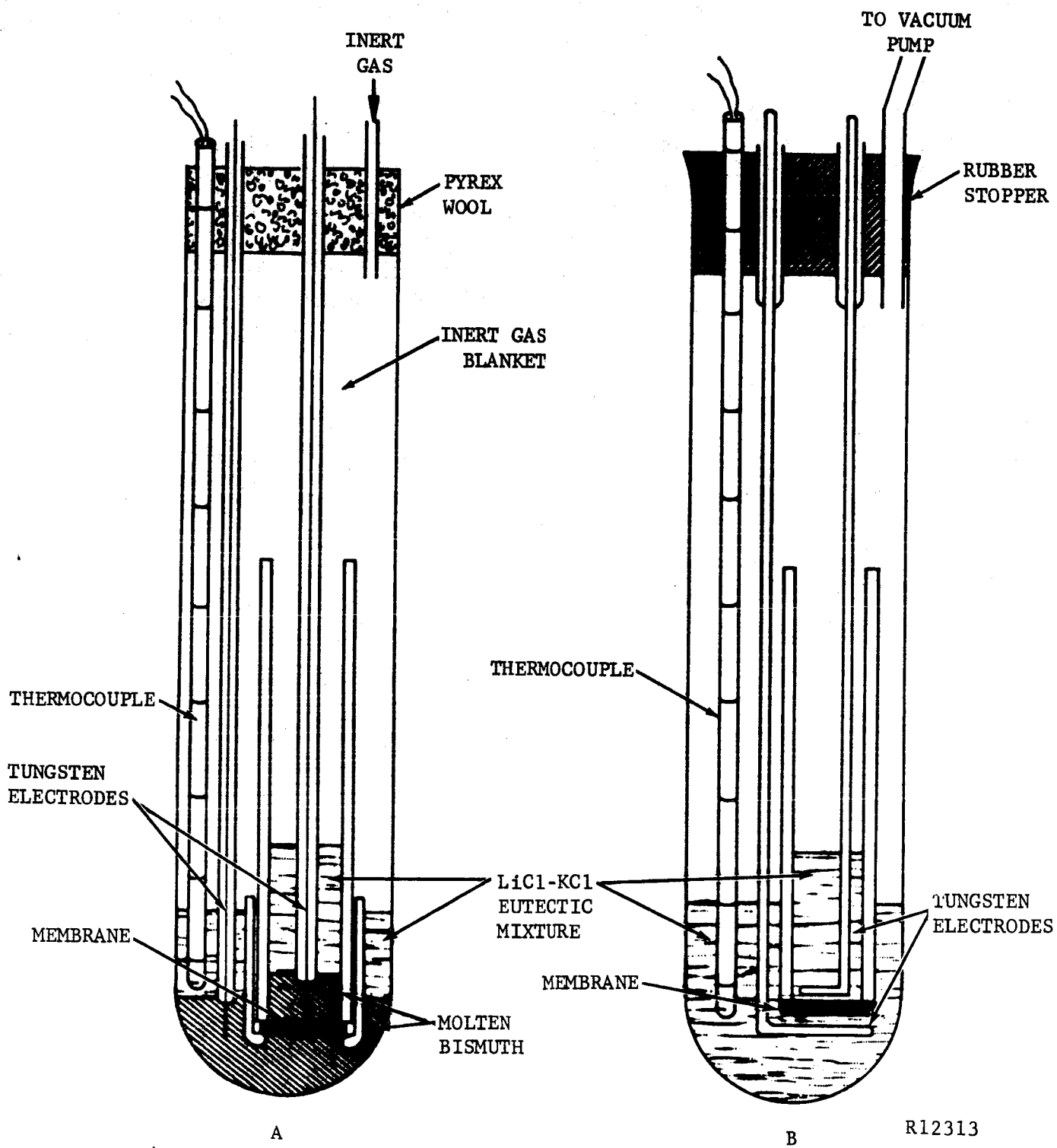
FIGURE 28. CONDUCTIVITY CELLS FOR MEASUREMENTS IN FUSED SALTS

between the membrane pellet and the support tube, the cell shown in Figure 29 was designed. In this cell the pellet was held between two glass tubes. Flexible gaskets used between the ends of the glass tube and the pellets were used to seal the pellet and separate the two electrolyte compartments. Tungsten electrodes in each compartment were used in conjunction with the conductivity bridge to measure resistances. This cell permitted the use of a variety of gasket materials.

In some cases d.c. resistance measurements were made on pellets which were acting as separators in complete cells. The d.c. resistances were calculated from the IR drop measured with the polarizer described in Section 4.1.1.

b. **Results in the Absence of Fused Salts**

The resistivities of NaA, NaX, NaY, LiX, LiY, AgX, LiX-PJ, and LiKX(aqueous) were determined as a function of temperature in the absence of fused salts. The effect of fabrication conditions, binders, and bonding techniques was investigated. The preparation of the various zeolites is described in Sections 5.2.1 and 5.2.2. The results are presented graphically in the form of Arrhenious type plots (log resistivity vs. the reciprocal of the absolute temperature).

The effect of zeolite type upon the resistivity of zeolites in the sodium ion form is shown in Figure 30. These pellets were prepared by vacuum, hot pressing with pressed gold foil electrodes. The Type Y zeolite was prepared according to the procedure given in Section 5.2.1. The diffraction pattern was that of a Type Y zeolite (Table XV). The activation energy for conduction for NaY was found to be 15.0 kilocalories per mole. Calculations using the activation energy yield the following composition of the unit cell after dehydration

$$Na_{63} \left[(AlO_2)_{63} \quad (SiO_2)_{129} \right]$$
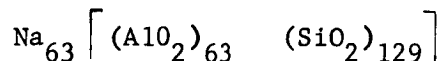
This composition for the unit cell is somewhat different from that reported in the literature, but confirms the observation that the chemical

PYREX
WOOL

INERT
GAS

GLASS TUBES

ELECTROLYTE

TUNGSTEN
ELECTRODES

GASKETS

MEMBRANE
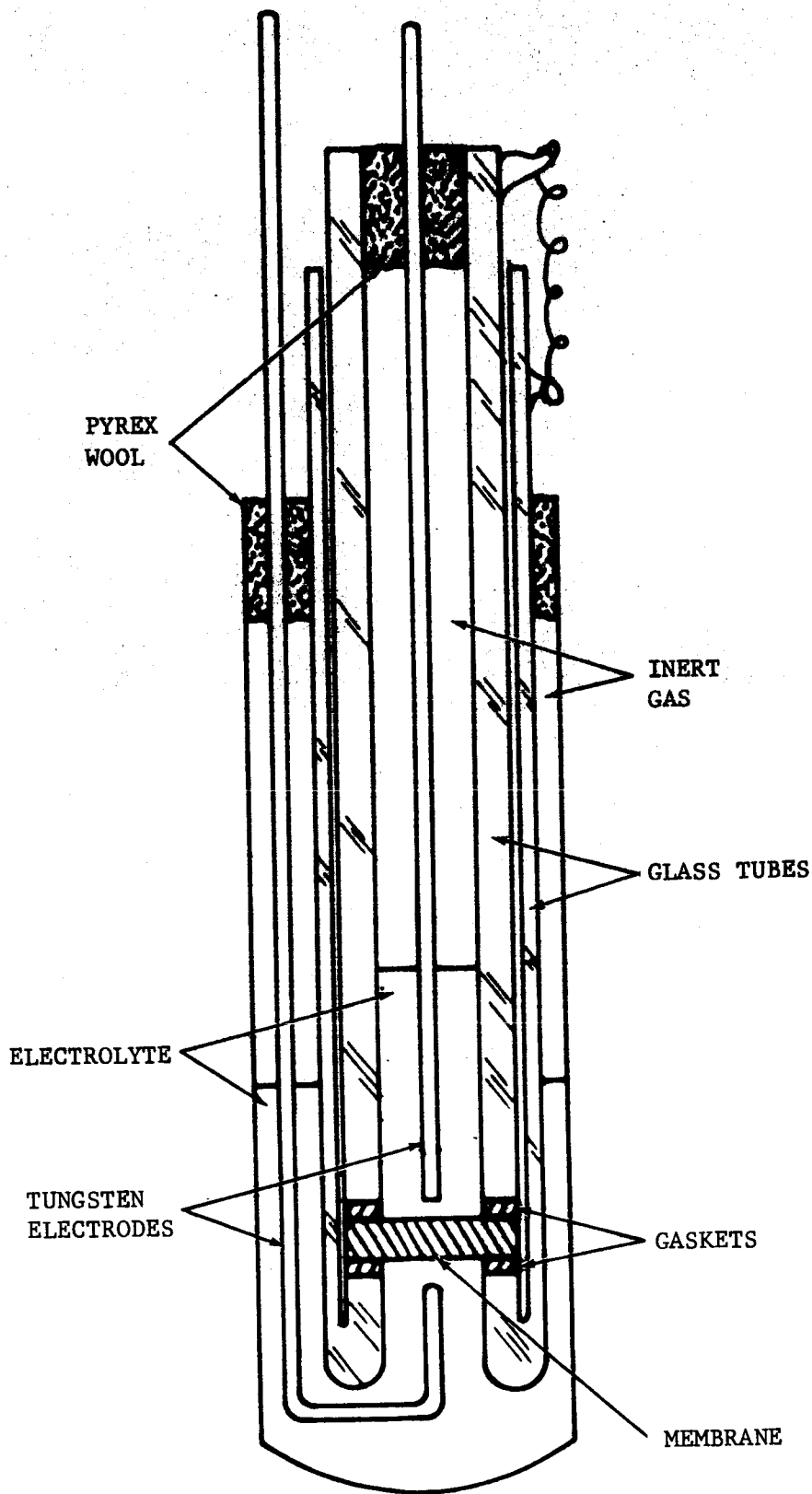
R13767

FIGURE 29. CONDUCTIVITY CELL WITH GASKET SEALS
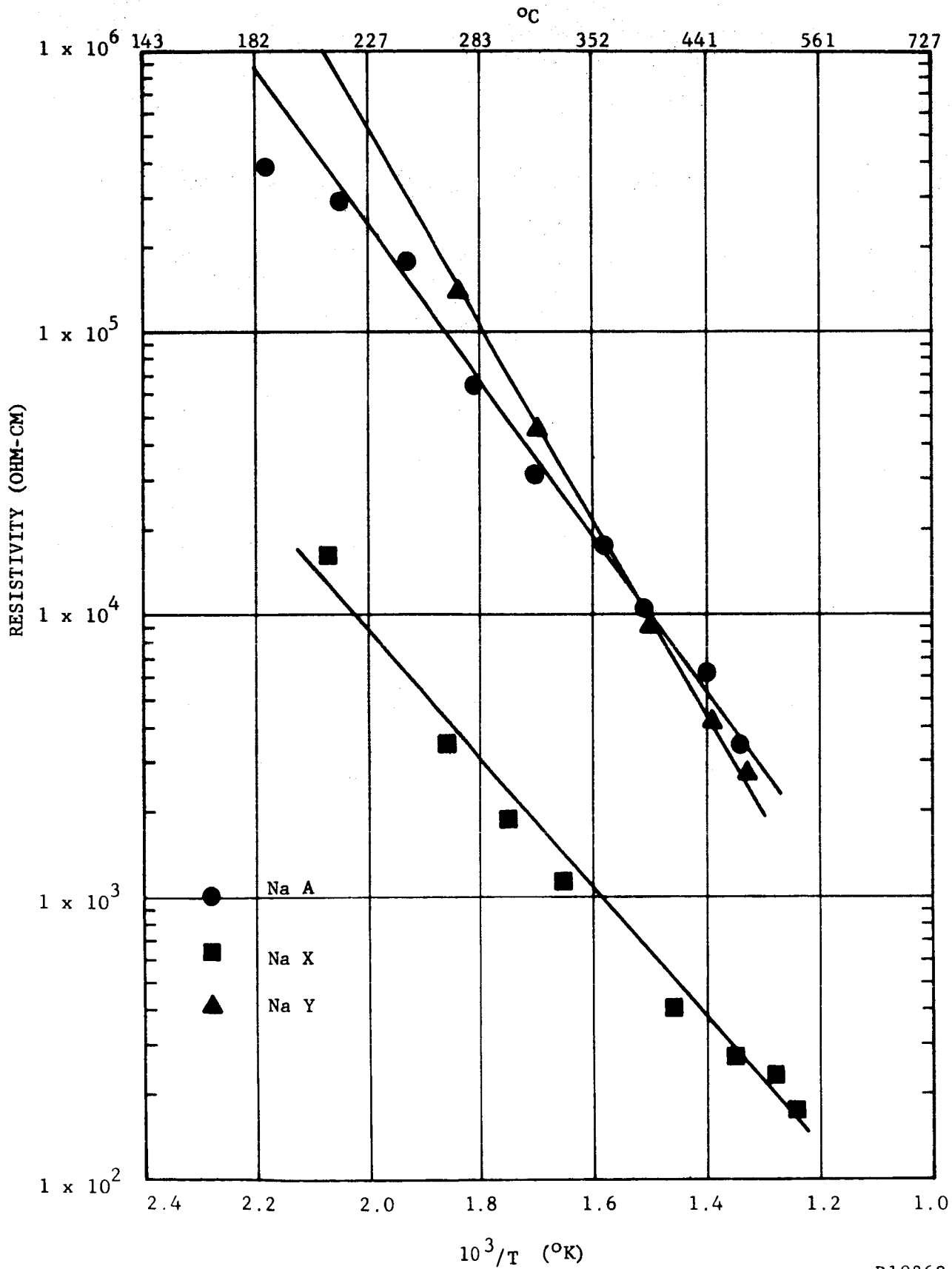
FIGURE 30. EFFECT OF ZEOLITE TYPE ON RESISTIVITIES OF SODIUM ZEOLITES

R10262

composition and hence, to a certain extent, the properties of the zeolites can be altered without changing the zeolite type.[20]

Both phosphoric acid and sodium silicate were used as bonding agents for the fabrication of thin zeolite membranes. The effect of these sintering aids upon the resistivity of NaA zeolite was investigated. For these investigations dry powders of either the pure NaA zeolite or NaA zeolite containing the desired sintering aid were fabricated into thin membranes having integral gold foil electrodes by the vacuum hot pressing technique. The results for the NaA and NaA containing phosphoric acid and sodium silicate are shown in Figure 31.

The silicate sample (Z-3) contained 20 weight percent of $Na_2O \cdot 2SiO_2$ and the phosphoric acid sample (Z-5) contained 18% phosphoric acid and 2% of an aqueous solution of polyvinyl alcohol. As the experimental results indicated, the addition of either phosphoric acid or sodium silicate caused an increase in the resistance of vacuum hot pressed NaA membranes. This effect of silicate was much smaller than that of phosphoric acid. A much greater increase in resistivity was noted with the H_3PO_4 treated material. It appears that the H_3PO_4 interacted with the zeolite alumino-silicate lattice in such a way as to reduce either the number of charge carriers or their mobility. This effect has also been noted with other acids.

Zeolite membranes prepared by sintering at higher temperatures using H_3PO_4 or sodium silicate as a binder had a smooth, hard surface. No suitable method of attaching gold leaf electrodes for conductivity measurements could be found for these membranes. Therefore, two other methods of attaching metallic electrodes were tried. In the first method, a silver electrode was formed on the surface of the fired zeolite membrane by covering with a silver conducting paste. This method was unsuccessful because of lack of adequate contact in some cases and penetration into porous pellets in other cases.

Considerably better results were obtained with gold electrodes placed on the surface of the membrane by vacuum evaporation. Figure 32 compares the
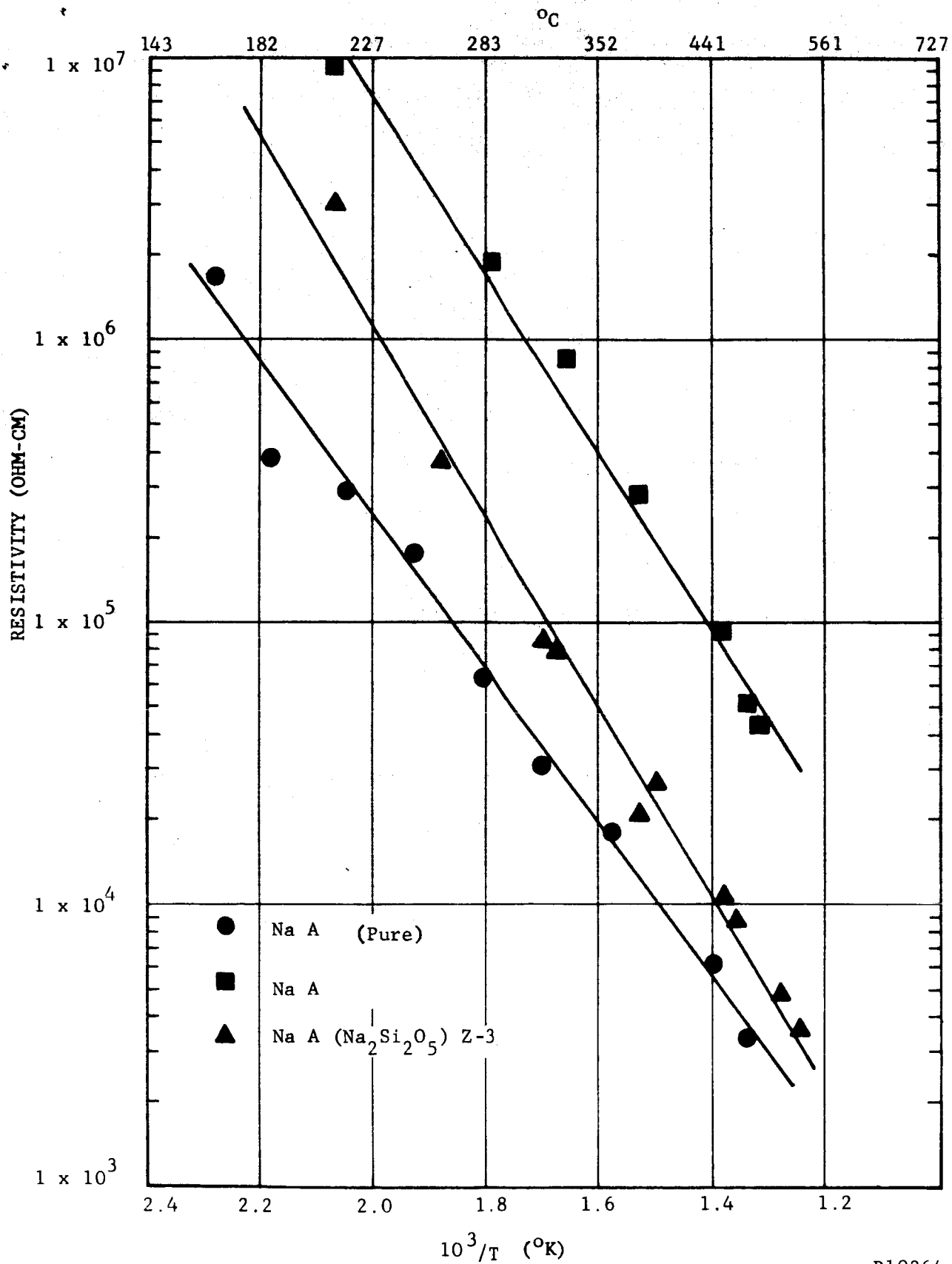
FIGURE 31. EFFECT OF H_3PO_4 AND $Na_2Si_2O_5$ BINDERS ON RESISTIVITY
OF NaA ZEOLITES

R10264

-117-
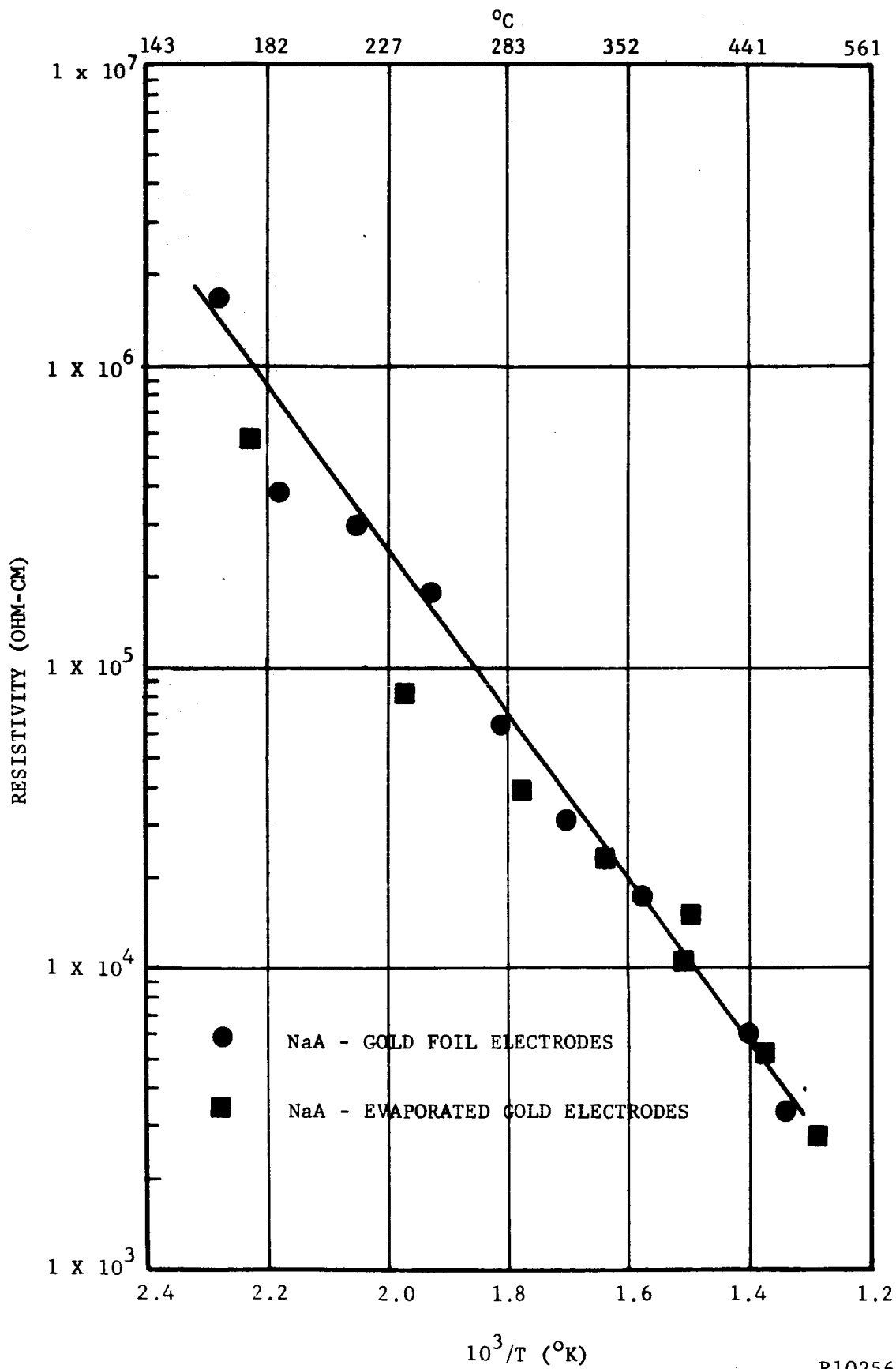
FIGURE 32. COMPARISON OF GOLD FOIL AND EVAPORATED GOLD ELECTRODES.

resistivity of hot pressed NaA membranes with gold leaf and with evaporated gold electrodes. The results indicated practically no difference in the two techniques. Thus vacuum evaporation of gold appeared to be one suitable method of attaching electrodes to formed zeolite pellets.

The effect of heat treatment at $740^{\circ}C$ and phosphoric acid upon the resistance of NaX is shown in Figure 33. The hot pressed membranes were made in the usual manner. The phosphate bonded zeolite (Z-14, 27 weight% H_3PO_4) had been heated to $740^{\circ}C$. Evaporated gold foil electrodes were used. From the results it appeared that the NaX could be heated to approximately $700^{\circ}C$ with no change in resistance unless phosphoric acid was present. In the experimental work upon bonding of NaX pellets, it had also been found that treatments at these higher temperatures would result in the loss of some zeolite structure.

It is readily seen that the Type X resistance is lower than that of the other types. Thus efforts were concentrated on this type of zeolite. The effects of several cations contained in Type X zeolites and to a certain extent fabrication techniques are shown in Figure 34. These measurements were made with aluminum foil electrodes pressed against the surface of the pellets. The material designated LiX-PJ ($700^{\circ}C$/90 minutes) was cold pressed and then sintered at $700^{\circ}C$ for 90 minutes. No binder was used. Both the thermal gravimetric analysis and x-ray diffraction patterns show a considerable amount of zeolite structure remained. The sample designated LiKX(1200#) was prepared by pressing a 1.27 cm diameter pellet of LiKX at a total force of 1200 pounds. No binder or thermal treatment was used. The LiKX was prepared by exchange of NaX with an aqueous solution having the composition of the LiCl-KCl eutectic. Since no thermal treatment was used, the zeolite structure was retained. The sample designated LiX-PJ(1100°) was fired at $1100^{\circ}C$ to destroy the zeolite structure. The Li porcelain material was prepared by exchange of an NBS porcelain with molten $LiNO_3$ as described in Section 5.1.1. The NaX sample was prepared by first calcining NaX at $950^{\circ}C$ for 30 minutes to destroy the zeolite structure. The resulting material was then pulverized, pressed, and finally sintered at $1260^{\circ}C$ for
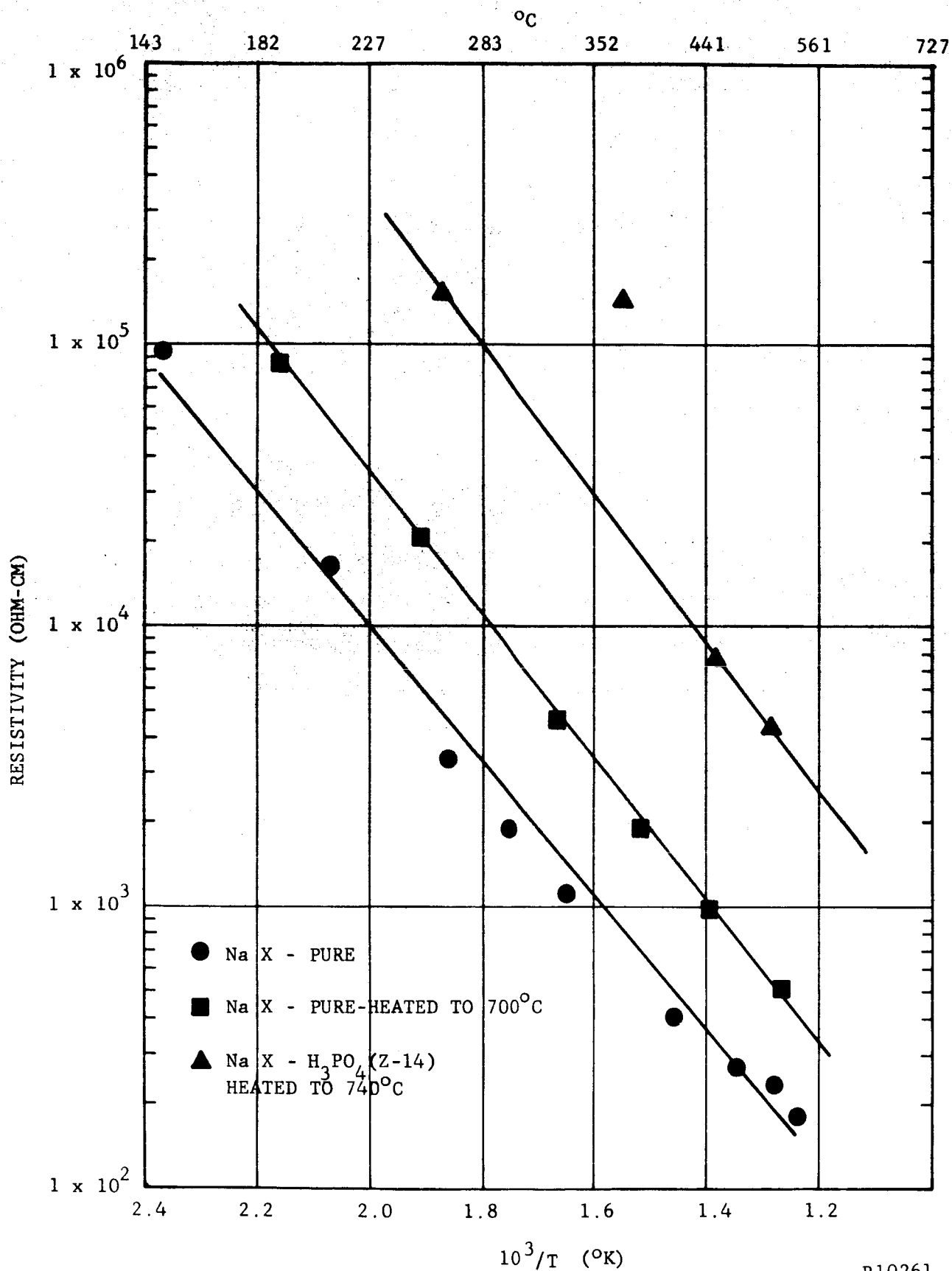
FIGURE 33. EFFECT OF HEAT TREATMENT AND H_3PO_4 ON THE
RESISTIVITY OF NaX

R10261
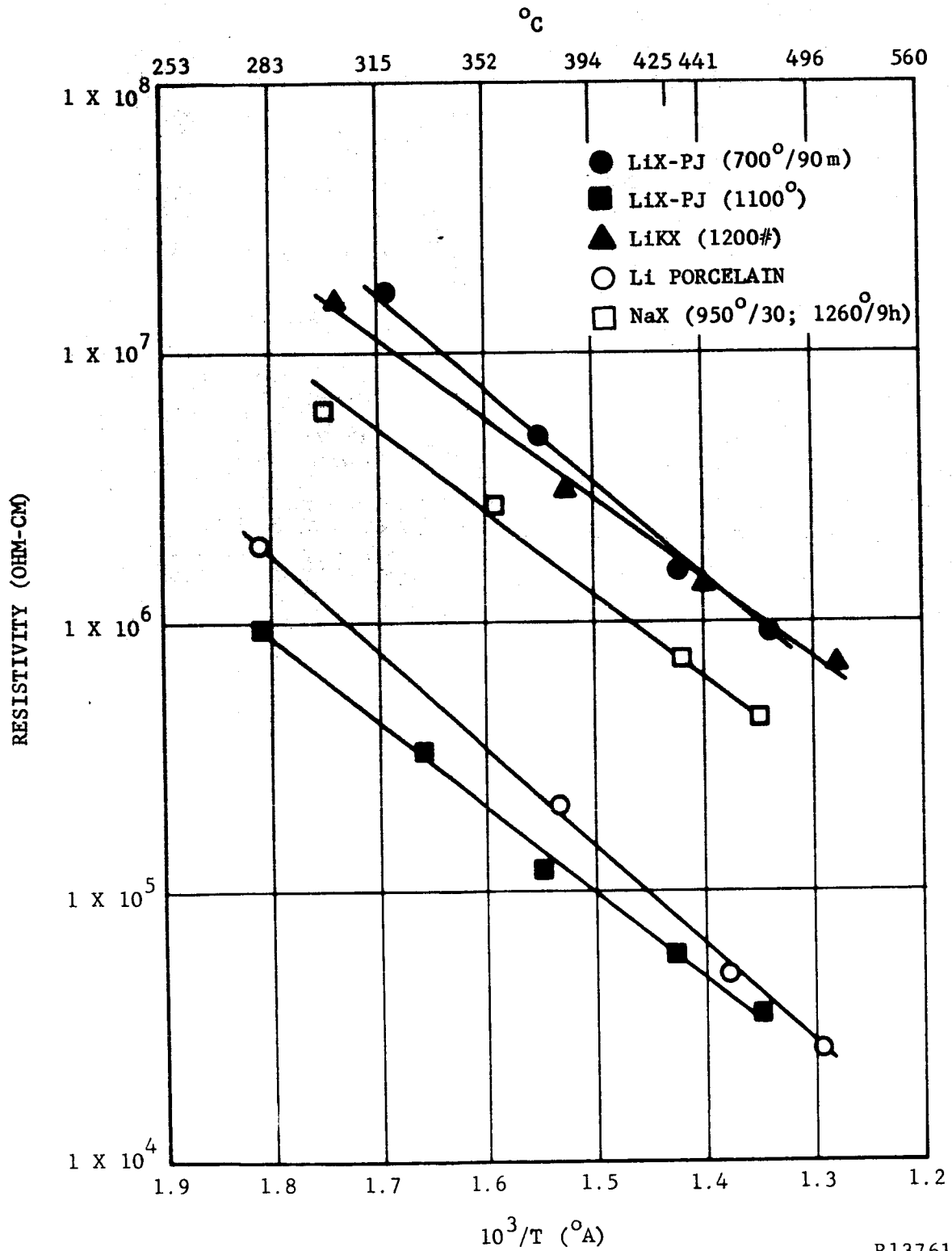
FIGURE 34.   RESISTIVITY OF ZEOLITE AND PORCELAIN MEMBRANES.
ALUMINUM FOIL ELECTRODES.

-121-

9 hours.

It would appear that the lithium containing nonzeolitic material have lower resistivities than the corresponding zeolitic materials. By contrast, when Na containing zeolitic materials were subjected to treatments which destroy the zeolite structure, the resistivity was found to increase. (See Figures 31 and 32.) Substitution of Li for Na in zeolites is also known to increase the resistivity. These results would indicate that the conduction mechanism in zeolites and in porcelain materials was different.

These resistivity measurements with aluminum foil electrodes were considerably higher than those reported previously. A series of experiments were performed to determine if the method of contact was responsible for the higher resistance. The results are shown in Figure 35. A pellet of NaA with gold electrodes was prepared by vacuum hot pressing according to the procedure given in Section 5.2.3. After the resistivity measurements were made the pressed gold electrodes were removed and measurements made with aluminum foil and gold foil electrodes backed with Fiberfrax. Finally, resistance measurements were made by contacting the pellet with a thin layer of a 50/50 weight percent tin-lead alloy which was molten at the temperatures of measurements. Not too much significance should be attached to this latter measurement. Damage to the pellet because of repeated handling along with a very thin layer of liquid alloy might have given rise to poor contacts and thus high results. However, the experiments do indicate that solid electrodes would be expected to give high pellet resistivities because of poor contacts.

Efforts were then renewed with evaporated gold electrodes. Vacuum evaporated gold had been shown to be suitable as electrodes for vacuum, hot pressed pellets (Figure 32). However, with other fabricating techniques, this method of electrode attachment presented some difficulties. These difficulties were essentially due to the rough and more porous surface of the zeolite pellets. It was found that a considerably heavier gold deposit was necessary to achieve a continuous gold film. Figure 36 shows some of
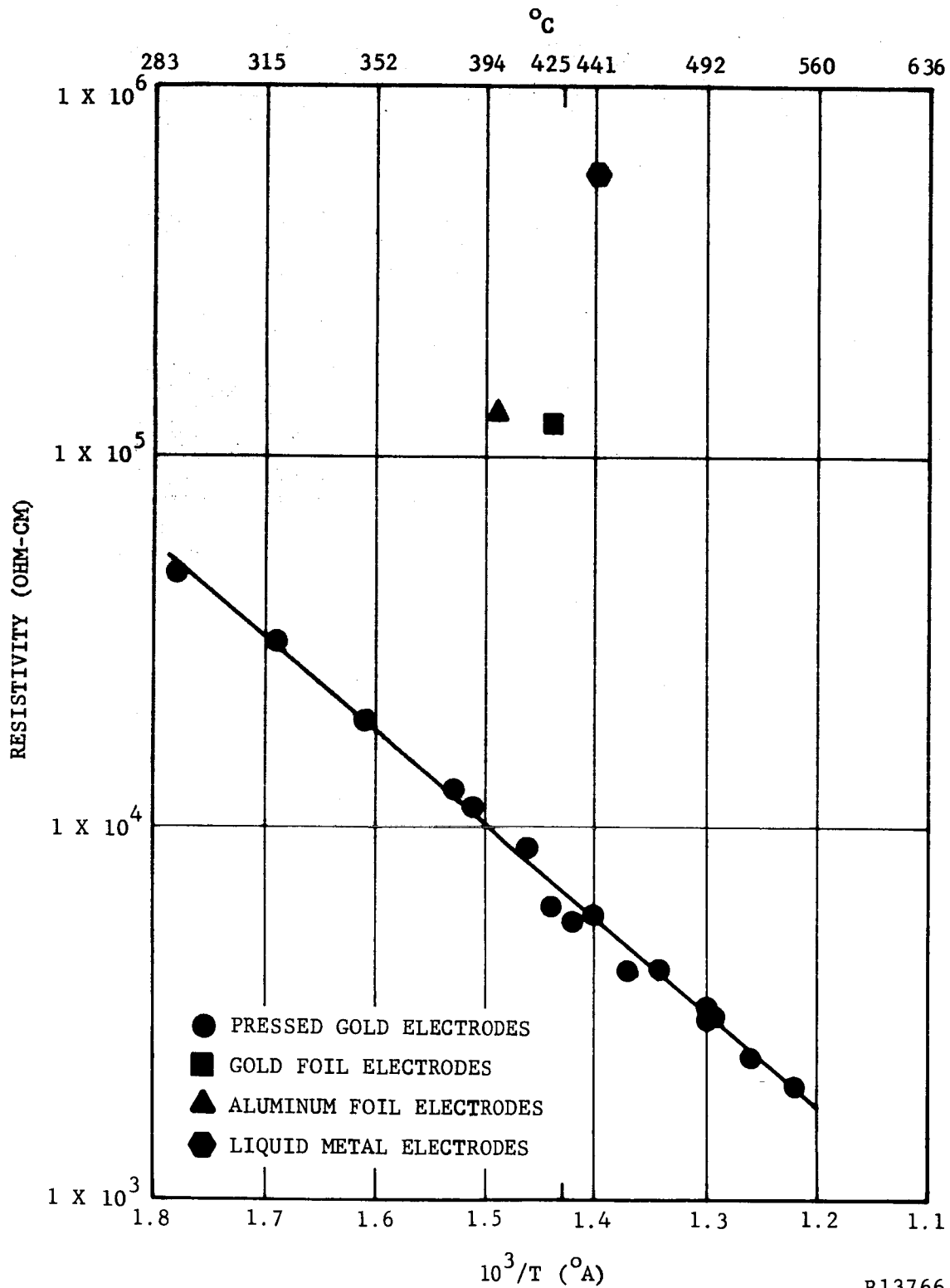
FIGURE 35. COMPARISON OF METHODS OF ELECTRODE CONTACTS.
NaA MEMBRANES.

R13766

-123-
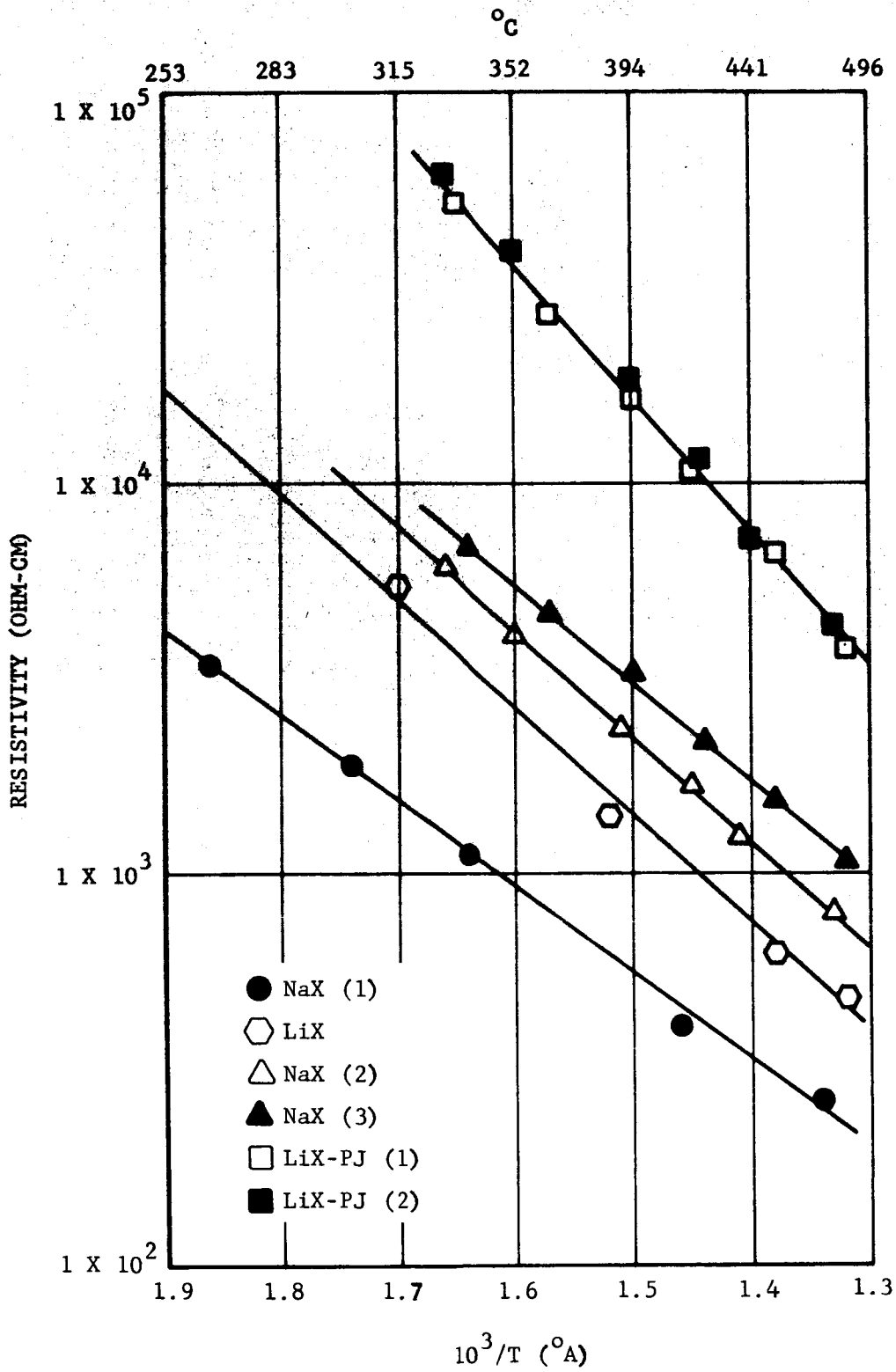
FIGURE 36. RESISTIVITY OF TYPE X ZEOLITES.

R13765

the results obtained with this heavier gold deposit.

Figure 36 also shows the effect of the cation type of variations in the vacuum hot pressing technique, and of the presence of a salt impurity as well as the reproducibility of the measurements. The sample markes NaX(1) had been formed by vacuum, hot pressing at 700 kgm/cm^2 and 150°C early in the program. Later, the pressing pressure and temperature were increased to produce stronger pellets. Samples marked NaX(2) and NaX(3) were formed at 2000 kgm/cm^2 and 200°C. They represent duplicate runs. The sample marked LiX was known to be a lithium exchanged zeolite containing additional LiCl. The samples marked LiX-PJ(1) and LiX-PJ(2) are duplicate runs of a lithium exchanged zeolite containing no additional salts. The effect of salt inclusions upon the resistivity is quite apparent and pronounced. All pellets were formed by vacuum hot pressing. Samples NaX(1) and LiX had gold foil electrodes. Samples NaX(2), NaX(3), LiX-PJ(1), and LiX-PJ(2) had vacuum, evaporated gold electrodes.

c. **Results in the Presence of Fused Salts**

Resistivities of membranes and separators used in complete cells assembled for discharge studies are given in Section 6. Those studies in which only resistivity of the membrane was measured are described in this section. These cells contained no electroactive materials.

An NaA membrane was formed by the vacuum, hot pressing procedure. The membrane was sealed to the inner glass tube with a silicone rubber (RTV560) as described in Section 5.3. Resistivities were measured as a function of time and temperature with a conductivity bridge using the cell shown in Figure 28A. The resistivities are shown in Table XXVII.

TABLE XXVII

RESISTIVITY OF NaA MEMBRANE

Time	Temperature (^{o}C)	Resistivity (ohm-cm)
0	408	20,700
30 min.	441	4,680
60 min.	445	4,080
15 hrs., 55 min.	445	208

The membrane was found slightly crazed after the test but was otherwise intact. The bonding of RTV 560 to the membrane and the Pyrex tube appeared unaffected by the treatment. When breaking the zeolite membrane, glassy material could be observed in contrast with the initial porous aspect of the material.

Experiments were initiated to determine the effect of intercrystalline and intracrystalline inclusion of salts in membranes immersed in ionic melts on the resistivities of these membranes. These results were obtained in a cell of the type shown in Figure 28B. The membrane attached to its support tube was subjected to vacuum for various periods of time. Resistance value obtained while the membranes were under vacuum were very erratic. Therefore, all reported measurements were taken when the cell was at atmospheric pressure. The results of these resistivity measurements and the condition of the membrane are given in Table XXVIII. The composition and fabricating procedures are described in Section 5.2.3.

In an effort to minimize the effects of the sealant upon the measured resistance, a vacuum, hot-pressed LiX-PJ was tested in the electrolytic cell with gasket sealing shown in Figure 29. The membrane was vacuum impregnated with LiCl-KCl at 370° for two hours. The membrane was then clamped between the two Pyrex tubes using gaskets of the silicone rubber, G.E. RTV 560, which had been precured at 370°C. Tungsten electrodes immersed in molten LiCl-KCl were used in both compartments of the cell. The assembly was evacuated to remove the gas pocket from beneath the membrane. The initial resistivity was 10.5 ohm-cm. This value increased slowly at first then very rapidly to about 55,000 ohm-cm. Following re-evacuation, the resistivity was 10.7 ohm-cm then again reached a very high value. In a second experiment, a sample of the cured RTV 560, from which the gaskets referred to above were cut, was placed in LiCl-KCl eutectic melt at 370°C. After evacuation for several minutes, the rubber was examined in the melt at atmospheric pressure. Tiny gas bubbles appeared on the surface of the sample within a few minutes. Presumably, this was responsible for the increase in membrane resistance referred to above.

TABLE XXVIII

RESISTIVITIES OF ZEOLITE MEMBRANES

Membrane Material	Tube Supporting Membrane	Sealant	Initial Resistivity (ohm-cm)	Final Resistivity (ohm-cm)	Duration of Impregnation	Remarks
Z-16*	Pyrex	RTV 560	--	242	3 hours	Part of membrane separated off when retrieving tube from melt
Z-16*	Pyrex	RTV 560	168K	248	12 hours	Membrane cracked
Z-16*	Pyrex	RTV 560	6050	5300	5½ hours	Tiny cracks visible with magnifying instrument
Z-22	AV30	80-20 glass	845	365	40 min.	Partial surface deterioration, no cracks
Z-22B	AV30	80-20 glass	154	154	30 min.	Vacuum not used, membrane cracked
Z-22B	Corning 7052	80-20 glass	945	945	25 min.	Failure of sealant
Z-22	AV30	80-20 glass	129	92	15-3/4 hrs.	Small cracks visible with microscope
Z-25	Pyrex	RTV 560	380K	3.79K	21½ hrs.	Sealed membrane heated to 400°C. for ½ hr. before immersion in fused salt, wetting of membrane prevented by strong hydrophobic action induced by RTV 560
Z-25	Corning 7052	80-20 glass	84	84	25 min.	Membrane cracked
Z-25	Corning 7052	80-20 glass	108	108	25 min.	Membrane cracked.
Z-28	Corning 7052	80-20 glass	86	107	24 hrs.	Membrane uncracked, bond good
Z-28	Corning 7052	80-20 glass	104	167	24 hrs.	Membrane uncracked, bond good
NaX**	Pyrex	RTV 560	11.4K	13.9K	65 hrs.	Small cracks mostly near edge of membrane
NaX**	Pyrex	RTV 560	22K	228	65 hrs.	Small cracks, failure of sealant
LiX**	Pyrex	RTV 560	8.9K	2240	65 hrs.	Membrane cracked throughout; failure of sealant

* Sintered at 700°C. for 30 minutes.

** Vacuum hot pressed.

Shifts of the membrane resistivity from a few ohm-cm to above 23,000 ohm-cm was repeatedly observed following a series of evacuation for time periods up to 60 hours. This seemed to indicate that decomposition of the silicone rubber gaskets in the eutectic melt was still occurring after 60 hours at 370°C under vacuum. It is interesting to note that in this experiment, the zeolite membrane was found intact following a 6-day immersion in fused LiCl-KCl. Furthermore, the electrolyte level in the inside compartment was found to have dropped from slightly over 5 cm at the start of the test to approximately 4 cm at the conclusion of the test. This corresponded to a rate of material transfer of 0.21 gms per day per cm^2 of membrane area under a liquid head equal to 8.4 gms/cm^2. This would indicate that the leakage rate through the pellet and/or around the seal was relatively low.

5.3 SEPARATOR SEALING

Three general methods of sealing were used between the membranes and their support tubes. These methods were rigid sealing with glasses or ceramics, flexible sealing with plastics or silicone rubbers, and pressure sealing with flexible gaskets. In addition to tests of laboratory cells and membrane resistivities, the sealing program was also directed toward the fabrication of complete cells. The eventual battery configuration, as described in Section 7.2 was designed to utilize an alumina ring for membrane support and to provide sealing surfaces for Kovar bellows on each side for the anode and cathode compartments. Suitable sealing glasses were required to mount the membrane and its support on a step in the I.D. of the alumina ring. The feasibility of this approach was applied to the development of glass seals between membranes and 1.27 cm diameter 96% alumina tubes (McDanel AV-30).

Dilatometry experiments and data were accumulated for the materials of interest in order to determine their thermal limitations. Table XXIX indicates that, in general, the Type A zeolite materials exhibited thermal expansions similar to Al_2O_3. However, as noted in Section 5.2.3, the Type

X zeolites on the other hand exhibit low thermal expansion characteristics together with large anomalies in their expansion data.

The initial sealing investigation was conducted with the Type A zeolite membranes utilizing Pyroceram sealing glasses 45 and 95. Thermal coefficients of the sealing glass were modified by blending glasses 45 and 95. Z-16 membranes were readily bonded to 1.27 cm diameter McDanel AV-30 alumina tubes with an 80/20 ratio of glass 45 to glass 95. (This mixture is usually referred to as 80-20 glass.) The lower fusion point of glass 95 also improved the wetting of the intersurfaces during sealing. Sealing was performed in a small tube furnace between 670°C and 700°C for 5 to 7 minutes, the time and temperature being governed by the transformation temperature of the particular zeolite composition.

TABLE XXIX

COMPARISON OF THERMAL COEFFICIENTS OF EXPANSION

Material	α in/in/^{o}C x 10^{-6}	Temp. Range ^{o}C	Remarks
Z-14	6.62	25-600	Sintered 740°C/30 min.
Z-14	9.38	25-600	Sintered 850°C/30 min.
Z-16	7.61	25-600	Sintered 700°C/30 min.
Z-19	14.02	25-600	
NBS Porcelain	5.00	25-600	
Al_2O_3	6.89	25-600	ΔRR Morganite
Pyrex (7740)	3.25	25-600	
Na-Ca Glass (0800)	9.2	0-300	Literature
Kovar Glass (7056)	5.1	0-300	Literature
ZrO_2	10.0	0-1000	Literature, CaO Stabilized
Rodar or Kovar	5.7	30-500	Manufacturers Data

These glasses have exhibited excellent resistance to attack by the LiCl-KCl electrolyte and molten CuCl. In some cases, successful glass seals with the 80/20 glass were made between phosphate and sodium silicate bonded lithium zeolites and AV-30 alumina or kovar glass. The concept of blending the Pyroceram sealing glass 45 and 95 and observing the mode of failure at the seal interface was applied throughout the

program to develop seals between various membranes and appropriate glass or ceramic tube. Glass seal integrity was never reproducibly attained with the Type X materials. The reasons for cell failures with Type X zeolites due to loss of seals became evident during the investigation of simulated cell dilatometry described in Section 5.2.3. Other sealing techniques were attempted using glass resins (Owens-Illinois Type 100) mixed with about 20% by weight of powdered mica. The mixture gave a satisfactory bond with metals such as nickel but not with glass or alumina in the experimental cells.

A material called Imidite (Whittaker Corp., Imidite 850) cured according to the manufacturer's instructions became hard and brittle at $425^{\circ}C$ and therefore was unsuitable for use.

The anomolous expansion behavior of the Type X zeolites when fabricated into rigid membranes seemed to indicate that adequate sealing would require the development of flexible seals or gaskets before the zeolites could be used in high temperature cells. Extensive testing was done with silicone products obtained from General Electric. Materials tested included the silicone resin SR-123 and the silicone rubbers RTV30, RTV106, and RTV560. All of these materials with the exception of the RTV560 became brittle when heated to 370° or higher.

Flexible silicone rubber seals capable of operation in the range of $370-380^{\circ}$ were obtained with RTV560. In the preparation of the seals, one drop of the curing agent was thoroughly mixed with 20 grams of the RTV560. The mixture was then cured first at room temperature for 24 hours, at 120° for 24 hours, and then at increasing temperature increment of about 30° per hour until the temperature reached 370°. The rubber was maintained at this temperature for an additional 20 hours.

RTV560 cured in the above manner was extensively used as a sealant for membranes in spite of the lyophobic action apparently created by a silicone film spreading from the sealant or vapor deposited on all surfaces in the vicinity of the bonded sites. Since the silicone film was destroyed by

sodium and cuprous chloride melts in initial cell experiments, the effect of the lyophobic film on the apparent resistivity of membranes was not truly evaluated until the active materials in the cells were separated from the membranes by the inert LiCl-KCl eutectic melt. In some cases, membranes bonded to supporting tubes with RTV560 were found to be "nonwetted" by the molten LiCl-KCl even after 24 hour immersion at 400°C.

In an effort to remove this volatile component from the curing system and especially the zeolite pellet, curing was attempted under vacuum and in a flowing gas stream. Vacuum curing experiments had to be discontinued because of bubbling and foaming of the silicone rubber during curing.

For the other experiment samples of the uncured silicone rubber and a vacuum, hot pressed NaX pellet were placed on microscope slides and inserted in a 25 mm i.d. glass tube which in turn was placed in a tube furnace. A vigorous stream of compressed air was passed through the tube during the curing operation. The following curing cycle was used: overnight at room temperature, five hours at 110°C, gradual heating (approximately 50° per hour) to 380°C, and finally two hours at 380°C.

At the end of the curing cycle an oily layer was found on the cooler downstream end of the tube. This layer was insoluble in acetone and was not wet by water. No analysis of the material was attempted because of its limited amount.

Following the curing operation, the samples of silicone rubber were removed from the tube and a small amount of powdered LiCl-KCl eutectic was placed on the zeolite pellet. The pellet and eutectic were heated to 400°C while in a stream of dry nitrogen. Upon melting the eutectic formed a sphere on the surface of the zeolite. No evidence of wetting of the zeolite could be observed. This experiment would indicate that neither vacuum curing or curing in a flowing gas system was capable of preventing the formation of a nonwettable pellet in the presence of the silicone rubber.

Experiments completed at the end of the program and described in Section 5.2.4 indicated that cured RTV slowly decomposed with a low rate of gas

evaluation when immersed in molten LiCl-KCl at $370^{\circ}C$. This gas evolution also created difficulties when pressure sealing with gaskets of precured RTV560 was attempted.

A limited effort on the use of Teflon as a flexible sealant or gasket was discontinued when it was completely decomposed within 24 hours when immersed in molten LiCl-KCl for 24 hours. Initially it was found that in air Teflon expanded slightly at first when heated briefly at $425^{\circ}C$. No further dimensional change was observed following reheating at $425^{\circ}C$ for 24 hours. The weight loss was very small and the initial elasticity appeared retained at room temperature.

5.4 POROUS MEMBRANE SUPPORTS

Porous membrane supports were fabricated by dry pressing and sintering. The objective of this work was to develop a porous material thermally compatible with the zeolite membranes. This approach would allow the fabrication of 5 cm diameter 0.25 mm membranes with the thicker porous substrate providing the structural strength.

Table XXX, Porous Membrane Substrate Materials, describes the materials fabricated. The ZrO_2 materials were selected to provide a match for the high expansion zeolites, approximately $10 \times 10^{-6}/^{\circ}C$. All materials fabricated contained open pore structures as shown by their relatively high porosities determined from water absorption measurements. A 5 cm disc, 0.16 cm thick of composition S-4, Table XIII, containing 90% Al_2O_3, 7% H_3PO_4, and 3% ball clay was sintered and lapped. A similar 5 cm disc of zeolite composition Z-14 was dry pressed, sintered, and lapped for mating to the S-4 substrate. An edge seal of the 80/20 Pyroceram blend was successfully achieved between the S-4 substrate and the Z-14 zeolite. The Z-14 disc was approximately 0.38 mm thick.

The material AL-300, shown in Table XXX, is a raw alumina material in block form supplied by Western Gold and Platinum Company, Belmont, California. Discs machined from AL-300 were sintered at $1400^{\circ}C$/16 hours and $1500^{\circ}C$/2½

TABLE XXX

POROUS MEMBRANE SUBSTRATE MATERIALS

Number	Material, Wt %	Sinter °C/Hrs.	% Porosity	Remarks
S-1	100 RMB-4F Ramming Mix (Zircoa)	1200/15	--	Strong, porous, ZrO_2 plate
S-2	88 RMB-4F, 17 No.36F Grain (Zircoa)	1400/4	27	Strong, porous, ZrO_2 plate
S-3	70 Al_2O_3* (-100 m.), 18 Al_2O_3* (325m) 12 H_3PO_4	1400/4	14	Strong, porous Al_2O_3 plate, poor green strength
S-4	60 Al_2O_3* (-100 m.), 30 Al_2O_3* (-325 m.) 7 H_3PO_4, 3 OM48 clay	1400/4	25	Better green strength
S-5	91 Al_2O_3 (-325 m.), 9 QS-13 Pemco Frit	1000/10	34	Good strength
	Al-300 Wesgo Product, 96% Al_2O_3	1400/16	39	Excellent strength @ 12-15 mil thick
	Al-300 Wesgo Product, 96% Al_2O_3	1500/2½	15	Excellent strength @ 12-15 mil thick

* Alcoa Tabular Alumina T-61

-133-

hours. Their respective porosities of 39 and 15% show the latitude one may have for the development of porous substrates. High temperatures will completely vitrify the material. AL-300 also exhibits excellent strength at 0.25-0.40 mm. In addition to substrate applications, this material may also be useful as a membrane. The use of these materials as porous separators is given in Section 5.1.3.

SECTION 6

CELL TESTS

During this program, complete cells of the following types were tested:

$$Na//Separator//CuCl,KCl/W \qquad (24)$$

$$Mg \text{ or } Li\text{-}Mg \text{ alloy}/LiCl,KCl//Separator//CuCl,KCl/W \quad (25)$$

$$Li\text{-}Mg \text{ alloy}/LiCl,KCl/Glass \text{ frit}//LiCl,KCl/CuO/W \quad (26)$$

To avoid decomposition of the silicone rubber sealant, cells with CuCl cathodes were discharged at temperatures below 415°. The CuCl was diluted with 10 mole percent of KCl to lower the melting point of the cathode. Cells with CuO cathodes did not use the silicone rubber sealant and therefore were discharged at $420\text{-}430^{\circ}$.

A schematic diagram of the cell used for the majority of the discharge tests is shown in Figure 37. The outer container was a 30x240mm Pyrex or Vycor test tube. The anode compartment was a Pyrex or alumina tube about 95 mm in length and 10 mm inside diameter utilizing various methods of supporting membranes as shown in Figure 38. Either molten sodium with a tungsten lead or a strip or slug of a Li-Mg alloy along with an Ag-AgCl reference electrode of the type described in detail in the Section 4.1.3 were used in the anode compartment.

The main body of the cell contained the cathode material, either a molten mixture of CuCl and KCl or solid CuO (not represented on Figure 37) in

GLASS WOOL

INERT GAS

INERT GAS BLANKET

PYREX OR VYCOR
TUBE

PYREX OR
ALUMINA
TUBE

Ag-AgCl
REFERENCE
ELECTRODE

ANODE

MEMBRANE

CATHODE
(TUNGSTEN)

THERMOCOUPLE

CATHODE
DEPOLARIZER
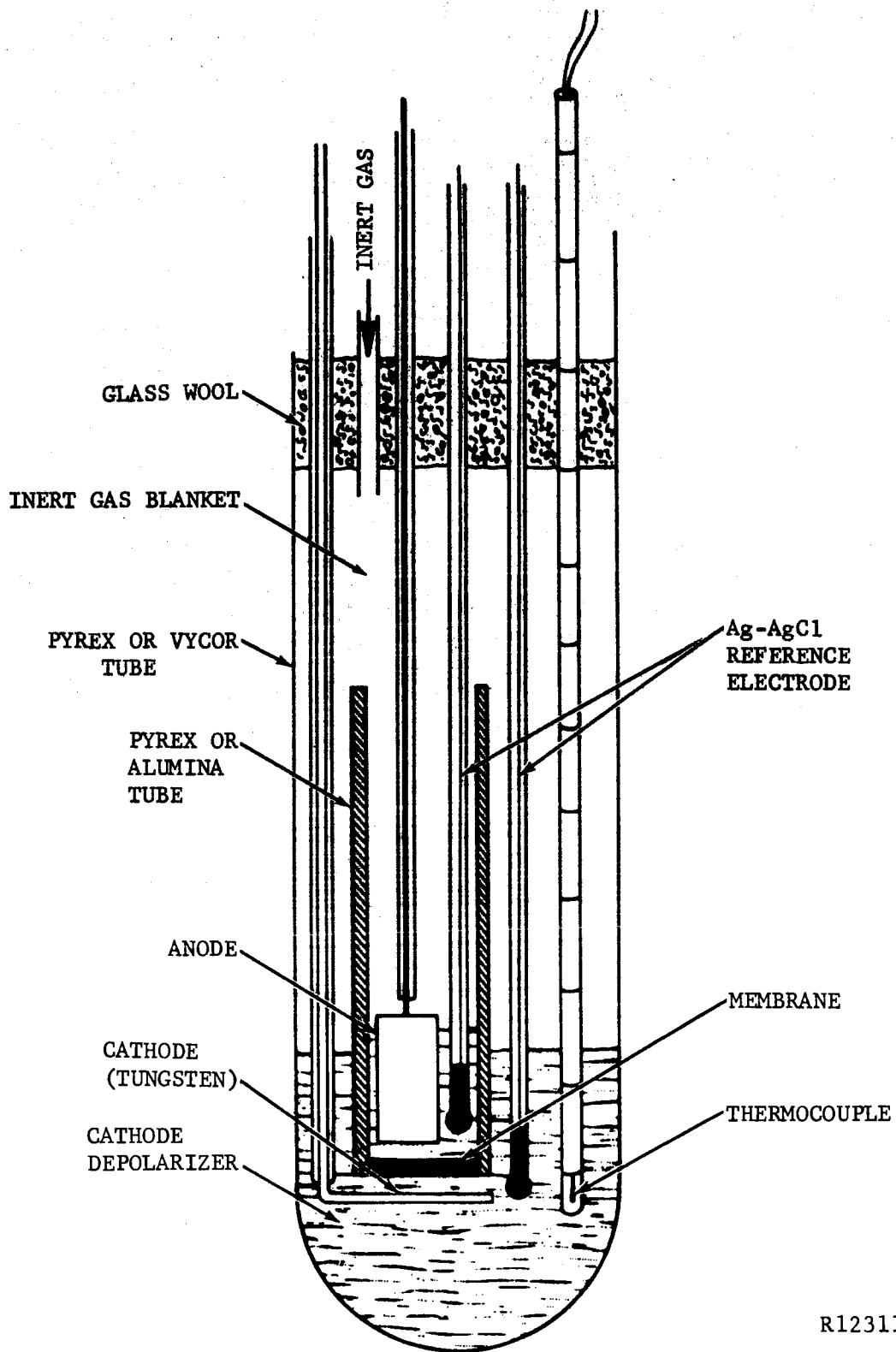
R12311

FIGURE 37. EXPERIMENTAL CELL FOR DISCHARGE TESTS

BOTTOM VIEW

(a)

ANODE COMPARTMENT

PYREX TUBES

PYREX BEAD

RTV 560 SEAL

MEMBRANE

CROSS SECTION A

(b)

PYREX OR ALUMINA TUBE

PYROCERAM GLASS

MEMBRANE
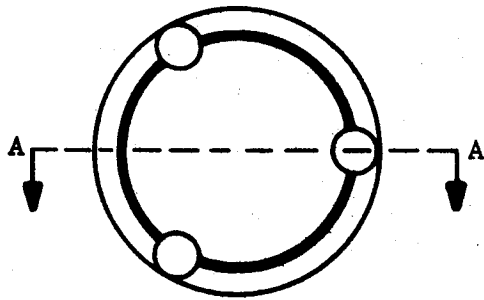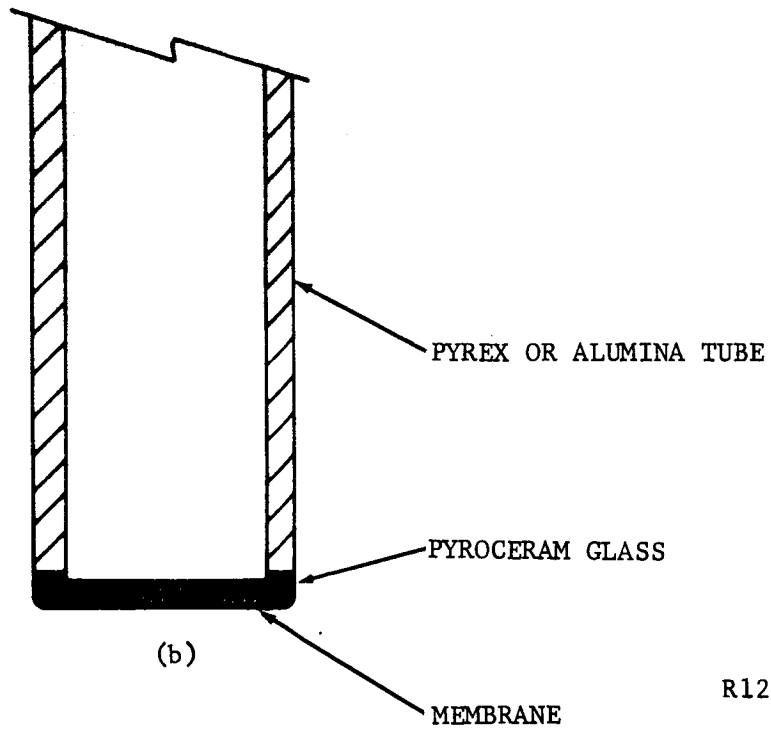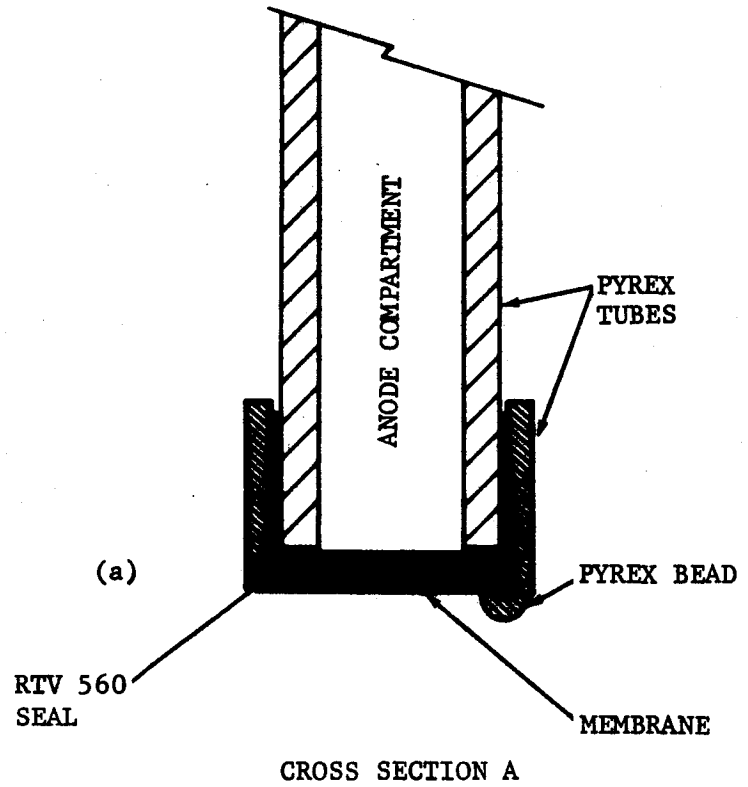
R12312

FIGURE 38. ANODE COMPARTMENTS

molten LiCl-KCl eutectic mixture, along with an Ag-AgCl reference electrode and a chromel-alumel thermocouple.

Tungsten rods were generally used as current collectors in the anode and the cathode compartments of the cells.

Current drains used throughout these tests were in general based on a current density of 6.7 mamps/cm^2 of the membrane area exposed to the electrolytes. The cells were discharged using the commutator described in Section 4.1.1. Both the IR drop and the IR free voltage of the cell during discharge were recorded.

6.1 CELL TYPE   Na//Separator//CuCl, KCl/W

Two types of separators were used in these cells. In one type, NaX zeolite membranes were fabricated by the procedures described in Section 5.2.3. The other type of separator was the NBS porcelain.[13] In all cases a membrane area of 1 cm^2 was used with a discharge current of 6.7 mamps. At this current drain, sufficient cathode material was available for 112 hours of operation. The capacity of the sodium anode at this current drain was 174 hours per gram.

The test conditions, membrane type, method of membrane sealing, performance, and nature of failure of the individual cells are summarized in Table XXXI. The IR free cell voltage and membrane resistivity of Cell No. 54 are also shown in Figure 39. The effect of temperature on the resistivity of the membrane in Cell No. 54 is given in Table XXXII. The resistivity measurements were made approximately five hours after the start of the test. Since the resistance of the separator was far greater than the combined resistances of all other parts of the cell, the resistivity of the membrane was computed directly from the total resistance of the cell.

TABLE XXXI

PERFORMANCE OF CELLS
Na//Separator//CuCl,KCl/W

Cell No.	54	57	55	56	58	59	60	61
Membrane								
Type	Z-16	Z-16	Z-16	Z-17	Z-17	Z-19	NBS	NBS
Sintering temp. °C.	700	700	780	940	960	1280	1150	1150
IR free voltage, volts								
a. At start of test	3.43	3.22	3.35	3.36	3.45	3.43	3.56	3.50
b. After Cu^{++} depletion	2.62	--	2.53	2.79	2.34	2.66	--	2.67
c. At end of test	2.58	1.45	2.22	2.44	1.30	2.60	2.63	2.30
Anode potential, volts	--	--	-2.33	-2.44	--	--	--	--
Cathode potential, volts								
a. Start of test	--	--	+1.02	+0.92	--	--	--	--
Resistivity, ohm-cm								
a. Start of test	6,240	13,900	4,150	16,700	16,700	3,800	12,900	14,000
b. End of test	3,010	2,030	797	3,880	2,490	3,000	6,755	5,200
Duration of test, hours	6	22	6	12	21½	13	23	28
Nature of failure								
Membrane cracked	X	X	X	X	X			
Seal failure			X					
Metallic copper shorts				X				X
Membrane disintegrated						X	X	
Support	Pyrex	Pyrex	Pyrex	Pyrex	Pyrex	Pyrex	7052 Glass	Pyrex
Sealant	RTV 560	RTV 560	RTV 560	RTV 560	RTV 560	RTV 560		RTV 560
Wt. of Na, gms	1.13	0.83	1.1	0.94	--	0.9	1.02	0.80
Wt. of CuCl, KCl, gms	3.0	3.0	3.0	3.0	3.0	3.0	3.0	3.0
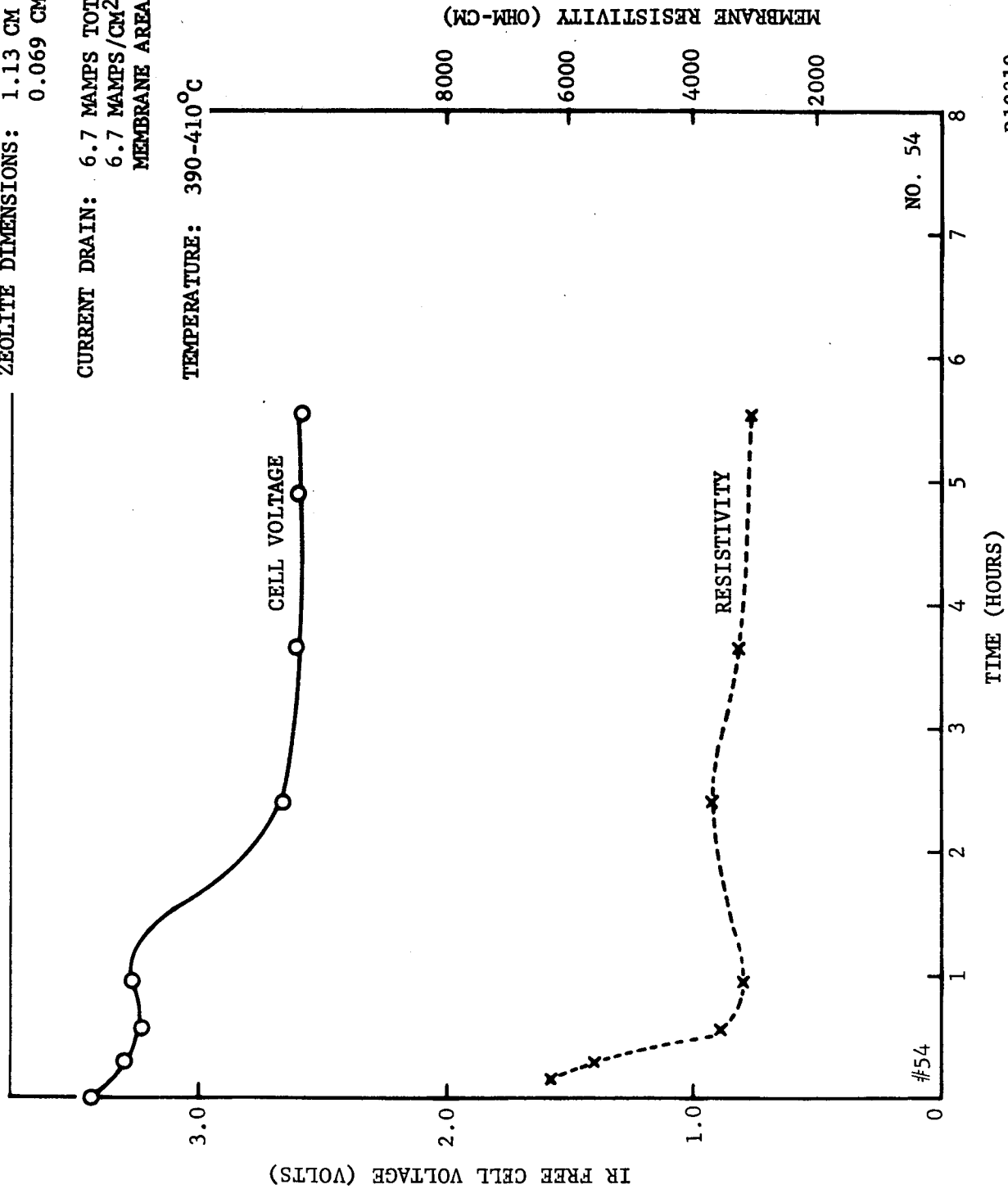
FIGURE 39. PERFORMANCE OF THE CELL Na//Z-16(700°/30M)// CuCl, KCl/W

TABLE XXXII

RESISTIVITY OF Z-16 (700°C/30 min.) MEMBRANE

Temperature (°C)	Resistivity (ohm-cm)
410	3010
422	2170
430	1921
440	1643

6.2 CELL TYPE: Li-Mg Alloy/LiCl,KCl//Separator//CuCl,KCl/W

The membranes tested in this type of cell were fabricated from samples of NaX zeolite Z-16 sintered at 700° for 30 minutes or from alumina (AL 300). Some of the zeolite membranes were bonded to porous zirconia to increase their strength. The membranes were sealed to Pyrex or alumina tubes using a silicone rubber compound (General Electric RTV 560), a pyroceram seal (Pyroceram 45), or a 80-20 glass seal. A number of these membranes were impregnated with the fused salts in the cells by applying vacuum for various periods of time before operating the cells.

Table XXXIII gives the results of the series of tests using cells with CuCl cathodes with Z-16 membranes sealed to a Pyrex tube with the silicone rubber. These cells were discharged at a current density of 6.7 mamps/cm^2 of membrane area and a total current of 6.2 mamps. Based upon this current drain and the composition of the cathode, the capacity of the cathode mixture was 39.5 hours per gram.

The IR free cell voltage and membrane resistivity for cell No. 62 as a function of time are shown in Figure 40. This cell was still running at 72 hours when the test was stopped and the cell dismantled for inspection. A slight reddish deposit was found on the lower edge of the anode. This deposit was nonadherent and was lost when the anode was washed with water. The deposit was probably metallic copper. No other copper was found in the anode compartment. A crack was noted across the zeolite pellet. Metallic copper was visually observed within this crack. However, the relatively

TABLE XXXIII

PERFORMANCE OF CELLS

$$\text{Li-Mg Alloy} \Big/ \begin{matrix} \text{LiCl,} \\ \text{KCl} \end{matrix} \Big/\!\!\Big/ \text{Z-16} \Big/\!\!\Big/ \begin{matrix} \text{CuCl,} \\ \text{KCl} \end{matrix} \Big/ \text{W}$$
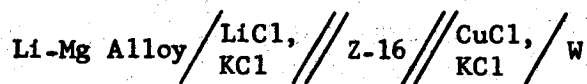
Cell No.	62	63	64	67	72	73*
IR free voltage, volts						
a. At start of test	3.29	3.50	3.49	3.24	3.40	3.40
b. After depletion of Cu^{++}	2.50	--	2.52	2.39	2.58	--
c. At end of test	1.93	--	0.94	1.02	1.47	2.51'
Anode potential vs. Ag-1m AgCl						
reference electrode, volts	-2.56	-2.53	--	-2.39	-2.55	--
Cathode potential vs. Ag-1m AgCl						
reference electrode, volts						
a. Start of test	+0.75	+0.98	--	+0.84	+0.87	--
Resistivity, ohm-cm						
a. Start of test	5030	6700	5140	4140	3960	3670
b. End of test	314	6700	785	596	short	548
Duration of test, hours	72	1	47	69	8½	22½
Weight of LiCl-KCl, gms.	2	2	2.5	--	2	2
Weight of CuCl-KCl, gms.	5	3.5	3.5	--	3	3
Weight of Li-Mg alloy, gm			Not Determined			
Nature of failure						
Cracked membrane		X	X			X
Cracking of tube						
supporting membrane				X	X	
Cell shorted by metallic copper at						
edge of membrane where seal failed					X	

* Cell 73 was left on open circuit throughout its operation.
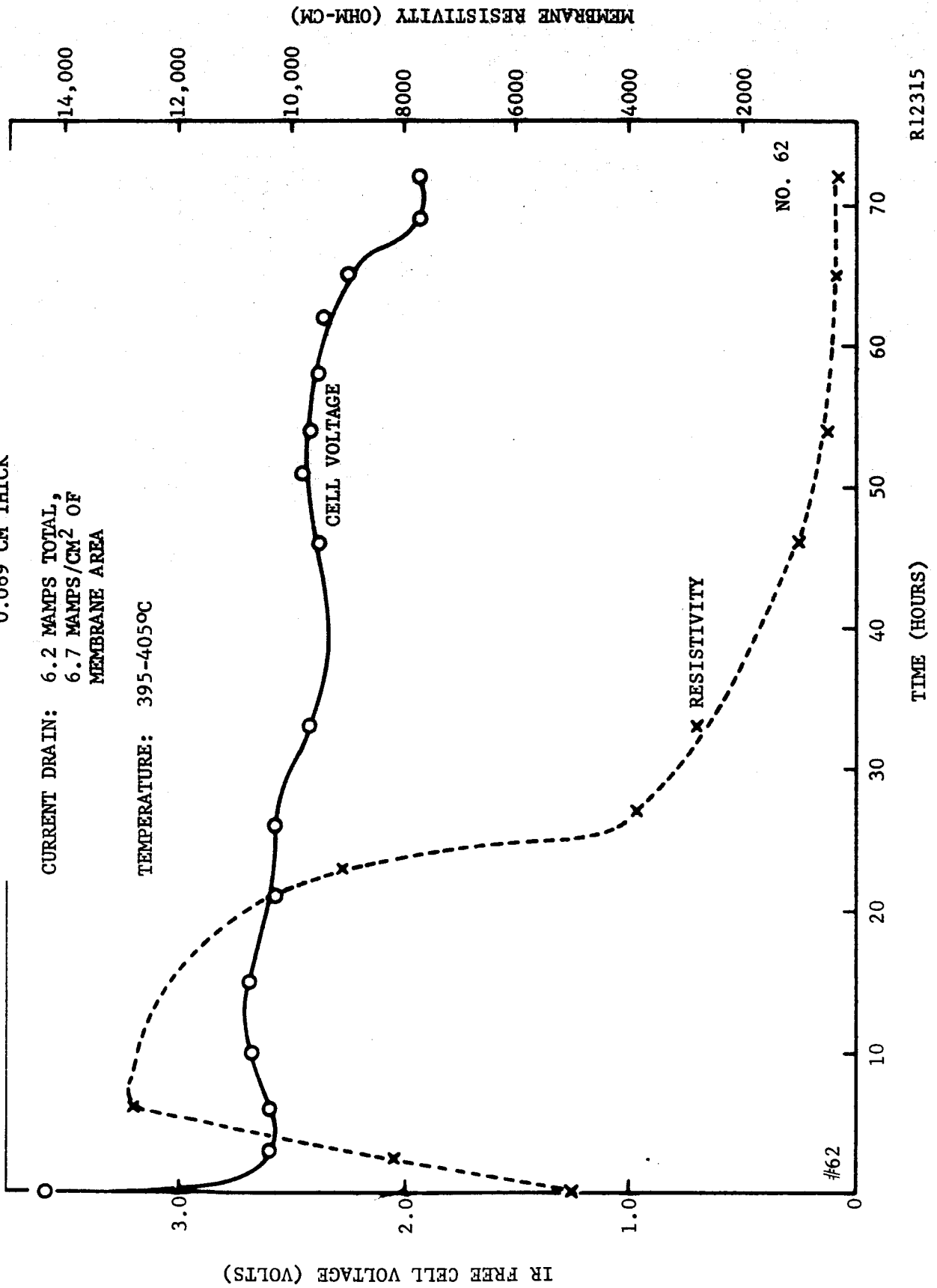
FIGURE 40. PERFORMANCE OF THE CELL: Li-Mg ALLOY/LiCl, KCl//   Z-16(700°/30m/CuCl, KCl/W.

- 143 -

high cell resistance and voltage at the end of the test would indicate that this copper did not lead to any significant shorting of the cell compartments.

High apparent resistivities for zeolite membrane had been observed when gasket composed of the RTV silicone rubber were used to seal zeolite pellets. In these experiments described in more detail in Section 5.3, the high resistivity seemed to be correlated with gas bubbles being liberated from the silicone rubber. Collection of gas bubbles on the face of the zeolite separator along the absorption of a volatile component from the silicone which rendered the surface nonwettable by the electrolyte would account for not only the initially high resistivity but also the increase in resistivity with time. The decrease in resistivity might be accounted for by the decrease in the rate of gas evolution and a chemical attack of the nonwetting film by the molten CuCl. If these conclusions are correct, it would indicate that the abnormally high resistivities sometimes found with zeolite were caused by the silicone rubber seal and were not an inherent property of the zeolite.

The correctness of this conclusion was supported by the experimental characteristics of cell using Z-16 zeolite membranes which were sealed with materials other than the silicone rubber. Three cells were constructed using Z-16 zeolite membranes sealed to alumina tubes (AV30) with Pyroceram 45. The membrane in one cell fell off the alumina tube within a few minutes following the start of the test. The two other cells gave the following results:

Cell Number	70	71
Initial Open Circuit Voltage, volts	2.98	2.95
Initial Anode Potential vs. Ag-1m AgCl, volts	-2.60	-2.53
Initial Cathode Potential vs. Ag-1m AgCl, volts	+0.40	+0.45
IR Free Voltage at End of Test, volts	2.37	2.35
Initial Resistivity of Membrane, ohm-cm	114	4647
Final Resistivity of Membrane, ohm-cm	- -	1954
Duration of Test, hours	2½	3

The significant point with these cells was the fact that from the beginning of the test a slow decrease in membrane resistivity was observed. During this same time period cells using the silicone rubber sealant were usually found to show large increases in cell resistance. The failure of these cells was attributed to substantial cracks in the rigidly bonded zeolite membrane.

Results obtained with two cells using porous alumina as membrane sealed to the AV30 alumina tubes with the 80-20 glass were as follows:

Cell Number	74	77
Initial Open Circuit Voltage, volts	3.08	3.14
Final Open Circuit Voltage, volts	1.1	1.3
Initial Resistivity, ohm-cm	98	<50
Final Resistivity, ohm-cm	535	407
Duration of Test, hours	16½	15

The membranes were found intact when dismantling the cells. The decrease in cell performance was attributed to diffusion of cuprous ions into the anode compartment of the cells and direct chemical reaction with sodium. These cells also support the conclusion that the use of silicone rubber sealants can lead to high resistances. In these cells with alumina separators the gradual increase in resistivity was attributed to a gradual loss of the anolyte through the porous separator.

In one of the last cells run under this program a vacuum hot pressed LiX-PJ membrane was sealed to a Pyrex support tube with AgCl. The membrane was pressed at 200° and 2000 kgm./cm.^{2} The seal was constructed to minimize contact between the AgCl and the electrolyte. A sketch of the cell is shown in Figure 41. A magnesium anode was used and the cell was discharged at 6.7 mamp/cm^2 of membrane area. The initial open circuit voltage was 2.18 volts and the voltage under load was 2.17. Within a short period of time the cupric ions present as an impurity in the cuprous chloride were removed and the open circuit voltage and the voltage under load were 1.68 and 1.67 volts, respectively. After 17.5 hours of operation, when the cell voltage under the 6.7 mamp/cm^2 drain was still 1.67 volts, the drain was increased
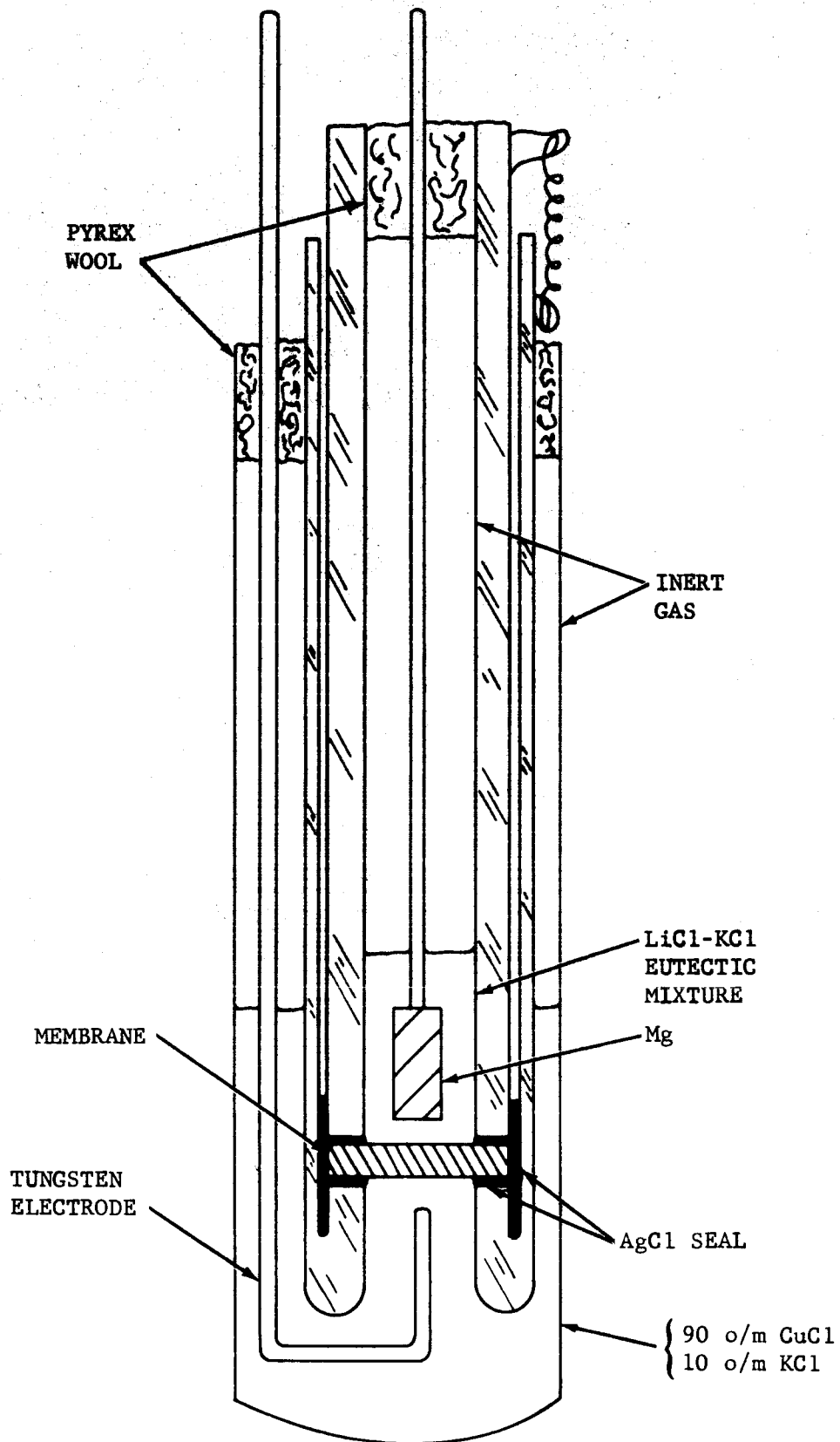
FIGURE 41.   ELECTROLYTIC CELL E

to 67 mamps/cm^2 for 6 minutes. The cell voltage under this increased load was 1.60 volts. The increase in cell resistance towards the end of the test was probably due to solid magnesium chloride formed in the anode compartment by the oxidation of the anode. Initial cell resistance was 4.9 ohms. After 51 hours of discharge, the test was discontinued because of difficulties which were not associated with the cell. At this time the cell voltage under load was 1.60 volts and the resistance was 10 ohms. The cell voltage under load and total cell resistance are shown in Figure 42. The zeolite membrane was found intact at the end of the test. No copper was visually observed in the anode compartment.

6.3   CELL TYPE: Li-Mg Alloy/LiCl,KCl//Glass Frit//LiCl,KCl/CuO/W
These cells utilized as a separator a 0.178 cm. thick, fine glass frit (nominal maximum pore diameter 4-5.5 microns) fused to the bottom of the Pyrex tube serving as the anode compartment. The tube contained the alloy immersed in about 3 grams of the LiCl-KCl eutectic mixture. The glass frit rested on top of approximately 10 grams of CuO in wire form placed in the bottom of a Vycor tube with 6-17 grams of the eutectic mixture and a W or Cu wire collector. These cells were operated at 420°-430°C. Voltage time and resistivity-time curves for one cell at a current density of 6.7 mamps/sq.cm. of glass frit are shown in Figure 43. The voltages shown on this curve have not been corrected for IR drop. Deterioration of the alloy section above the anolyte rather than the coulometric dissolution of the immersed section compelled the replacement of the anodes during cell discharges. This deterioration was ascribed to chemical attack by trace amount of oxygen present in the argon atmosphere maintained above the electrolytes. The transformation in the cell voltage as the lithium on the surface of the alloy anode was consumed was readily apparent. Before this transformation the anode acted essentially as though it were a solid lithium electrode; after the transformation it acted essentially as a magnesium electrode.

With this cell the anode compartment was removed after 48 hours of operation.
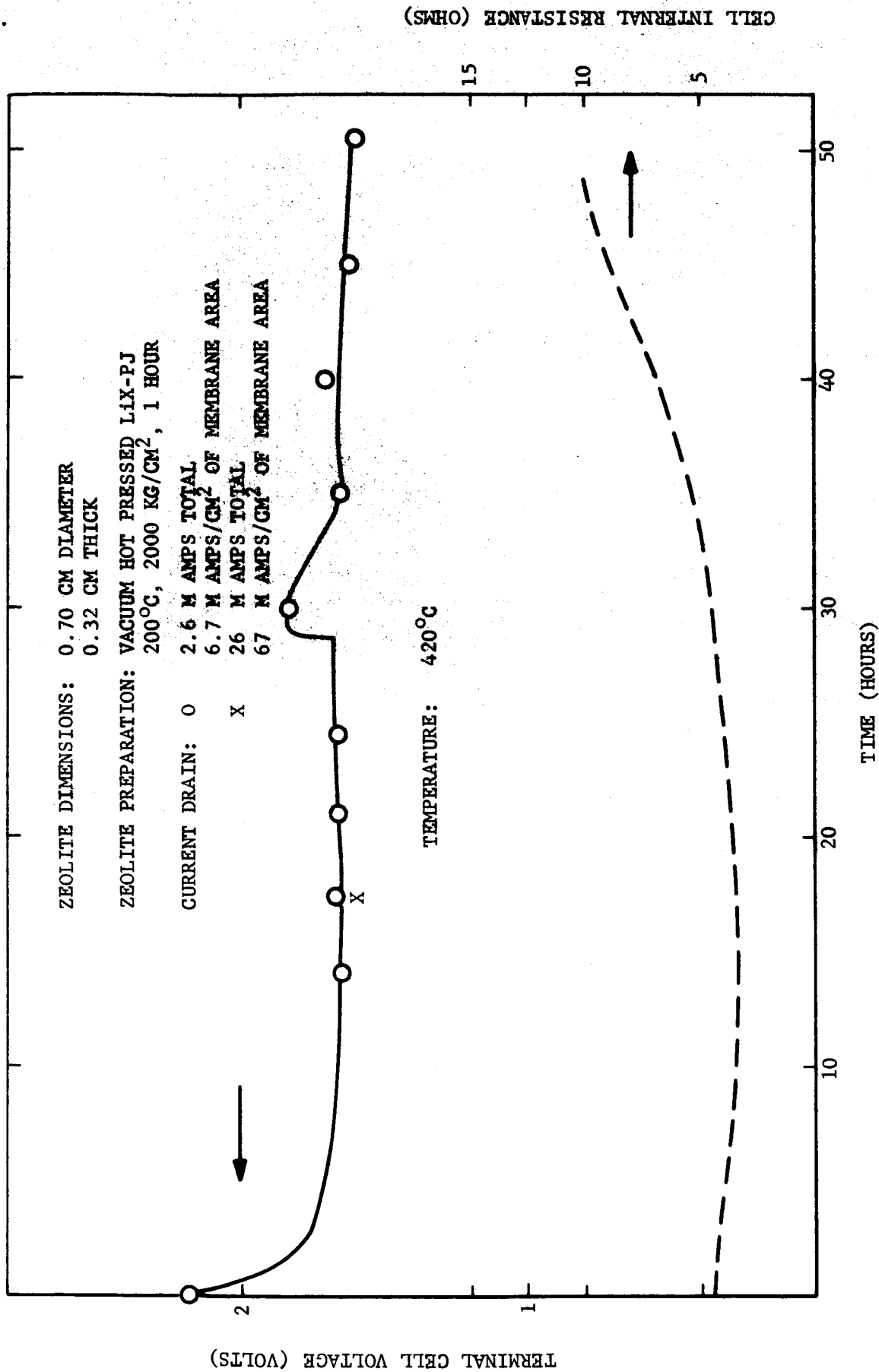
FIGURE 42. PERFORMANCE OF THE CELL: Mg/LiCl,KCl//LiX-PJ//CuCl,KCl/W.
(VHP)
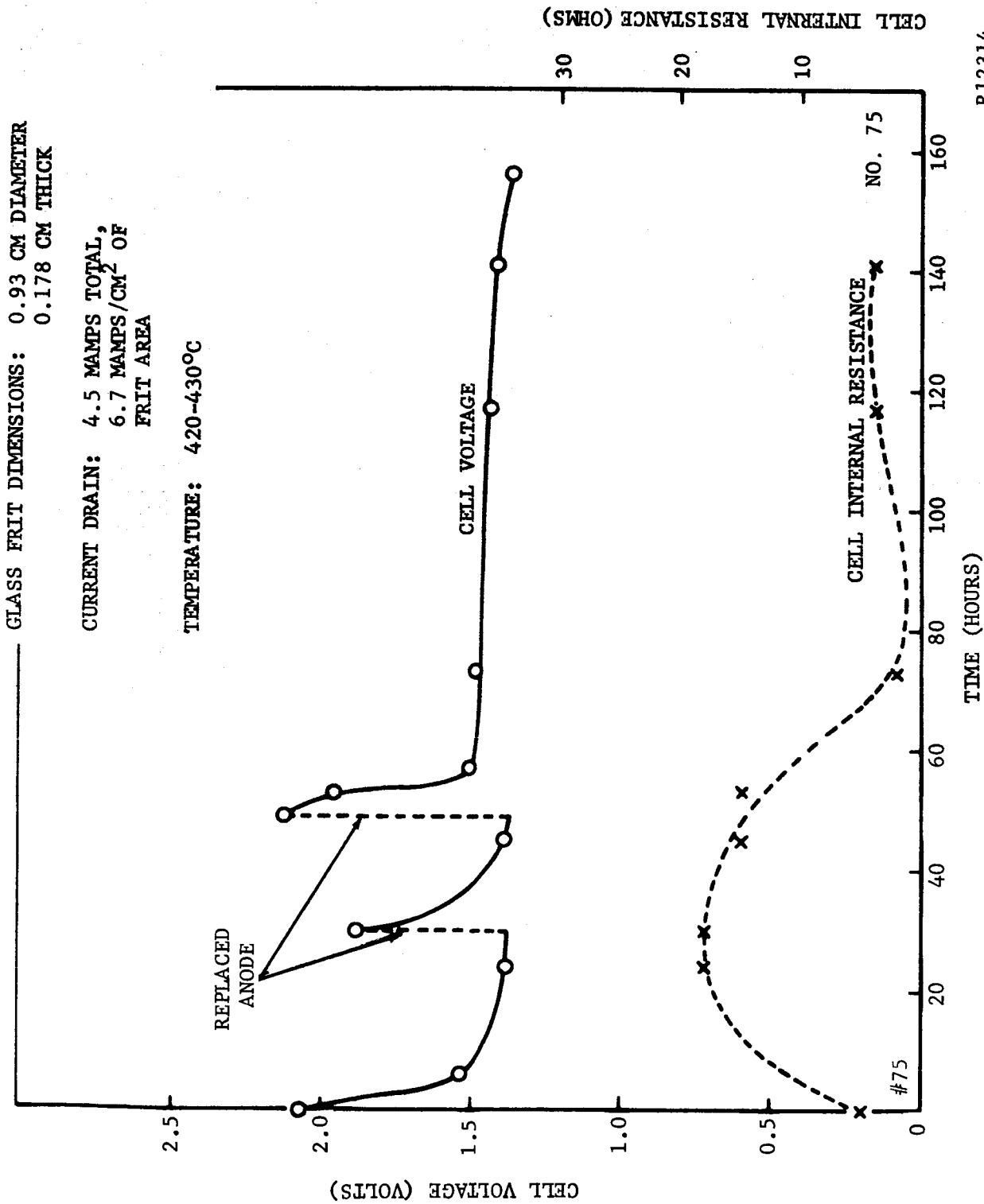
FIGURE 43. PERFORMANCE OF THE CELL: Li-Mg ALLOY/LiCl, KCl//GLASS FRIT//LiCl, KCl/CuO/W

-149-

Chemical analysis of this compartment showed a total of 46.2×10^{-6} moles of Cu(II) present. A new anode and anode compartment was added and the test continued. No analysis could be made of the cells after the tests because failure of the glass tube forming the anode compartment permitted mixing of the catholyte and anolyte.

Similar results, with the exception of a higher resistance, were found with another cell of this same type. The higher resistance was ascribed to a deficiency of electrolyte in the anode compartment. At the end of 72 hours of operation under the same discharge conditions as used in the preceeding cell, the IR free voltage was 1.36 volt and after 96 hours of operation the cell voltage was 1.28.

The results of cells of this type should be compared with cells using a porous Al_2O_3 separator but a molten cathode (previous section). Within a relatively short period of time the molten CuCl diffused through the porous alumina separator and caused shorting. With the solid cathode with a relatively low solubility at the operating temperature of the cell, the diffusion of cupric ions through the separator was relatively slow and no difficulties with shorting occurred.

It is significant to note that cells of this type function satisfactorily, with the exception of anode replacement as previously noted, for discharge times in excess of the required 72 hours. As a matter of fact, cell #75 performed for a total of 156 hours at cell voltages in excess of 1.35 volts. This cell ran 107 hours after the replacement of the anode compartment. During the final 73 hours of discharge, no changes or additions were made to this cell. At the request of the NASA Technical Monitor, no further work was done with porous separators and solid cathodes.

6.4 SUMMARY AND CONCLUSIONS
The results of cell testing and membrane sealing experiments lead to the

conclusion that the principal difficulty associated with zeolite membranes was connected with the seals. With proper seals zeolite membranes were suitable as separators in high temperature batteries. Both the resistance and leakage rate of the zeolite membranes were sufficiently low to make a practical cell for 72 hours of operation.

If rigid seals were used either the zeolite membrane or the seal would crack because of the anomalous expansion behavior of the zeolites. Either flexible sealants or gaskets would be satisfactory. However, these materials must be stable in the environment of the battery.

Cells for 72 hours of operation can be obtained with porous separator and insoluble cathodes. Use of an insoluble cathode will probably result in a low cell voltage.

SECTION 7

CELL DESIGN AND CONSTRUCTION

In anticipation of assembly and testing of complete cells and batteries, a preliminary cell design was formulated in an attempt to determine areas in which special problems might arise.

7.1 CELL VOLUME CHANGES

One of the first points which had to be taken into account in the design of a cell for this application was the change in volume which will occur during discharge. Using a zeolite as a solid electrolyte permitting only cation transfer between the anode and cathode compartment would result in a decrease in volume in the anode compartment and an increase in volume in the cathode compartment. In the anode compartment the active metal anode would be oxidized to form ions. The transfer of these ions as the charge carriers through the zeolite would result in a net volume decrease in the anode compartment. In the cathode compartment there would be a volume change due to the reduction of the cathode material from one oxidation state to a lower one and the introduction of cations from the anode compartment through the zeolite.

As an example of the volume changes to be encountered, consider one proposed

cell having a sodium anode and a CuCl cathode. The individual half reactions
expected are:

$$\text{Anode} \qquad Na \longrightarrow Na^+ + 1e^- \qquad\qquad (27)$$

$$\text{Cathode} \qquad CuCl + 1e^- \longrightarrow Cu + Cl^- \qquad\qquad (28)$$
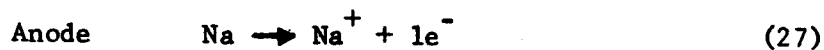
with one Na+ passing from the anode compartment through the zeolite membrane
to the cathode compartment for each electron transferred.

For a total capacity of 14 ampere-hour, the amount of metallic sodium
oxidized, sodium ion transferred, and CuCl reduced are each 0.523 faradays.
The loss of 0.523 faradays (12.0 grams) of metallic sodium is equivalent to
a volume decrease at 450°C. of

$$\frac{12.0 \text{ grams}}{0.842 \text{ grams/cm}^3} = 14.25 \text{ cm}^3 \qquad\qquad (29)$$

The density of molten sodium was calculated from data given in Reference 47.
The situation in the cathode compartment is more complex since there is a
transformation of 0.523 equivalents of CuCl to Cu and the introduction of
0.523 equivalents of NaCl. Assume that CuCl and NaCl from ideal solution;
i.e., their individual volume are additive, and that the volume of NaCl
dissolved in CuCl can be extrapolated from the high temperature molten
volumes of NaCl. Then the decrease in volume of CuCl is,

$$0.523 \text{ equiv.} \times \frac{98.99 \text{ grams}}{\text{equiv.}} \times \frac{\text{cm}^3}{3.655 \text{ grams}} = 14.16 \text{ cm}^3 \qquad\qquad (30)$$

The volume increase due to formation of Cu is

$$0.523 \text{ equiv.} \times \frac{63.54 \text{ grams}}{\text{equiv.}} \times \frac{\text{cm}^3}{8.73 \text{ grams}} = 3.81 \text{ cm}^2 \qquad\qquad (31)$$

and the formation of NaCl is

$$0.523 \text{ equiv.} \times \frac{59.44 \text{ grams}}{\text{equiv.}} \times \frac{\text{cm}^3}{1.746 \text{ grams}} = 17.81 \text{ cm}^3 \qquad\qquad (32)$$

The densities of CuCl and NaCl at 450°C. were obtained from Reference 60.
The density of Cu at 450° was calculated from its known density at 0°C. and

its coefficient of thermal expansion. Thus the total volume change in the cathode compartment is

$$-14.16 + 3.81 + 17.81 = 7.46 \text{ cm}^3 \tag{33}$$

Similar calculations show that using a potassium anode the volume of the anode section would decrease 27.8 cm^3 while the cathode section would increase 12.4 cm^2. The results for these two systems are summarized in Table XXXIV.

TABLE XXXIV

VOLUME CHANGES IN 14 AMPERE-HOUR CELL

	Volume Change, cm^3		
Cell	Anode	Cathode	Cell
Na/Zeolite/Cucl	-14.25	+7.46	-6.79
K/Zeolite/Cucl	-27.8	+12.4	-15.4

7.2 CELL DESIGN

To accommodate these volume changes, a preliminary cell design utilizing movable bellows as containers for the anode and cathode sections was formulated. This preliminary design using a liquid metal anode is shown in Figure 44. For cells using solid anodes, the anode compartment would contain the solid anode and a LiCl-KCl anolyte. The bellows would be fabricated from a Kovar type metal or stainless steel. It would appear from preliminary information that molybdenum-manganese ceramic to metal seals utilizing iron or nickel brazing alloys would have the best chance of surviving in contact with either a liquid metal anode or a fused salt anolyte. Glass sealants, e.g., pyroceramic types or sodium phosphate glass, would be usable in the configuration where an anolyte is used.

7.3 COMPATIBILITY TESTS

Compatibility tests were run for various materials proposed for use in cell construction. In these tests the materials were vacuum sealed in Pyrex ampoules. The tests were run by holding the materials in contact with each

FUSED Al_2O_3

ZEOLITE

KOVAR METAL
INTERIOR Cu-PLATED

Na OR K ANODE
or
Mg IN LiCl-KCl ANOLYTE

KOVAR METAL BELLOWS

CuCl
CATHODE

Mo - Mn SEAL WITH Fe
BRAZING ALLOY

SINTERED POROUS
Al_2O_3

GLASS SEAL
(PYROCERAM TYPE)
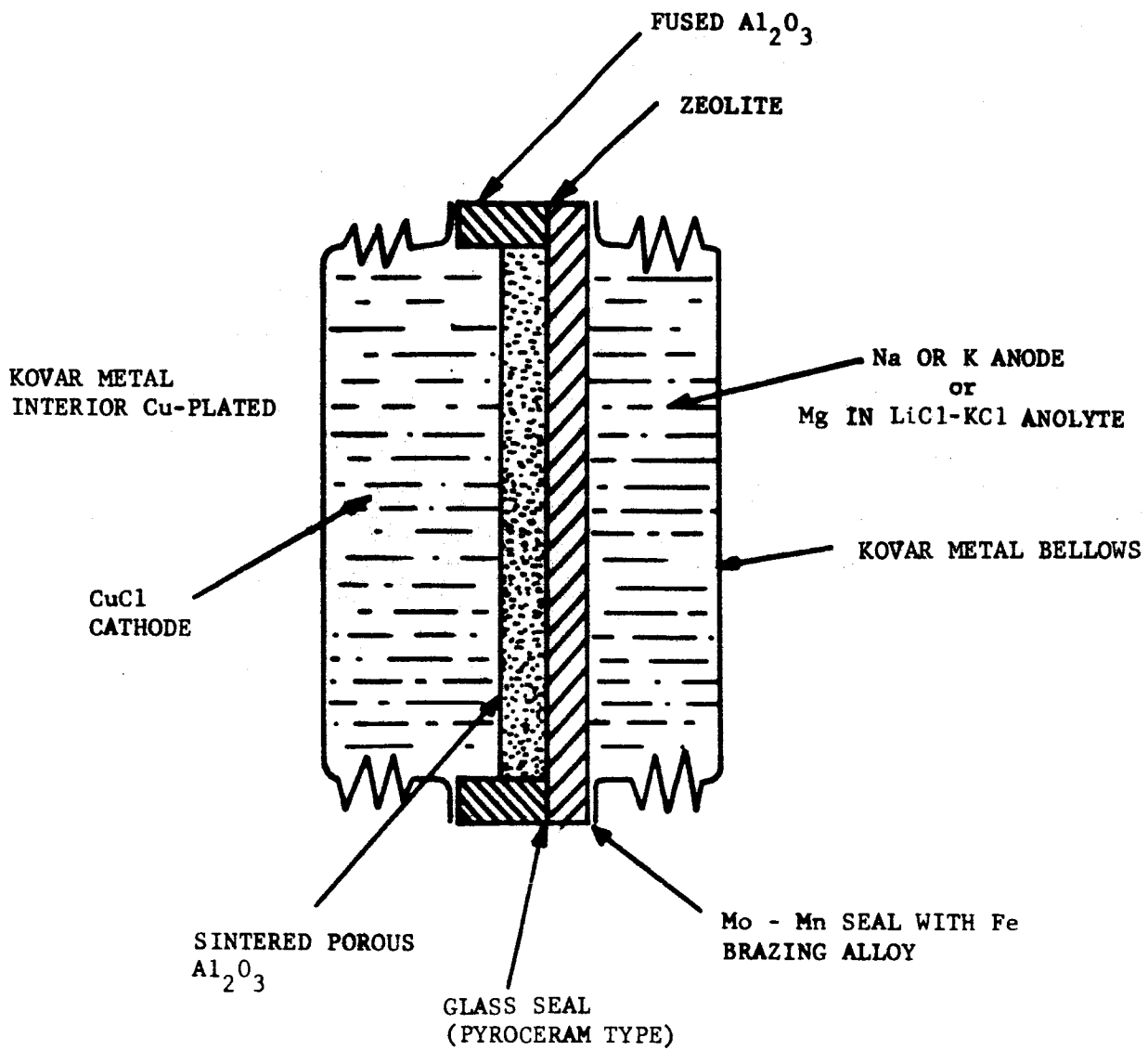
R10254

FIGURE 44. PRELIMINARY CELL DESIGN

-155-

other at $450^{\circ}C.$ for a minimum of 72 hours. In most cases visual examination was used to determine changes.

Some of the results have been presented in previous sections on anodes and cathodes, but the results are also presented here for completeness. These results can be summarized as follows:

Metallic Sodium With:

Zeolites, Types A, X, and Y formed by vacuum, hot pressing	Varied from complete disintegration to penetration and discoloration depending on the relative amounts of the zeolite and Na
NaX, vacuum, hot pressed and impregnated with molten LiCl-KCl	Completely disintegrated
NaX formed by silicate or phosphate bonding	Completely disintegrated
Sodium-alumino-phosphate, composition C-9	Completely disintegrated
Porcelain, NBS formulation	Completely disintegrated
Porcelain on porous ZrO_2	Completely disintegrated
Armco iron	No apparent reaction
Nickel	No apparent reaction
Recrystallized Al_2O_3	No apparent reaction

Metallic Lithium With:

LiX + LiCl, vacuum hot pressed	Completely disintegrated
Glass ampoules	Etched
Recrystallized Al_2O_3	Destroyed structural integrity

Metallic Potassium With:

KA, vacuum, hot pressed	Completely disintegrated

Molten CuCl With:

Zeolites, Types A, X, and Y formed by vacuum, hot pressing	No apparent reaction

Recrystallized Al_2O_3	No apparent reaction
Armco iron	Formed an adherent layer of metallic copper
Nickel	No apparent reaction
Kovar A (29% Ni, 17% Co, 0.3% Mn, bal. Fe)	14% weight gain; grainy but apparently adherent layer of protective copper deposited
Au-Cu Brazing alloy (Incoro 60)	No apparent reaction

Molten $BiCl_3$ With:

Zeolites, Types A, X, and Y formed by vacuum hot pressing	No apparent reaction
Armco iron	Iron completely dissolved
Nickel	Nickel completely dissolved
Recrystallized Al_2O_3	No apparent reaction

Molten LiCl-KCl Eutectic With:

Zeolites, Types A, X, and Y formed by vacuum, hot pressing	No apparent reaction, penetration of the fused salt into the zeolite pellet
Recrystallized Al_2O_3	No apparent reaction
Armco iron	No apparent reaction
Nickel	No apparent reaction
Kovar A (29% Ni, 17% Co, 0.3% Mn, bal. Fe)	No apparent reaction, approx. 1% weight loss
Au-Cu brazing alloy (Incoro 60)	Fused salt slightly green, 0.25% weight loss

SECTION 8

CONCLUSIONS

The objective of this program was to develop a high energy density battery capable of operating for three days at $800^{\circ}F$ in an environment approximately the same as exists on the planet Venus. Initially a battery composed of an alkaline earth or alkali metal anode separated from a molten cathode by a solid ionic conductor was proposed as capable of achieving the discharge temperature and duration. The synthetic zeolites, by reason of their known cationic conductivity at these temperatures, were proposed as the solid ionic conductors to be used as separators.

During the course of the program, the problems associated with the development of cell configurations most suitable for long discharge duration were extensively studied. Realization of the program objectives required finding an optimum combination of a large number of variables. To this end it was necessary to follow a number of paths and subsequently to abandon those found to be least promising. The preceding sections contain a complete presentation of all work performed. It is believed desirable at this point to review the findings which are most pertinent to the development of a long duration thermal battery, and the path which they suggest as most promising of success.

Solid anodes (the alkaline earths) were initially eliminated from consideration because of difficulties implied in maintaining adequate electrolytic

contact between the solid anode and the solid separator particularly when the anode was being consumed by electrolytic oxidation. The use of the solid alkaline earth elements with a fused salt anolyte to achieve electrolytic contact was considered. However, in order to have an anolyte which was molten at the operating temperature of the battery, salts containing lithium ions must be used. The alkaline earths (except Mg) reacted with such salts to form liquid lithium alloys. Consequently this concept was regarded as equivalent to a liquid alkali metal anode.

The alkali metals were initially favored since they are liquids at the operating temperature of the battery and thus adequate contact with the separator would be achieved. However, the experimental results showed that the liquid alkali metals caused complete disintegration of the solid separators. Solid alloys of the less active alkaline earths, e.g., magnesium, and alkali metals are known but to obtain an alloy with a melting point that is high enough to be usable, the alkali metal content must be so low that the alloys offer no advantage over the unalloyed Mg. Thus within the scope of this effort, it was concluded that magnesium with a LiCl-KCl eutectic as the anolyte would be the most suitable for use as the anode half cell.

The halides of silver (I), copper (I), copper (II), iron (III), bismuth (III), and compounds of chromium (V) and vanadium (VI) were all considered initially as cathode material. The properties of these compounds were studied in half cells either as pure salts or in the presence of the products from the cell discharge reaction. In half cell test with coulometric addition of the anode reaction product by ionic transfer through a porcelain membrane, CuCl was reduced with a utilization efficiency of at least 67% in a 72 hour test. In a similar manner an efficiency of 71% was found for the reduction of $BiCl_3$ in a 115 hour test in which sodium ions were coulometrically added. Based upon electrochemical performance, equivalent weight, and compatibility with other cell components, cuprous chloride was found to be the most suitable for this application. In addition to half cell tests, CuCl was extensively tested in complete cells.

Various methods of forming thin zeolite membranes were developed. These methods included vacuum hot pressing; cold pressing and sintering; hot pressing; and bonding with sodium silicate or phosphoric acid. The effect of these fabrication procedures upon the various properties of the zeolites was investigated. In general thin membranes with suitable strengths could be produced by all of these methods. With all methods, except vacuum hot pressing, strength was achieved at the expense of zeolite structure. Vacuum, hot pressing yielded strong membranes with no loss of zeolite properties. However, as with all zeolite materials, water was strongly absorbed and must be avoided in formed membranes if the strength were to be preserved.

The effect of fabrication technique, zeolite type, and cation upon the ionic resistivity was studied. In general, fabrication techniques which tended to destroy the zeolite structure increased the resistivity. Of the three zeolite types studied the Type X had the lowest resistivity. Of the cations studied, sodium zeolites had the lowest resistance. Many of the earlier problems associated with the use of zeolites were traced to contamination by and decomposition of the silicone rubber used to obtain flexible seals. When these effects were eliminated, resistivities of the order of 10-40 ohm-cm were obtained in fused salts for period up to 72 hours. In addition mass transfer across the zeolite membrane appears acceptable. In a six day test the average rate of material transport was 0.21 gms/day/cm^2 of membrane area under a liquid head equal to 8.4 gms/cm^2.

Cell testing demonstrated two approaches to the development of a battery capable of operating for 72 hours at 800°F. In one case the cell consisted of a magnesium alloy anode and a molten CuCl cathode separated by a zeolite membrane. This cell operated for 72 hours and had an IR free voltage at the end of test of 1.93 volts while under a current drain of 6.7 mamps/cm^2 of membrane area. The membrane resistivity was 300 ohm-cm at the end of test. Similar cells using a sodium anode lasted a maximum of 28 hours. Failure was attributed to attack of the zeolite by the molten sodium. In general, the cells with sodium anodes had voltages in excess of 2 volts during test.

In another case two cells with magnesium alloy anodes and cupric oxide
cathode with a porous glass separator were discharged for 96 and 156 hours
respectively. In the latter case the cell produced terminal voltages in
excess of 1.35 volts at 6.7 mamps/cm^2 during the entire test period. Cells
using porous separators and molten CuCl cathode had life time less than
17 hours.

REFERENCES

1. R. E. Panzer, Electrochem. Tech. $\underline{2}$, 10 (1964).

2. W. J. Hamer, M. S. Malmberg, and B. Rubin, J. Electrochem. Soc. $\underline{103}$, 8 (1956).

3. G. F. Zellhoefer, U.S. Patent 3,110,632, Nov. 12, 1963.

4. S. Senderoff, E. M. Klopp, and M. L. Kronenberg, Progress Report Contract NOrd-18240 AD 277433.

5. S. M. Selis, L. P. McGinnis, E. S. McKee, and J. T. Smith, J. Electrochem. Soc. $\underline{110}$, 469 (1963).

6. H. A. Laitinen and B. B. Bhatia, J. Electrochem. Soc. $\underline{107}$, 705 (1960).

7. H. A. Laitinen and J. W. Pankey, J. Amer. Chem. Soc. $\underline{81}$, 1053 (1959).

8. E. O. Black and T. DeVries, Anal. Chem., $\underline{27}$, 906 (1954).

9. H. A. Laitinen and C. H. Liu, J. Amer. Chem. Soc. $\underline{80}$, 1015 (1958).

10. H. A. Laitinen, et al, Monthly Progress Reports on Contracts DAI-49-186-502-ORD(P)-50; DAI-49-186-502-ORD(P)-187; and DA-11-022-ORD-1987.

11. Z. S. Volchenkova and S. F. Palquev, "Electrochemistry of Molten and Solid Electrolytes", Vol. I, Consultants Bureau, New York, 1961.

12. J. O'M. Bockris, G. J. Hills, D. Inman, and L. Young, J. Sci. Inst. $\underline{33}$, 438 (1956).

13. R. J. Labrie and V. A. Lamb, J. Electrochem. Soc. $\underline{106}$, 895 (1959).

14. R. J. Labrie, J. Electrochem. Soc. $\underline{111}$, 473 (1964).

15. E. F. Uhler and G. S. Lozier, Final Report Contract AF33(616)-7505, AD 277197, April 1962.

16. D. C. Hamby, B. W. Steller, and J. B. Chase, J. Electrochem. Soc. $\underline{111}$, 998 (1964).

17. B. W. King, W. A. Hedden, A. B. Tripler, Jr., D. J. Bowers, and B. O. Austin, Ceramic Bul. $\underline{43}$, 117 (1964).

18. D. W. Breck, W. G. Eversole, R. M. Milton, T. B. Reed, and T. L. Thomas, J. Amer. Chem. Soc. $\underline{78}$, 5963 (1956).

19. R. L. Broussard and B. P. Shoemaker, J. Amer. Chem. Soc. $\underline{82}$, 1041(1960).

20. D. C. Freeman, Jr. and D. N. Stamires, J. Chem. Phy. $\underline{35}$, 799 (1961).

21. R. M. Milton, U.S. Patent 2,882,243, April 14, 1959.

22. D. W. Breck, E. M. Flanigen, and R. M. Milton, Paper No. 81, 137th ACS Meeting, Cleveland, April 1960.

23. D. W. Breck and N. A. Acara, British Patent 868,846, May 25, 1961.

24. D. W. Breck and N. A. Acara, U.S. Patent 2,962,355, November 29, 1960.

25. R. M. Milton, British Patent 847,057, September 7, 1960.

26. Union Carbide Corp. (by D. W. Breck and N. A. Acara), German Patent 1,100,008, September 19, 1957.

27. Union Carbide Corp. (by D. W. Breck and N. A. Acara), German Patent 1,100,009, January 28, 1958.

28. D. W. Breck and N. A. Acara, U.S. Patent 2,995,423, August 8, 1961.

29. D. W. Breck and N. A. Acara, U.S. Patent 2,991,151, July 4, 1961.

30. R. M. Milton, British Patent 841,812, July 20, 1960.

31. Union Carbide Corp. (by D. W. Breck), German Patent 1,100,010, March 31, 1958.

32. D. W. Breck and N. A. Acara, U.S. Patent 2,950,952, August 30, 1960.

33. R. M. Milton, British Patent 864,707, April 6, 1961.

34. R. M. Milton, U.S. Patent 2,882,244, April 14, 1959.

35. Union Carbide Corp. (by D. W. Breck), German Patent 1,098,929, April 14, 1958.

36. R. M. Barrer, J. Chem. Soc., 1948, 127.

37. R. M. Barrer and N. McCallum, J. Chem. Soc., 1953, 4029.

38. R. M. Barrer and E.A.D. White, J. Chem. Soc., 1951, 1267.

39. R. M. Barrer, Proc. Intern. Symposium Reactivity of Solids, Gothenberg, 1952, Pt. 1, 373 (Pub. 1954).

40. P. C. Huang, A. Mizany, and J. L. Pauley, J. Phys. Chem. 68, 2575(1964).

41. H. E. Rabinowitsch and W. C. Wood, Elektrochem. 39, 562 (1933).

42. D. N. Stamires, J. Chem. Phy., 36, 3174 (1962).

43. W. L. Haden, Jr. and F. J. Dzierzanowski, U.S. Patent 2,992,068, July 11, 1961.

44. C. Berger, F. C. Arrance, D. W. Cleaves, and M. J. Plizga, Final Report Contract NAS7-150, March 1964.

45. Societe D'Etudes, De Recherches et D'Application Pour L''Industrie, Final Report Contract DA-91-591-EUC-2773 OI-360308-D; AD433803, October 31, 1963.

46. R. P. Hamlen, J. Electrochem. Soc., 109, 746 (1962).

47. R. N. Lyon, "Liquid-Metals Handbook", Second Edition, June 1962.

48. Brooks & Perkins, Inc. Specification BP-S-125 Revision B.

49. G. F. Pallnow and R. M. Kay, J. Electrochem. Soc. 109, 648 (1962).

50. K. Kordesch and A. Marko, J. Electrochem. Soc. 107, 480 (1960).

51. E. M. Levin, C. R. Robbins, and H. F. McMurdie, "Phase Diagrams for Ceramists", The American Ceramic Society, Columbus, Ohio (1964).

52. R. J. Labrie--private communication to M. R. Unger, March 25, 1965.

53. H. A. Laitinen and D. R. Rhodes, J. Electrochem. Soc., 109, 413 (1962).

54. N. A. Saltykova and A. N. Baraboshkin, in "Electrochemistry of Molten and Solid Electrolytes" Vol. 2, M. V. Smirnov, Editor, p. 26 Consultants Bureau, New York (1964).

55. Z. N. Syritskaya, "The Structure of Glasses", Vol. 2 Consultants Bureau, New York (1960).

56. G. L. Clark, "Applied X-rays", Fourth Edition, McGraw-Hill Co., Inc., New York, pp. 420-2 (1955).

57. R. J. Brumbaugh and W. E. Fanus, Anal. Chem. 26, 463 (1954).

58. D. N. Stamires, et al, Second International Congress on Surface Chemistry, Paris, 1960.

59. M. Hansen, "Constitution of Binary Alloys", McGraw-Hill, New York, 1958.

60. M. Blander, Editor, "Molten Salt Chemistry", Interscience Publishers, New York, 1963.

APPENDIX A

SOLID STATE BATTERY

One of the principal problems associated with most battery systems for aerospace applications is to find suitable method to hermetically seal the battery and prevent leakage and loss of electrolyte. This problem becomes particularly severe as the operating temperature of the battery increases. The use of ion exchange membranes, both organic and inorganic, as solid electrolytes in fuel cells represents an attempt to solve this problem by minimizing the amount of liquid present.

The synthetic zeolites, because of their ionic conductivity, particularly at high temperatures, are suitable for use as solid electrolytes. In addition, zeolites which have been exchanged with reducible metal ions such as Ag^+, Cu^{++}, Hg^{++}, Ni^{++}, and Au^+ can be used in a dual role as a solid electrolyte and a cathode depolarizer.

The electrical properties of zeolites discussed above, together with the fact that zeolite crystals can be very easily ion-exchanged with reducible metal ions, have made possible the preparation of a primary cell.[58] The features of such a cell are long life and operation over a wide temperature range. Since the only mass transfer across the lattice is the diffusing ions, it can be considered to be a true solid-state cell. To illustrate the principle, consider a cell made up from a catholyte Ag^+Z^- bonded to Na^+Z^- electrolyte which in turn is bonded to a Zn anode. Gold foil can be used as a current collector at the cathode. This cell can be represented as

$$Zn/Na^+Z^-/Ag^+Z^-/Au \tag{34}$$

This system can be compacted to small discs: for example, 1/2 inch diameter with 1/4 inch thickness.

The operation of the completely solid cell formed in this way can best be illustrated by the series of reactions at the various parts of the cell

$$\text{Anode reaction} \qquad Zn \rightarrow Zn^{++} + 2e^{-} \qquad (35)$$

$$\text{Cathode reaction} \qquad 2\,Ag^{+} + 2e^{-} \rightarrow 2\,Ag \qquad (36)$$

$$\text{Electrolytic reaction} \qquad Zn^{++} + 2\,Ag^{++}Z^{-} \rightarrow Zn^{++}Z_2^{-} + 2\,Ag^{+} \qquad (37)$$
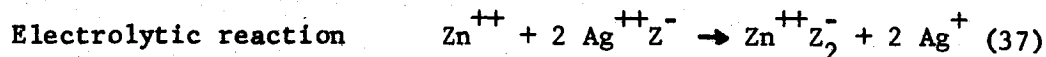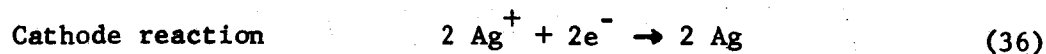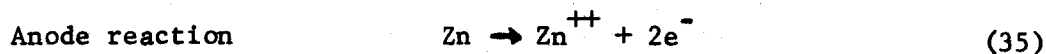
Other combinations of catholyte/electrolyte/anode systems are possible; for example,

$$Zn/Ca^{++}\,Z_2^{-}/Hg^{++}Z_2^{-}/Au \qquad (38)$$

The power output of the system depends on the following factors:

    (1)   Temperature

    (2)   Type of phase and amount of absorption

    (3)   Type of catholyte

    (4)   Type of electrolyte and anode

Preliminary experimental results have been obtained with such a cell and indicate that it can operate from $-79^{\circ}C$. up to $700^{\circ}C.-800^{\circ}C$. Voltages in the range of 2 to 3 volts have been measured. These cells can be stacked together to form high-voltage solid-state batteries. An advantage of this type of porous crystal over the ion-exchange resins is their high electro-chemical equivalent (700-750 coulombs/cc) and their tolerance to considerably higher temperature, i.e., stability of some zeolites extends up to $1000^{\circ}C$.

The weight requirements of the cathode portion of such a solid state battery can be calculated. For 14 ampere-hours of operation, a total of 0.523 equivalents of the cathode would be required. A comparison of this amount of various cathode depolarizers is shown in Table XXXV. The amounts of cathode depolarizer required for 14 ampere-hours of operation were calculated with the assumption that the cathode depolarizer was reduced at 100 percent efficiency with the number of electron per molecule as given by the "n" value. No provisions have been made in the calculations for the amount of electrolyte which might be required with the conventional depolarizers. It appears that the active weight of a cathode composed of a zeolite containing

a reducible cation will be heavier than that of a conventional depolarizer. However, it must be emphasized that the zeolite also serves as the electrolyte. When the electrolyte requirements of conventional depolarizers are taken into account, the use of a zeolitic cathode becomes more attractive. In addition, it would appear that the zeolite type of cell might be easier to fabricate and might contain less inert materials.

TABLE XXXV

COMPARISON OF CATHODE DEPOLARIZERS

Cathode Depolarizer	n	Equivalent Weight, grams	Weight for 14 ampere-hours
Type A Zeolite in Ag^+ form	1	226.9	119
Type A Zeolite in Cu^{++} form	2	149.8	79
Type A Zeolite in Ni^{++} form	2	147.42	77
Type X Zeolite in Ag^+ form	1	237.9	124
Type X Zeolite in Cu^{++} form	2	161.8	85
$CuCl_2$	2	67.2	35
$FeCl_3$	1	162.2	84
$BiCl_3$	3	105.1	55
$AgCl$	1	144.3	75
CuO	2	39.8	20.8

APPENDIX B

VOLUME CHANGE IN TYPE X ZEOLITE

The Type X zeolites have a face-centered, cubic structure. The length of the unit cell, a_o, can be determined from the equation

$$a_o = d_{hkl} (h^2 + k^2 + l^2)^{1/2} \tag{39}$$

where d_{hkl} is the spacing for the crystal plane having the indices h, k, and l.

The data for NaX and LiX given in the following table is taken from Table XIV, Section 5.2.2.

CRYSTAL PARAMETERS OF NaX and LiX

$h^2+k^2+l^2$	LiX(59% exchanged)		NaX	
	d_{hkl}	a_o	d_{hkl}	a_o
3	14.37	24.889	14.47	25.062
8	8.79	24.858	8.85	25.028
11	7.49	24.844	7.54	25.010
19	5.70	24.846	5.73	24.977
27	4.79	24.889	4.81	24.993
32	4.40	24.891	4.42	25.004
35	4.21	24.906	4.23	25.025
40	3.931	24.864	3.946	24.958
43	3.794	24.877	3.808	24.969
44	3.749	24.867	3.765	24.973
Averages		24.873 ± 0.021		25.000 ± 0.032

Since these zeolites have a cubic structure, the volume of the unit cell is

$$V_o = a_o^3 \tag{40}$$

$$\text{For LiX} \quad V_o = 1.5388 \times 10^4$$

$$\text{NaX} \quad V_o = 1.5625 \times 10^4$$

$$\text{Volume Change} \quad 1.52\%$$

-168-

DISTRIBUTION

National Aeronautics and Space
Administration
Washington D. C. 20546

Attn: Ernst M. Cohn, Code RNW

1 Copy

National Aeronautics and Space
Administration
Washington D. C. 20546

Attn: George F. Esenwein, Code MSA

1 Copy

National Aeronautics and Space
Administration
Washington D. C. 20546

Attn: A. M. Andrus, Code FC

1 Copy

National Aeronautics and Space
Administration
Washington D. C. 20546

Attn: J. R. Miles, Code SL

1 Copy

National Aeronautics and Space
Administration
Washington D. C. 20546

Attn: Welfred M. Redler, Code PE

1 Copy

National Aeronautics and Space
Administration
Goddard Space Flight Center
Greenbelt, Maryland

Attn: Thomas Hennigan, Code 632.2

1 Copy

National Aeronautics and Space
Administration
Goddard Space Flight Center
Greenbelt, Maryland

Attn: Joseph Shirfey, Code 652

1 Copy

National Aeronautics and Space
Administration
Goddard Space Flight Center
Greenbelt, Maryland

Attn: Paul Donnelly, Code 636.2

1 Copy

National Aeronautics and Space
Administration
Lewis Research Center
21000 Brookpark Road
Cleveland, Ohio 44135

Attn: N. D. Sanders MS 302-1   1 Copy

National Aeronautics and Space
Administration
Lewis Research Center
21000 Brookpark Road
Cleveland, Ohio 44135

Attn: Martin J. Saari MS 500-201

1 Copy

National Aeronautics and Space
Administration
Lewis Research Center
21000 Brookpark Road
Cleveland, Ohio 44135

Attn: Robert L. Cummings MS 500-201

1 Copy

National Aeronautics and Space
    Administration
Lewis Research Center
21000 Brookpark Road
Cleveland, Ohio 44135

Attn: Harvey J. Schwartz MS 500-201
                         1 Copy

National Aeronautics and Space
    Administration
Lewis Research Center
21000 Brookpark Road
Cleveland, Ohio 44135

Attn: J. J. Weber MS 15-1
                        1 Copy

National Aeronautics and Space
    Administration
Lewis Research Center
21000 Brookpark Road
Cleveland, Ohio 44135

Attn: J. E. Dilley MS 500-309
                        1 Copy

National Aeronautics and Space
    Administration
Lewis Research Center
21000 Brookpark Road
Cleveland, Ohio 44135

Attn: B. Lubarsky MS 500-201
                        1 Copy

National Aeronautics and Space
    Administration
Lewis Research Center
21000 Brookpark Road
Cleveland, Ohio 44135
                   1 Copy
Attn: M. R. Unger MS 500-201   + 1 Repro

National Aeronautics and Space
    Administration
Lewis Research Center
21000 Brookpark Road
Cleveland, Ohio 44135

Attn: Library
                        1 Copy

National Aeronautics and Space
    Administration
Lewis Research Center
21000 Brookpark Road
Cleveland, Ohio 44135

Attn: Report Control Office
     Mail Stop 5-5   1 Copy

National Aeronautics and Space
    Administration
Scientific and Technical Information Facility
P. O. Box 5700
Bathesda 14, Maryland

Attn: NASA Representative   2 Copies
                        + 1 Repro

National Aeronautics and Space
    Administration
Marshall Space Flight Center
Huntsville, Alabama

Attn: Philip Youngblood
     Bldg. 4487-BB
     M-ASTR-EC   1 Copy

National Aeronautics and Space
    Administration
Manned Space Craft Center
Houston 1, Texas

Attn: William R. Dusenbury
     Propulsion and Energy Systems
     Branch, Energy Systems Div.
     Bldg 16, Site 1   1 Copy

National Aeronautics and
    Space Administration
Manned Space Craft Center
Houston 1, Texas

Attn: Robert Cohen
    Gemini Project Office
                    1 Copy

National Aeronautics and
    Space Administration
Manned Space Craft Center
Houston 1, Texas

Attn: Richard Ferguson, EP-5
                    1 Copy

National Aeronautics and
    Space Administration
Manned Space Craft Center
Houston 1, Texas

Attn: Forrest E. Eastman, EE-4
                    1 Copy

National Aeronautics and Space
    Administration
Ames Research Center
Pioneer Project
Moffett Field, California

Attn: James R. Swain   1 Copy

Jet Propulsion Laboratory
4800 Oak Grove Drive
Pasadena, California

Attn: Aiji Uchiyama   1 Copy

U. S. Army Engineer Research
    and Development Labs
Fort Belvoir, Virginia 22060

Attn: Dr. Galen Frysinger
    Electrical Power Branch
    SMOFB-EP   1 Copy

U. S. Army Engineer Research
    and Development Labs
Fort Monmouth, New Jersey

Attn: David Linden (Code SELRA/PS)
                    1 Copy

U. S. Army Research and Development
Liaison Group (9851 DV)
APO 757
New York, New York

Attn: B. R. Stein   1 Copy

Army Research Office
Office, Chief Research and Development
Department of the Army
3D 442, The Pentagon
Washington D. C. 20546

Attn: Dr. Sidney J. Magram
                    1 Copy

Harry Diamond Labs
Room 300, Bldg 92
Connecticut Avenue and
    Van Ness Street, N. W.
Washington D. C.

Attn: Nathan Kaplan   1 Copy

Army Materiel Command
Research Division
AMCRD-RSCM T-7
Washington 25, D. C.

Attn: John W. Crellin   1 Copy

U. S. Army TRECOM
Fort Eustis, Virginia 23604

Attn: Dr. R. L. Echols
       (SMOFE-PSG)   1 Copy

U. S. Army TRECOM
Fort Eustis, Virginia 23604

Attn: Leonard M. Bartone
       (SMOFE-ASE)
       Physical Sciences Group
       Mechanical Systems Subgroup,
       ASE   1 Copy

U. S. Army Research Office
Box CM, Duke Station
Durham, North Carolina

Attn: Paul Greer   1 Copy

U. S. Army Research Office
Box CM, Duke Station
Durham, North Carolina

Attn: Dr. Wilhelm Jorgensen
                                1 Copy

U. S. Army Mobility Command
Research Division
Center Line, Michigan 48090

Attn: O. Renius (AMSMO-RR)
                                1 Copy

Headquarters, U. S. Army
   Materiel Command
Development Division
Washington 25, D. C.

Attn: Marshall D. Aiken
       (AMCRD-DE-MO-P)   1 Copy

Office of Naval Research
Washington D. C. 20360

Attn: Dr. Ralph Roberts, Code 429
       Head, Power Branch   1 Copy

Naval Research Laboratory
Washington D. C. 20390

Attn: Dr. J. C. White, Code 6160
                                1 Copy

Office of Naval Research
Department of the Navy
Washington D. C. 20360

Attn: H. W. Fox, Code 425   1 Copy

Bureau of Naval Weapons
Department of the Navy
Washington 25, D. C.

Attn: Whitwell T. Beatson
       (Code RAAE-52)
                                1 Copy

Bureau of Naval Weapons
Department of the Navy
Washington 25, D. C.

Attn: Milton Knight (Code RAAE-50)
                                1 Copy

Bureau of Ships
Department of the Navy
Washington 25, D. C.

Attn: Bernard B. Rosenbaum
(Code 340)   1 Copy

Naval Ordnance Laboratory
Department of the Navy
Corona, California

Attn: Mr. William C. Spindle
(Code 441)   1 Copy

Naval Ordnance Laboratory
Department of the Navy
Silver Spring, Maryland

Attn: Philip B. Cole (Code WB)
                         1 Copy

Wright-Patterson AFB
Flight Vehicle Power Branch
Air Force Aero Propulsion
    Laboratory
Dayton, Ohio

Attn: J. E. Cooper, APIP   1 Copy

AF Cambridge research Lab
L. G. Hanscom Field
Bedford, Massachusetts

Attn: Francis X.Doherty   1 Copy
       Edward Raskind   1 Copy

Rome Air Development Center, ESD
Griffiss AFB, New York 13442

Attn: Commander (RAALD)
                         1 Copy

Headquarters, USAF (AFRDR-AS)
Washington 25, D. C.

Attn: Lt. Col. William G. Alexander
                         1 Copy

Mr. Charles F. Yost
Asst Director, Material Sciences
Advanced Research Projects Agency
The Pentagon, Room 3E 153
Washington 25, D. C.
                         1 Copy

Dr. John H. Huth
Advanced Research Projects Agency
The Pentagon, Room 3E 157
Washington 25, D. C.
                         1 Copy

U. S. Atomic Energy Commission
Auxiliary Power Branch (SNAP)
Division of Reactor Development
Washington 25, D. C.

Attn: LCOL George H. Ogburn, Jr.
                         1 Copy

Lt. Col. John H. Anderson
Advanced Space Reactor Branch
Division of Reactor Development
U. S. Atomic Energy Commission
Washington 25, D. C.   1 Copy

Mr. Donald B. Hoatson
Army Reactors, DRD
U. S. Atomic Energy Commission
Washington 25, D. C. 20545

1 Copy

Office, DDR and E: USW and BSS
The Pentagon
Washington 25, D. C

Attn: G. B. Wareham   1 Copy

Institute for Defense Analyses
Research and Engineering
    Support Division
1666 Connecticut Avenue, N. W.
Washington 9, D. C.

Attn: Dr. George C. Szego   1 Copy

Power Information Center
University of Pennsylvania
Moore School Building
200 South 33rd Street
Philadelphia 4, Pennsylvania

1 Copy

Office of Technical Services
Department of Commerce
Washington 25, D. C. 20009   1 Copy

Battelle Memorial Institute
505 King Avenue
Columbus 1, Ohio

Attn: Dr. C. L. Faust   1 Copy

Aerojet General Corporation
Chemical Products Division
Azusa, California

Attn: Dr. S. O. Rosenberg

1 Copy

Aeronutronic Division
Philco Corporation
Ford Road
Newport Beach, California

Attn: Dr. S. W. Weller   1 Copy

Allis Chalmers Manufacturing
    Company
1100 South 70th Street
Milwaukee 1, Wisconsin

Attn: Dr. Joyner   1 Copy

Arthur D. Little, Incorporated
Cambridge, Massachusetts

Attn: J. H. B. George   1 Copy

Douglas Aircraft Company, Incorporated
Astropower Laboratory
2121 Paularino Avenue
Newport Beach, California

Attn: Dr. Carl Berger   1 Copy

Atomics International Division
North American Aviation, Inc.,
Canoga Park, California

Attn: Dr. H. L. Recht   1 Copy

Electric Storage Battery Company
Carl F. Norberg Research Center
Yardley, Pennsylvania

Attn: Library   1 Copy

Eagle-Picher Company
Post Office Box 290
Joplin, Missouri

Attn: E. M. Morse   1 Copy

Dr. Arthur Fleischer
466 South Center Street
Orange, New Jersey   1 Copy

Electrochimica Corporation
1140 O'Brien Drive
Menlo Park, California

Attn: Dr. Morris Eisenberg
                                 1 Copy

General Electric Corporation
Schenectady, New York

Attn: Dr. William Carson
      General Engineering
      Laboratory
                                 1 Copy

Globe Union, Incorporated
900 East Keefe Avenue
Milwaukee, Wisconsin

Attn: Dr. C. K. Morehouse
                                 1 Copy

Gould-National Batteries, Inc.,
Engineering and Research Center
2630 University Avenue, S. E.
Minneapolis 14, Minnesota

Attn: J. F. Donahue   1 Copy

Gulton Industries
Alkaline Battery Division
Metuchen, New Jersey

Attn: Dr. Robert Shair   1 Copy

Hughes Research Laboratories
    Corporation
Malibu, California

Attn: T. M. Hahn   1 Copy

Livingston Electronic Corporation
Route 309 opposite Springhouse Quarry
Montgomeryville, Pennsylvania

Attn: William F. Meyers
                                 1 Copy

Lockheed Aircraft Corporation
1123 N. Mathilda Avenue
Sunnyvale, California

Attn: J. E. Chilton   1 Copy

P. R. Mallory and Company
Northwest Industrial Park
Burlington, Massachusetts

Attn: Dr. Per Bro
                                 1 Copy

Hoffman Electronics Company
Research Laboratory
Santa Barbara, California

Attn: Dr. J. Smatko
                                    1 Copy

Magna Corporation
Division of TRW, Incorporated
101 South East Avenue
Anaheim, California

Attn: Dr. G. Rohrbach   1 Copy

Marquardt Corporation
16555 Saticoy Street
Van Nuys, California

Attn: Dr. H. G. Krull   1 Copy

Melpar, Incorporated
3000 Arlington Boulevard
Falls Church, Virginia

Attn: Dr. R. T. Foley   1 Copy

Monsanto Research Corporation
Everett 49, Massachusetts

Attn: Dr. J. O. Smith   1 Copy

Radio Corporation of America
Somerville, New Jersey   1 Copy

Space Technology Laboratories, Inc.,
2400 E. El Segundo Boulevard
El Segundo, California

Attn: Dr. A. Krausz   1 Copy

Southwest Research Institute
8500 Culebra Road
San Antonio 6, Texas

Attn: Dr. Jan Al   1 Copy

Power Sources Research Laboratory
Whittaker Corporation
9601 Canogo Avenue
Chatsworth, California 91311

Attn: Dr. M. Shaw   1 Copy

University of Pennsylvania
Electrochemistry Laboratory
Philadelphia 4, Pennsylvania

Attn: Prof. J. O'M. Brockris

Yardney Electric Corporation
New York, New York

Attn: Dr. Paul Howard   1 Copy

Union Carbide Corporation
Parma Research Center
Advanced Developments Department
12900 Snow Road
Parma, Ohio

Attn: Dr. R. A. Charpie   1 Copy

Westinghouse Electric Corporation
Research and Development Center
Churchill Borough
Pittsburgh, Pennsylvania

Attn: Dr. A. Langer
                                   1 Copy

P. R. Mallory and Company, Inc.
3029 East Washington Street
Indianapolis, Indiana 46206

Attn: Technical Library

                     1 Copy

Naval Research Laboratory
Washington, D. C. 20390

Attn: Dr. Roger Labrie   1 Copy